Harnessing phages for supramolecular and materials chemistry

Marcozzi, Alessio

university of groningen

Harnessing phages for supramolecular and materials chemistry

PhD thesis

to obtain the degree of PhD at the
University of Groningen
on the authority of the
Rector Magnificus Prof. E. Sterken
and in accordance with
the decision by the College of Deans.

This thesis will be defended in public on

Tuesday 7 June 2016 at 09.00 hours

by

Alessio Marcozzi

born on 20 September 1982
in Rome, Italy

Supervisor
Prof. A. Herrmann

Assessment committee
Prof. A.K.H. Hirsch
Prof. H.A. Klok
Prof. O.A. Scherman

Harnessing phages
for supramolecular and materials chemistry

Chapter,1

Introduction,to,M13,and,Phage,Display

Abstract

The filamentous bacteriophage M13 is a popular tool in molecular biology. The most important applications that take advantage of this virus are the selection of peptide binders (aptamers) and refinement of antibodies through a technique called "phage display". Moreover, thanks to the modularity of its capsid and to its filamentous structure, M13 is used in materials science as a scaffold for nanostructures. Here, we introduce the biology of M13 and we review examples of its applications.

1.1 - The biology of M13

M13 is a filamentous bacteriophage of the genus Inovirus that exclusively infects male *Escherichia coli* (*i.e.* with conjugative pilus, or F pilus).[1] The M13 has a circular single stranded DNA genome (ssDNA, Figure 1) that is 6407 nucleotides long.[2,3] This sequence carries 11 genes that are often overlapping or separated only by a few nucleotides. These genes code for three classes of proteins that play roles in replication (p2, p5 and p10), or have morphogenetic (p1, p4 and p11) and capsidic (p3, p6, p7, p8, p9) characteristics.

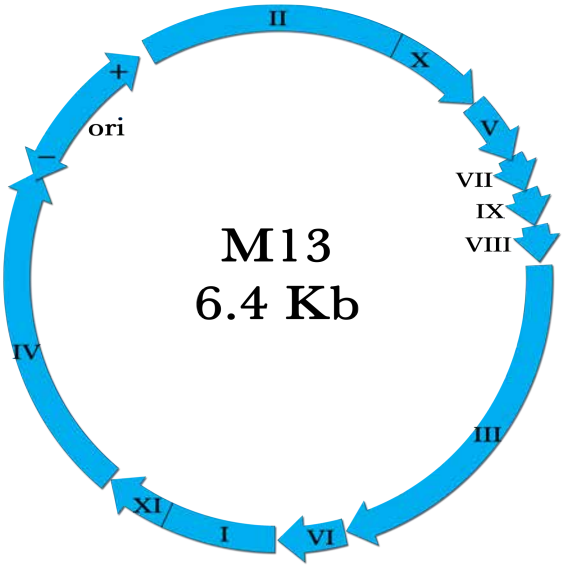

Figure 1. ***Genome map of M13.*** *Note that the genome carries 11 protein coding genes that could partially overlap or that are separated by only a few base pairs.*

Virion structure

The capsid of M13 is composed of 5 coat proteins (p3, p6, p7, p8 and p9; Figure 2). The protein p8, coded by gene 8, is made up of 50 residues adopting an alpha-helix structure. About 2700 copies of p8 assemble to form the major component of the capsid.[4] This assembly is approximately 900 nm long and 7 mm wide and forms a cylindrical structure that envelopes the genome. The four remaining capsid proteins are present in the capsid at

much lower numbers and are placed at either end of the virion. Five copies each of the proteins p3 and p6 are forming the head, whereas five copies of proteins p7 and p9 assemble into the tail.[2,4] The eleven M13 proteins coordinate to play seven distinct roles namely formation of the capsid head (p3 and p6), the capsid tail (p7 and p9), the capsid coat (p8), assembly of the new phage particles (p1, p4 and p11), binding of ssDNA (p5), DNA replication (p10) and replication of strand + (p2).

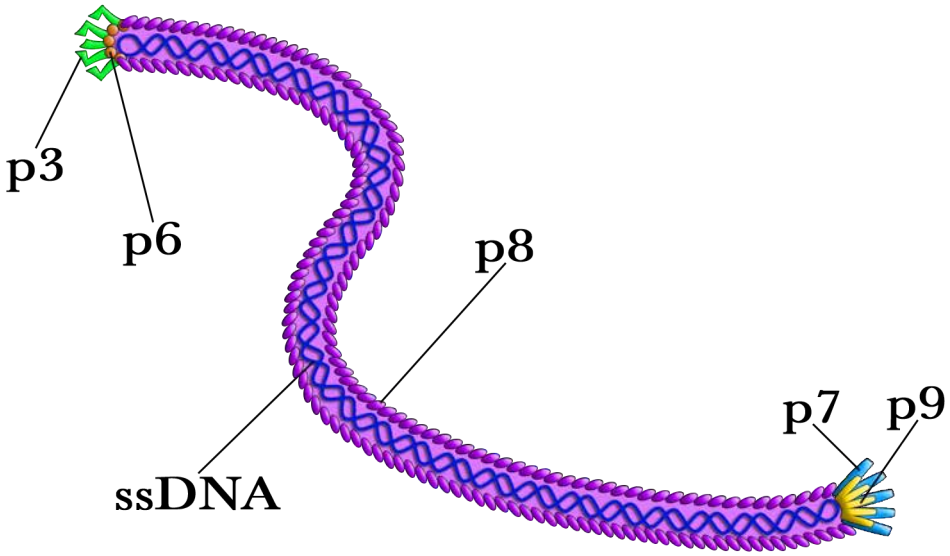

Figure 2. ***Schematic illustration of the arrangement of M13 capsid proteins.*** *Note, the tube-like structure is formed by about 2700 units of p8 with additional proteins p3 and p6 forming the head and p7 and p9 forming the tail.*

Life cycle

M13 follows the typical life cycle pattern of bacteriophages, except that it can only infect a male *E. coli* organism.[1] Typically, it completes the life cycle in four distinct steps; *infection of the host, replication of the viral genome using host factors, assembly of new viral particles, and external release of viral progeny by the host organism*. Figure 3 illustrates all stages of the life cycle of M13.

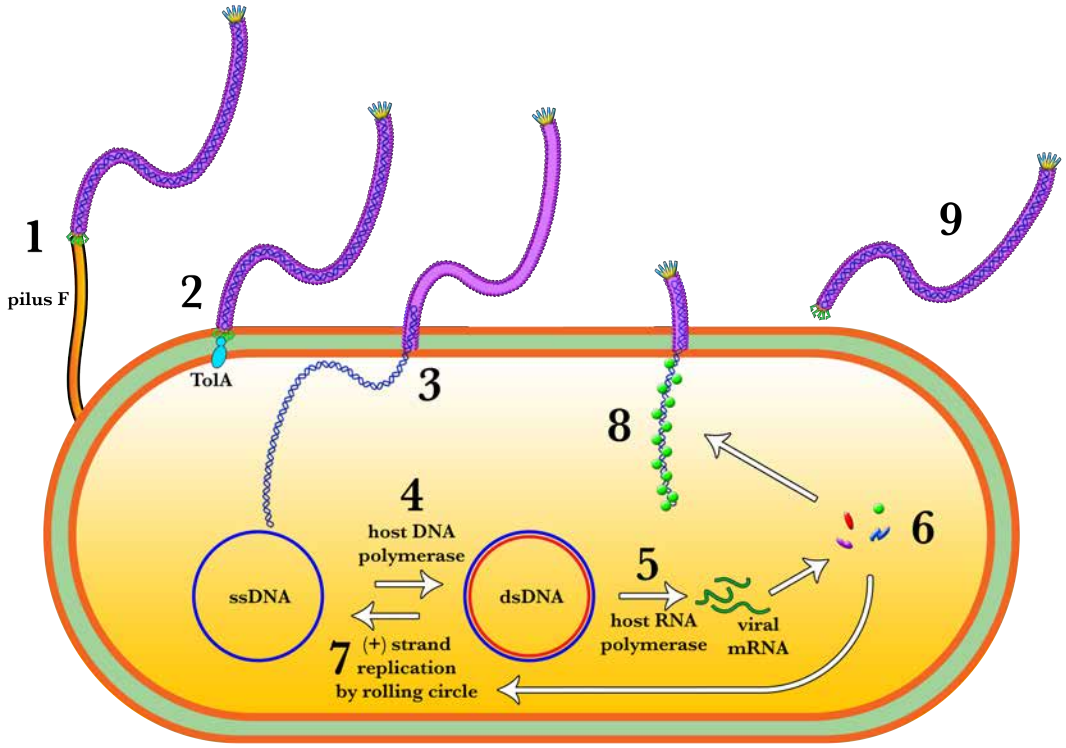

Figure 3. ***The life cycle of M13.*** *Stages 1 through 3 depict the infection of the host, stages 4 to 7 illustrate the replication of the genome, stages 5 and 6 show the expression of the viral proteins, and stages 8 and 9 sketch the assembly and extrusion of new viral particles.*

Infection. The infection of the host is mediated through p3, located on the head of M13[1]. The protein 3 (p3) initiates interactions through its N-terminus with the receptors of the F pilus of *E. coli*. Upon binding of p3 with the F pilus, M13 is retracted into the proximity of the host. Once M13 approaches very close to the host membrane, bacterial proteins TolQ, TolR and TolA mediate the uncoating of the viral DNA.[5-7] This dissolves the attached p8 protein, which allows the ssDNA genome to enter the host cytoplasm. This infection causes formation of turbid plaques in the *E. coli* colonies without lethal consequences. Further, the infection is of chronic type that is neither of temperate nor lytic nature. A characteristic outcome is significant reduction in the growth rate of the host cells.[8]

Replication of the viral genome. Following entry into the cytoplasm, the single-stranded phage genome, called "+ strand" is converted by the host enzymes into a double-stranded supercoiled circular DNA called replicative form (RF-1 or RF). The RF is used both as a template for the production of new viral ssDNA genome and for the expression of viral proteins.[9]

The next stage involves *amplification of the M13 genome*. M13 proteins p2, p5 and p10 play critical roles at this stage.[10-12] The endonuclease p2 remains bound to the 5' phosphate end of the nicked strand, and the free 3' hydroxyl end is released to serve as a primer for DNA synthesis by host DNA polymerase III. Using the un-nicked strand as a template, replication proceeds around the circular DNA molecule, displacing the nicked strand as ssDNA. Displacement of the nicked strand is carried out by a host-encoded helicase. Continued DNA synthesis can produce multiple single-stranded linear copies of the original DNA in a continuous head-to-tail series called a *concatemer*.[9,10] These linear copies can be converted to double-stranded and single-stranded circular molecules through the rolling-circle mechanism of DNA replication (Figure 4).

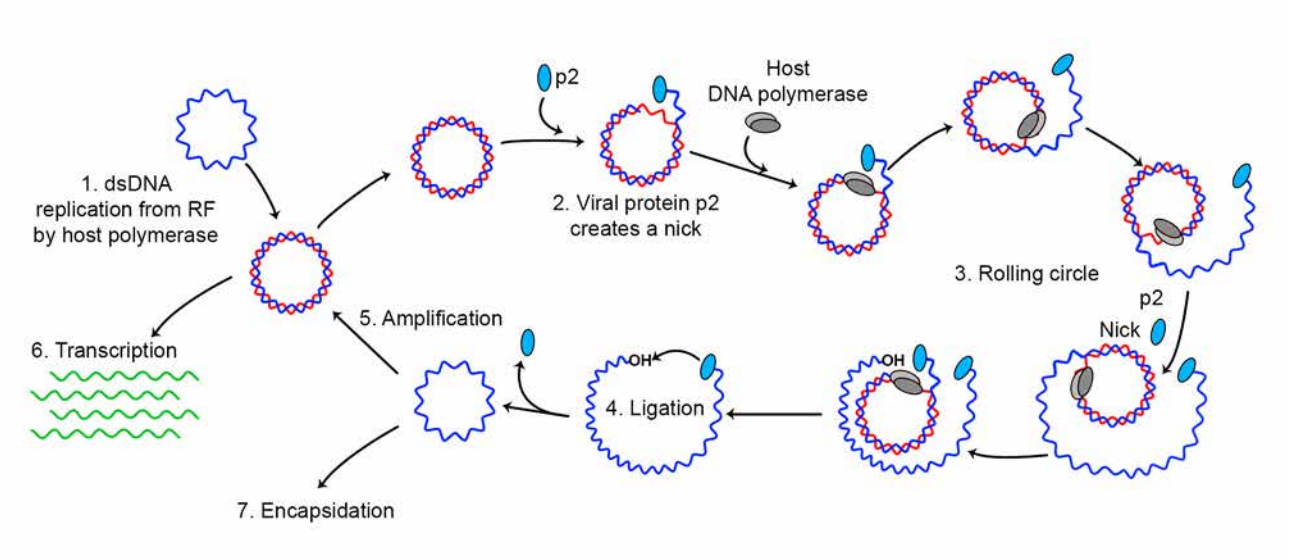

Figure 4. ***Schematic view of M13 DNA replication by rolling circle mechanism.*** *See text for details.*

At a later stage, p5 regulates the level of total viral DNA in the host by binding the new formed M13 ssDNA genome and withdrawing it from the replication machinery.[13] The protein p5 also directs the DNA towards the inner membrane of the host where virion assembly occurs. The p10 protein is important in the regulation of the number of dsDNA genomes inside the host. In the absence of p10, ssDNA accumulation does not occur. The p10 protein is identical to the C-terminus of p2 protein as they are produced by overlapping coding sequences. This identity reduces the size of the genome, but poses a challenge during genetic engineering as manipulation of this sequence will have a high likelihood of resulting in structural or functional detrimental changes. Though a puzzle for the genetic engineers, it is a marvelous example of the compactness coupled with efficiency that is often observed in viruses.

Assembly and extrusion of viral particles. As the concentration of ssDNA and capsid proteins increases, assembly and extrusion processes are initiated simultaneously when reaching an optimal quantity. The newly assembled virions are extruded from the host cell without inducing host-cell lysis. The last set of three M13 proteins, p1, p4 and p11 are required for maturation of the newly formed phages. These proteins assemble to form an extrusion channel in the host-cell membrane through which the mature phages are released. About twelve copies of p4 protein assemble to form the outer end portion of the channel, whereas five molecules of p1 and p11 combine to form the inner part of the channel. Hence, p4 remains in contact with extracellular surface whereas p1 and p11 communicate with the cytoplasm.

The ssDNA and p5 complex reach the extrusion channel where proteins p7 and p9 are assembled to form one end of the phage particle.[4] The p7 and p9 complexed interact with the extrusion channel to properly guide and direct the exit of newly formed phages. While passing through the inner membrane, these proteins are substituted with p5 and p8 that form the body of the mature phage. As this substitution is completed, five copies each of proteins p3 and p6 assemble to form the head region on the terminal end[14]. Immediately afterwards, the phage is released from the host cell.

1.2 - The phage display technology

The design and engineering of biological molecules is following two distinct strategies: the *rational* and the *irrational* approach.[15]

Rational design aims to create new molecules having certain properties based on the prediction of their structure-function relationship and simulation of their behavior through physical models. On the contrary, irrational design is based on the selection of molecules with a specific function with no *a priori* knowledge of their structural, chemical or physical characteristics. However, irrational design utilizes the powerful concept of *in vitro* evolution.

Phage display is a molecular bio-technology invented by George P. Smith in 1985[16] and was subsequently developed in the 1990s by several research groups in order to select antibodies, therapeutic proteins and in general as a support methodology for protein engineering.[17-19] This technique is applied to the irrational design approach since it serves the purpose of obtaining peptides or proteins with particular characteristics using evolution as a unique tool for their selection.

As Smith himself wrote in 1997, this strategy implies a true paradigm shift in the field of drug discovery. Phage display relies on the assumption that each single molecule is an individual within a large population. By applying selective pressure on the population, it is possible to drive the evolution of molecules whose fitness is higher for a desired property. This also implies that the molecules under selection possess characteristics that govern the evolution of organisms, namely the ability to reproduce and mutate. Not all the molecules can satisfy these criteria. However, a variety of biological molecules, including peptides and proteins, posses these features. Peptides and proteins do not mutate or reproduce by themselves. However, their coding genes have the potential to reproduce and generate variants due to a variety of mutations. This provides a powerful tool for genetic engineers. If one could generate a pool of closely related (structurally or functionally) peptides or proteins with minor alterations in the coding DNA sequence, it

might be possible to select and evolve peptides and proteins with highly specific and desired characteristics.

Until the discovery of phage display, construction of a peptide or protein library with known phenotypic and genotypic details was a fundamental problem in genetic engineering. Phage display elegantly solved this problem as it enables using phages for encoding and expressing peptide libraries.

Phages are bacterial viruses composed of a protein capsid that houses its genome.[20] It is easy to modify one (or more) capsidic proteins in order to express a peptide sequence of varying length, such that it is expressed on the outer surface of the viral capsid.

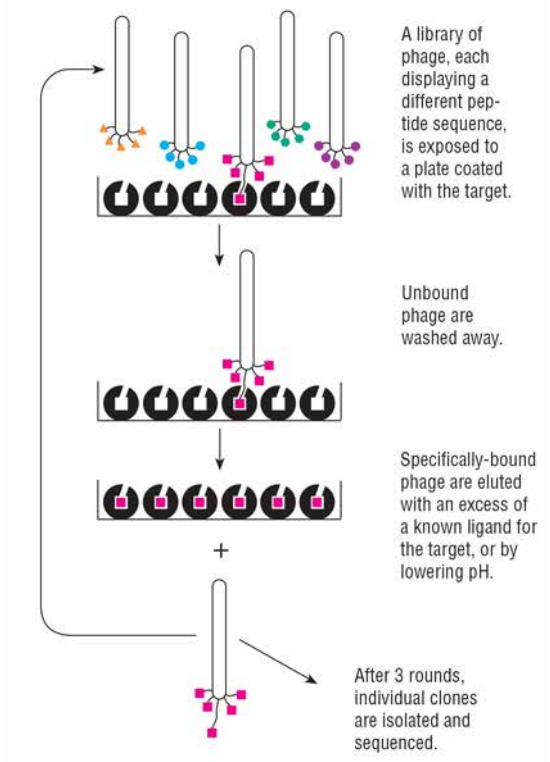

Figure 5. ***Overview of phage display.*** *The typical form of phage display selection protocol consists of incubation-washing-elution (Picture from phage display manual – New England Biolabs).*

The nucleotide sequence coding for the recombinant protein is retained within the capsid. This makes the viral particle a single connecting link between the phenotype (expressed protein) and genotype (the recombinant DNA sequence). Establishment of this

connecting link makes it possible to proceed with the irrational selection of molecules with desired functions.

A typical phage display selection protocol involves a few well-defined steps.[21] In its simplest form, the selection protocol is carried out by 1) incubating a library of phage-displayed peptides with a target that is immobilized on a solid support, 2) washing away the unbound phage, and 3) eluting the specifically bound phage (Figure 5). The eluted phages are then amplified and subjected to additional binding/amplification cycles to enhance the purity. After few rounds, selected clones are characterized by DNA sequencing and enzyme-linked immunosorbent assays (ELISA).

It is possible to express different type of libraries on the phage capsid.[22] Furthermore, different coat proteins can be used to expose the peptides. The present thesis work is based on two libraries expressed as N-terminal fusion to M13's minor coat protein p3. The first library, called "Ph.D.-12", encodes 12 random amino acid long linear peptides followed by a short C-terminal linker Gly-Gly-Gly-Ser. The library can be schematically representated as N-term-X_{12}-GGGS-p3-C-term.The second library, called "Ph.D.-C7C", is made of cyclic peptides consisting of an N-terminal Ala-Cys motif followed by seven random amino acids long peptides ending with Cys-Gly-Gly-Gly-Ser. The two Cys form a disulfide bond that constrains the peptide in its final cyclic conformation (N-term-A-C-X_7-C-GGGS-p3-C-term). Such libraries have an enormous theoretical complexity, in fact Ph.D.-C7C may code for $1.28X10^9$(20^7) unique peptide sequences, while Ph.D.-12 may code for $4.1X10^{15}$(20^{12}) peptide sequences. The successful production of such libraries is limited by the DNA transformation efficiency, which is around 10^9 transformants per electroporation in *E. coli*. Both libraries have complexities on the order of 10^9 independent clones, which is sufficient to encode most, if not all of the possible 7-mers but only a tiny fraction (less than 1 millionth) of the possible 12-mers sequences. This limitation, however, does not invalidate the potential of the method and, generally speaking, phage display is still the most efficient way to produce and test large peptide libraires that would not be accessible by other methods.

1.3 - Applications of phage display

Although the full impact of phage display as invented by Smith was not immediately appreciated, the advantages of using bacteriophages as tools for the display of ligands became evident when methods to fuse larger molecules, such as antibody fragments and phage coat protein p3, were developed.[17,23] Indeed, discovery of antibodies has led to the largest practical applications of the phage display technology. However, when libraries of immunoglobulin fragments were used to optimize standard antibodies, it turned out to be very difficult, although it is possible to express these proteins in bacteria.[24] For this reason, investigators have turned to single-chain variable region fragments (scFvs) and antigen-binding fragments (Fabs).[25-28] These novel approaches are widely used by pharmaceutical companies to speed up the whole and fragment antibody optimization, which has revolutionised the complete field of antibody discovery and production.

Phage display is used commonly for its powerful ability to assist in the selection of improved protein stability. Unlike classical panning methods that depend on protein-protein or protein-ligand interactions, phage display helps to identify improved protein variants based solely on their resistance to proteolysis or denaturation.[29] The procedure leverage the facts that 1) large proteins can be inserted between N and the C-terminal domain of the protein p3 without significant loss of infectivity and 2) filamentous bacteriophages are naturally resistant to most proteases. Hence, a library of protein variants cloned between N and the C-terminal domain can be subjected to proteases, followed by infection to identify proteolysis-resistant inserts. This principle can also be exploited to select for folding stability. A phage library can be subjected to a set of conditions, say exposure to a specific solvent for example, followed by infection to identify a protein insert that remains stable under these conditions. Using this strategy, it was possible to increase protein stability at high temperatures by selecting protein variants from a library with randomized surface residues.[30] A slightly different approach allows using phage-displayed libraries for the identification of protease substrates. In this case, peptide libraries are cloned at the N-terminus of the protein p3 followed by an epitope tag.

The recombinant phages are then immobilized via the epitope tag and treated with the proteasome of the randomized regions. The susceptible peptides will be dissolved owing to protease cleavage, and the eluted phage can be analysed further.[31]

Numerous researchers have developed clever applications of the phage display technology during the three decades since its invention, opening doors to a new kind of *in vitro* evolution strategy for novel enzymatic activity.[32] Many researchers have also tried to select proteins from phage-displayed libraries on the basis of their catalytic activity relying on substrate homologues designed to covalently bind the enzyme during or after catalysis. A typical approach in this area is the incubation of a library of enzyme variants with an immobilized substrate homologue. If an enzyme variant reacts with the substrate, the phage is retained and thus selected. A brilliant example of this approach is represented by the evolution of catalytic antibodies, a new class of proteins developed by several research groups. One such successful example is the work by Tanaka and colleagues on aldolases [33,34], who succeded in evolving aldolase activity using 1,3-diketones as substrate.

Other fields where phage display has been extensively used are enzyme-inhibitor discovery and selection of binders for inorganic materials and nanostructures, that will be presented in chapter 2 and 3, respectively.

1.4 - Summary

M13 is a filamentous bacteriophage that exclusively infects male *E. coli* that carries a conjugative pilus. M13 carries a circular ssDNA genome that codes for eleven proteins necessary for its replication, structural, morphogenetic and capsidic characteristics. The proteins play distinct roles in formation of capsid head (p3 and p6), formation of capsid tail (p7 and p9), formation of capsid coat (p8), assembly of the new phage particles (p1, p4 and p11), binding of ssDNA (p5), DNA replication (p10) and replication of strand + (p2).

Apart from its requirement for a sex-specific host, M13 completes its life cycle in four stages like any other bacteriophage through *infection of the host, replication of the viral genome using host factors, assembly of new viral particles, and external release of viral progeny by the host organism*. Interestingly, apart from inducing turbid plaques in host colonies and reducing growth, M13 neither integrates its DNA in the host's genome, nor causes lysis.

Use of phages is one of the most common methods for design and engineering of biologically active molecules. These methods can either be rational, where molecules with specific function are created or irrational, where molecules with specific function are selected for based on the principles of biological evolution. Phage display is an irrational design method that employs bacteriophages to select antibodies, therapeutic proteins and in general as support methodology for protein engineering. This method is commonly used for the selection of proteins with improved stability, enzyme inhibitor discovery and selection of binders for inorganic materials and nanostructures.

Assuming that each molecule is an individual representative of a wider population, application of selection pressure can drive the evolution of molecules with greater fitness for a desired trait. Though peptides and proteins do not mutate and reproduce by themselves, their nucleic-acid-coding sequences do, which provides a powerful tool for genetic engineering. Phage display works by creating a pool of structurally or functionally closely related peptides or proteins (through minor genetic variations), from which desired molecules are selected in three simple steps. Phage display has become a powerful tool in constructing protein/peptide libraries using phages.

A pool of M13 can be engineered to express protein variants on the coat that can be selected using its specific ligands. The phage becomes a connecting unit between the genotype and the expressed phenotype, making it possible to irrationally select desired molecules. The protocol proceeds with incubation of a library of phage-displayed peptides with a target that is immobilized on a solid support, followed by washing away the unbound phages, and elution of the specifically bound phage that can be further purified and characterised using ELISA or DNA sequencing. Furthermore, different libraries can be expressed as well as different coat proteins can be used to expose the peptides.

The present thesis work is based on two libraries "Ph.D.-12" and "Ph.D.-C7C" that have an enormous complexity on the order of 10^9 clones, which is sufficient to encode most, if not all of the possible 7-mer but only a tiny fraction of the possible 12-mer sequences. Although this limits the number of variants, phage display is still the most efficient way to produce and test vast peptide libraires.

1.5 - Thesis overview

In recent years, several research groups have made the effort to bridge chemistry and biology for the production of new hybrid materials. This is achieved by exploring of the interface between these two disciplines. In this context, this PhD work represents a clear example such an explorational approach in which molecular biology has been leveraged to exploit the potentials of bacteriophages in —but not only— materials science. The aim of this work is to give the reader an overview of such potentials and to report the results obtained. This thesis is organized as follows:

The first chapter "Introduction to M13 and Phage Display" aims to give a broad introduction about the biology of bacteriophage M13 and to review its current uses in biotechnology and materials science. Particular attention is dedicated to explain the technique called "phage display" and the evolutionary concepts behind it.

The purpose of the next two chapters is to depict practical applications of phage display for the selection of peptide aptamers against two very different targets and for two

very different purposes. In particular, Chapter 2 introduces the problem of increasing antibiotic resistance among infectious bacteria and delineates our strategy to deal with it. In this chapter, it is described how phage display has been successfully applied to evolve small peptide inhibitors against a bacterial enzyme. The selection process and the characterization of such promising peptides are reported, especially in regard to its activity to block the functionality of the bacterial target enzyme.

In Chapter 3, called "Exploring peptide libraries for CB8-based supramolecular host–guest chemistry", we will see an example of the utilization of phage display for the selection of peptides able to form host-guest interaction with a small organic molecule and how that specific interaction can be exploited to broaden our knowledge about such host-guest systems and for a practical application as well.

Chapter 4, "M13 as biomaterial", introduces the concept of using biological entities — like viruses— as versatile building blocks for materials science and how, by means of genetic engineering, it is possible to tune the properties of the building blocks and of the bulk material properties themselves. A successful example of this approach, liquid crystalline material made by genetically engineered M13 particles is reported.

While in the second chapter an antibiotic peptide was selected by phage display, the aim of the last chapter of this thesis, "Evaluation of new aminoglycoside antibiotics", is to evaluate the antimicrobial properties of new aminoglycoside derivatives. These carbohydrate-based antibiotics were not evolved by phage display but generated by a new method named "aptameric protective group" technology.

1.6 - References

1. Tzagoloff, H. & Pratt, D. The initial steps in infection with coliphage M13. *Virology* 24, 372–380 (1964).
2. van Wezenbeek, P. M. G. F., Hulsebos, T. J. M. & Schoenmakers, J. G. G. Nucleotide sequence of the filamentous bacteriophage M13 DNA genome: comparison with phage fd. *Gene* 11, 129–148 (1980).
3. Henry, T. J. & Pratt, D. The proteins of bacteriophage M13. *Proceedings of the National Academy of Sciences of the United States of America* 62, 800–807 (1969).
4. Marvin, D. A. Filamentous phage structure, infection and assembly. *Current Opinion in Structural Biology* 8, 150–158 (1998).
5. Riechmann, L. & Holliger, P. The C-Terminal Domain of TolA Is the Coreceptor for Filamentous Phage Infection of E. coli. *Cell* 90, 351–360 (1997).
6. Deprez, C. *et al.* Solution Structure of the E.coli TolA C-terminal Domain Reveals Conformational Changes upon Binding to the Phage g3p N-terminal Domain. *Journal of Molecular Biology* 346, 1047–1057 (2005).
7. Karlsson, F., Borrebaeck, C. A. K., Nilsson, N. & Malmborg-Hager, A.-C. The mechanism of bacterial infection by filamentous phages involves molecular interactions between TolA and phage protein 3 domains. *Journal of Bacteriology* 185, 2628–2634 (2003).
8. Brown, L. R. & Dowell, C. E. Replication of coliphage M-13. I. Effects on host cells after synchronized infection. *Journal of Virology* 2, 1290–1295 (1968).
9. Ray, D. S. Replication of bacteriophage M13. *J Mol Biol* 43, 631–643 (1969).
10. Fidanián, H. M. & Ray, D. S. Replication of bacteriophage M13. *Journal of Molecular Biology* 72, 51–63 (1972).
11. Yen, T. S. B. & Webster, R. E. Translational control of bacteriophage f1 gene II and gene X proteins by gene V protein. *Cell* 29, 337–345 (1982).
12. Stassen, A. P. M., Folmer, R. H. A., Hilbers, C. W. & Konings, R. N. H. Single-stranded DNA binding protein encoded by the filamentous bacteriophage M13: structural and functional characteristics. *Molecular Biology Reports* 20, 109–127 (1994).

13. Salstrom, J. S. & Pratt, D. Role of coliphage M13 gene 5 in single-stranded DNA production. *Journal of Molecular Biology l* 61, 489–501 (1971).
14. Simons, G. F., Konings, R. N. & Schoenmakers, J. G. Genes VI, VII, and IX of phage M13 code for minor capsid proteins of the virion. *Proceedings of the National Academy of Sciences of the United States of America* 78, 4194–4198 (1981).
15. Nixon, A. E. & Firestine, S. M. Rational and 'irrational' design of proteins and their use in biotechnology. *IUBMB Life* 49, 181–187 (2000).
16. Smith, G. P. Filamentous fusion phage: novel expression vectors that display cloned antigens on the virion surface. *Science* 228, 1315–1317 (1985).
17. McCafferty, J., Griffiths, A. D., Winter, G. & Chiswell, D. J. Phage antibodies: filamentous phage displaying antibody variable domains. *Nature* 348, 552–554 (1990).
18. Sidhu, S. S. Phage display in pharmaceutical biotechnology. *Current Opinion in Biotechnology* 11, 610–616 (2000).
19. Willats, W. Phage display: practicalities and prospects. *Plant molecular biology* (2002).
20. Messing, J. Cloning in M13 phage or how to use biology at its best. *Gene* (1991).
21. Barbas, C. F., Burton, D. R., Scott, J. K. & Silverman, G. J. *Phage display: a laboratory manual*. (2004).
22. Uchiyama, F., Tanaka, Y., Minari, Y. & al, E. Designing scaffolds of peptides for phage display libraries. *Journal of Bioscience and Bioengineering* 99, 448–456 (2005).
23. Barbas, C. F., Kang, A. S., Lerner, R. A. & Benkovic, S. J. Assembly of combinatorial antibody libraries on phage surfaces: the gene III site. *Proceedings of the National Academy of Sciences of the United States of America* 88, 7978–7982 (1991).
24. Simmons, L. C. *et al.* Expression of full-length immunoglobulins in Escherichia coli: rapid and efficient production of aglycosylated antibodies. *Journal of Immunological Methods* 263, 133–147 (2002).
25. Sheets, M. D. *et al.* Efficient construction of a large nonimmune phage antibody library: the production of high-affinity human single-chain antibodies to protein antigens. *Proceedings of the National Academy of Sciences of the United States of America* 95, 6157–6162 (1998).

26. de Haard, H. J. *et al.* A large non-immunized human Fab fragment phage library that permits rapid isolation and kinetic analysis of high affinity antibodies. *Journal of Biological Chemistry* 274, 18218–18230 (1999).

27. Mullaney, B. P., Pallavicini, M. G. & Marks, J. D. Epitope mapping of neutralizing botulinum neurotoxin A antibodies by phage display. *Infection and Immunity* 69, 6511–6514 (2001).

28. Krebs, B. *et al.* High-throughput generation and engineering of recombinant human antibodies. *Journal of Immunological Methods* 254, 67–84 (2001).

29. Chu, R. *et al.* Redesign of a Four-helix Bundle Protein by Phage Display Coupled with Proteolysis and Structural Characterization by NMR and X-ray Crystallography. *Journal of Molecular Biology* 323, 253–262 (2002).

30. Perl, D., Mueller, U., Heinemann, U. & Schmid, F. X. Two exposed amino acid residues confer thermostability on a cold shock protein. *Nature Structural & Molecular Biology* 7, 380–383 (2000).

31. Deperthes, D. Phage Display Substrate: A Blind Method for Determining Protease Specificity. *Biological Chemistry* 383, 1107–1112 (2002).

32. Fernandez-Gacio, A., Uguen, M. & Fastrez, J. Phage display as a tool for the directed evolution of enzymes. *Trends in Biotechnology* 21, 408–414 (2003).

33. Tanaka, F., Lerner, R. A. & Barbas, C. F. Reconstructing aldolase antibodies to alter their substrate specificity and turnover. *Journal of the American Chemical Society* 122, 4835-4836 (2000).

34. Tanaka, F. & Barbas, C. F., III. Phage display selection of peptides possessing aldolase activity. *Chemical Communications* 8, 769–770 (2001).

Chapter,2

Developing,peptide,inhibitors,of,DXS

Abstract

The non-mevalonate pathway (MEP/DOXP pathway) is an essential cellular pathway in all higher eukaryotes and some bacterial species. Many important human pathogens like malarial protozoa and tuberculosis bacteria use the non-mevalonate pathway for the synthesis of isoprenoids. DXS is one of the enzymes involved in this alternative pathway that is essential for the pathogens but it is fully absent in humans. These characteristics make it an ideal target for the development of antibacterial agents. In this chapter, we describe the use of phage display for the selection of an aptamer able to inhibit DXS. This represents the first step toward the development of new antibacterial peptides.

2.1 - Introduction

Bacterial infections are ubiquitous in nature and one of the major causes of death across the world. In addition to loss of life, these infections produce morbidity that directly affects the individual but indirectly the economy of the nation. Owing to this, most of the African nations are fairly poor on almost all indices of growth and prosperity. Furthermore, infectious bacteria like *Mycobacterium tuberculosis* parasitize immune-compromised individuals, including human immunodeficiency virus (HIV) affected patients, with lethal consequences.[1,2] Mortality rates are similarly increased by malarial parasites, especially in resource-poor nations. These factors, combined with various shortcomings like lack of compliance, over-dosing, under-dosing, misuse and abuse of antibiotics have become major reasons for recent emergence of multidrug resistant bacteria. These strains are resistant to most of the available antibacterial drugs.[3] This can only be prevented by proper dispensing and dosing of antibacterial agents. However, there is also an urgent need to develop new agents or variants of existing antibacterials to tackle multidrug-resistant pathogens.

An antibacterial agent needs to possess specific properties that make it suitable for treating infections. The drugs should be effective, potent, and should cause no side effects. Further, these agents should be selectively toxic to the target organism at the same time being absolutely safe for the patient. For instance sulfonamide antibiotics specifically inhibit the sysnthesis of folic acid in targeted bacteria that leads to cessation of DNA and RNA synthesis and bacterial growth inhibition. At the same time, sulfonamides do not induce this effect in humans or animals. This property of sulfonamides has made it one of the most succesful antibacterials that is still prescribed in its original form since its development more than five decades ago. To develop antibiotics able to harm bacteria but not humans, it is therefore necessary to determine a proper target first.

One such promising target is the non-mevalonate pathway or 2-C-methyl-D-erythritol 4-phosphate/1-deoxy-D-xylulose 5-phosphate pathway (MEP/DOXP pathway; Figure 1),

which is an essential cellular pathway in all higher eukaryotes and some bacterial species.[4]

The group leaded by Prof. Anna Hirsch at the University of Groningen is actively working on finding drugs able to target this patway. The current work is a collaborative effort between the Herrmann group and the laboratory of Anna Hirsch.

2.1.1 - The MEP pathway

The MEP pathway (Figure 1) produces isopentenyl pyrophosphate (IPP) and dimethylallyl pyrophosphate (DMAPP) that are required for the synthesis of biomolecules, which are involved in important cellular activities like protein anchoring, protein prenylation, cell membrane maintenance, hormone synthesis, and N-glycosylation.

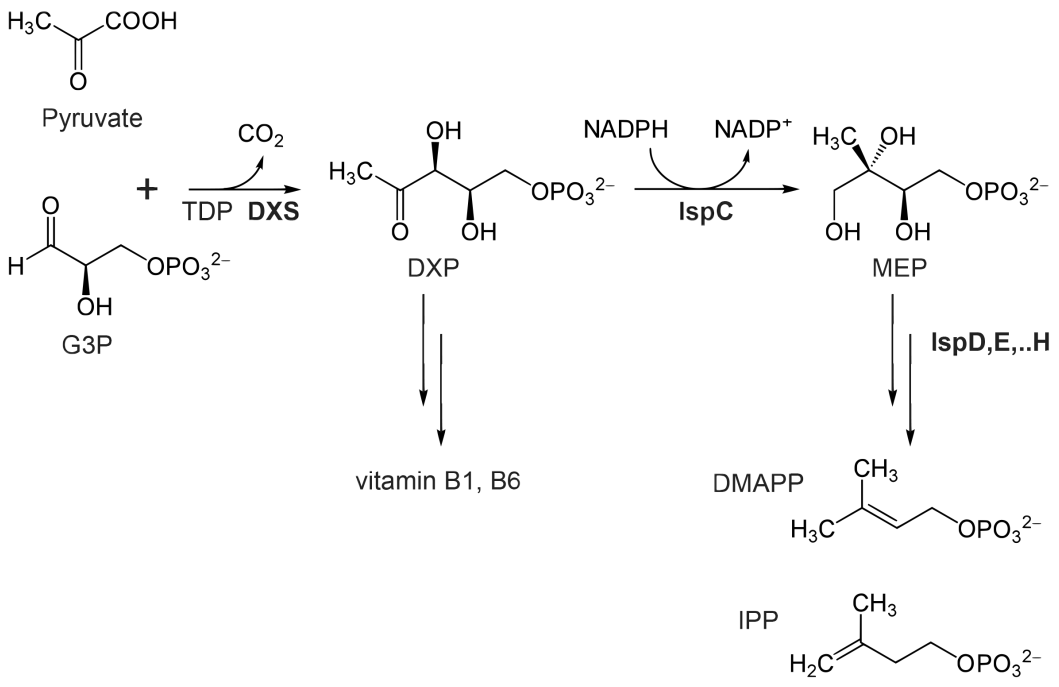

Figure 1. ***The MEP (2-C-methyl-D-erythritol-4-phosphate) pathway for the synthesis of isopentenyl diphosphate (IPP).*** *The first step, the condensation of pyruvate and glyceraldehyde 3-phosphate (G3P) to 1-deoxy-D-xylulose-5-phosphate (DXP) is catalysed by DXS. DMAPP = dimethylallyl pyrophosphate, TDP = thiamine diphosphate.*

Owing to the significance of the MEP pathway in the survival of human pathogens, research has been conducted towards exploring the possibility of selectively targeting this pathway for therapeutic applications. Specifically, the enzyme isopentenyl diphosphate isomerase (IPP isomerase) was found to be a suitable target in bacterial pathogens.[4] Medicinal chemists have high hopes of success in developing selectively toxic agents against these targets as this pathway has been genetically validated to be absent in humans[5,6] but critical for the existence of numerous pathogens, including *M. tuberculosis*[7] and *P. falciparum*[8], both of which kill over two million individuals in addition to morbid effects on another 200 million individuals every year. Humans exclusively utilise the alternative mevalonate pathway for the synthesis of IPP and DMAPP.[9,10] This is crucial in developing highly selective agents with minimal toxic effects in humans.[11]

The parallel research on crystal and co-crystal structures of the enzymes of the MEP pathway that are being deposited regularly in the Protein Data Base (PDB),[4,12]have fuelled the discovery of specific inhibitors. Among these agents, fosmidomycin–inhibitor for IspC has become the most promising agent as it has all the properties that make a good antibacterial. This is the reason behind its extensive clinical investigation.[13]

2.1.2 - DXS

Among the enzymes involved in the MEP pathway, 1-deoxy-D-xylulose-5-phosphate synthase (DXS) catalyses the rate-limiting step of TDP-dependent decarboxylative condensation of pyruvate and D-glyceraldehyde 3-phosphate to 1-deoxy-D-xylulose-5-phosphate (Figure 1). In addition to the MEP pathway, DXS is involved in pyridoxal phosphate and thiamine biosynthesis in many bacteria, which would qualify DXS inhibitors a triple-edged sword. However, despite this appeal, DXS is the least-studied enzymes of the MEP pathway as indicated by the availability of only two structures in the Protein Data Bank (PDB entries:2O1S, from *Escherichia coli* and 2O1X (Figure 2) from *Deinococcus radiodurans*)[14] both of which are from non-pathogenic bacteria. Furthermore, research on the development of DXS inhibitors is difficult with very few agents targeting

this enzyme reported in the literature (Figure 3). Most of these reports provide limited information on the structural features of DXS.[15-17]

Among the known agents, a pyruvate-competitive inhibitor belonging to the class of phosphonates (*compound 4*, Figure 3) has a micromolar K_i value against *M. tuberculosis* DXS with remarkable selectivity over mammalian TDP-dependent enzymes.[18,19] Furthermore, *compound 11* was reported to posses moderate inhibitory activity against *D. radiodurans* DXS (IC_{50} = 595 μM) by Hirsch and co-workers [20]. This group also validated its binding modes in liquid phase using nuclear magnetic resonance techniques.

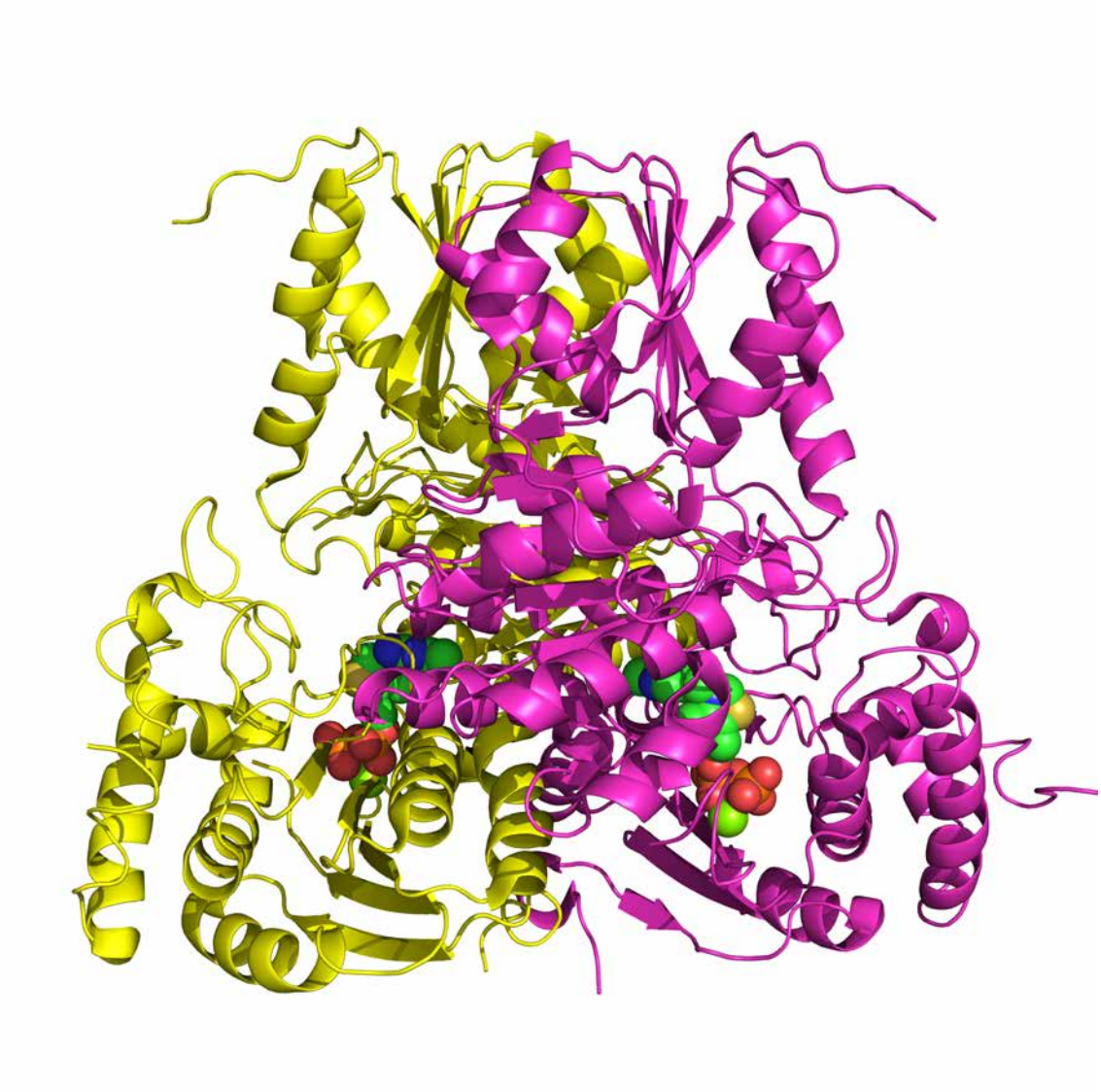

Figure 2. ***Structure of DXS dimer from Deinococcus radiodurans.*** *PDB entry 2O1X rendered as cartoon model using two colors to distinguish the monomers. TDP and Mg^{2+} ions in the active site are rendered as space-fill models.*

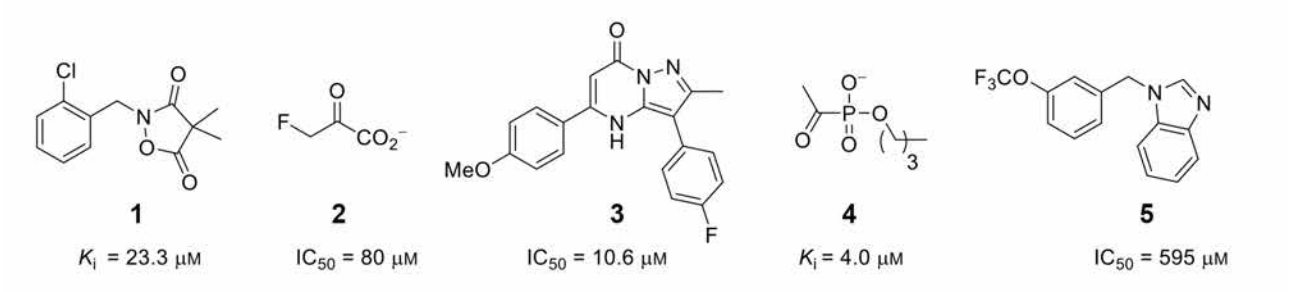

Figure 3. ***DXS inhibitors.*** *As reported in the literature with their respective IC_{50} values.*

2.1.3 - Peptides as enzyme inhibitors

All the reported DXS inhibitors are small organic molecules. No peptide DXS inhibitors have been developed, even though it has been shown that peptides can be effectively selected to bind functional sites of target enzymes with high specificity.[21-23] Moreover, peptides have few advantages over small organic molecules that encouraged medicinal chemists to reconsider their potential as drug candidates. For example, the risk of systemic toxicity associated with their administration is reduced and thanks to their short half-life, they do not tend to accumulate in tissues, with a reduced risk of complications caused by their metabolites.

Peptides are among the oldest and best known enzyme inhibitors[24] and play vital roles in all cellular activities as regulatory elements[25-28], signal molecules[29], and biological poisons.[30-32] Peptides have been extensivey studied with numerous applications developed during the past 25 years especially as enzyme inhibitors[33,34] and antiviral agents.[35-39] They work with different modes of inhibition, which provides an option to use multiple inhibitors to target different sites on the same enzyme and block its activities by interference with the enzyme-substrate active site, the allosteric regulatory sites, or even by altering the surface properties of the enzymes to affect their solubility. [33,34,40,41]

2.1.4 - Selection strategy

Combinatorial peptide libraries have been used as a source of ligands for a variety of macromolecules and different methods are known to select high-affinity binders from such libraries. In this study, phage display, one of the most efficient and cost-effective methods to select peptide binders,[42] was used as the method of choice for screening of peptide libraries to select DXS inhibitors employing *D. radiodurans* DXS as target. The phage display selection was done using a two-step protocol (Table 1).

	Phage Display I	**Phage Display II**
Library	X12GGGS	XSSX9GGGS
Competitors	None	Wild-type M13
Rounds I and II		
Target	Desthiobiotin-DXS	His-tag-DXS
Solid support	Streptavidin-coated beads	Nickel-coated beads
Eluent	Biotin	TDP
Round III		
Target	His-tag-DXS	not performed
Solid support	Nickel-coated beads	not performed
Eluent	Imidazole	not performed

Table 1. ***Overview of the two-step protocol for the selection of DXS inhibitors.*** *The first phage display consisted of three rounds of selection using the commercial library Ph.D-12, where streptavidin-bound DXS target was used for the first two rounds followed by nickel-bound target for the last round. In the second phage display, two rounds of selection were carried out using a custom-made library with nickel beads displaying immobilized DXS targets. The eluent used during the first display is meant to elute the target from the beads while the one used during the second one specifically competes with peptides interacting with the enzyme's active site.*

In the first step, the complexity of the library was narrowed down by selecting DXS-binding peptides with low inhibitory activity. In the second step, specific active-site-

binding peptides were selected by deep screening of the library using a Darwinian evolution process. The interaction between a phage library and a target occurs in solution or on a solid support during the incubation step. Aftewards, the target needs to be separated from the solution so that the phages that interact with the target can be retained while the ones with no affinity to the targed are discarded.

A common problem with the selection process employed is that the phages can interact with the solid support that may lead to selection of support-binders over target-binders. Considering this limitation, we used two types of magnetic beads and several elution buffers to avoid background-selection bias.

In our first selection, we screened a fully random M13 bacteriophage peptide library to specifically detect sequences, which are able to bind any part of the surface of DXS.

A new library was constructed based on the analysis of the selected peptides during the first step. This stringent library was used for the second phage display step, to select aptamers that specifically bind the active site of the enzyme. TDP was used as a competitive eluent to explicitly drive the selection process towards active-site-specific binders. Also, since nonspecific binders can be retained after the second round of phage display selection, wild-type M13 was co-incubated with the library. Wild-type phages efficiently compete with the nonspecific binding sites. Further, these can be easily filtered out during post-selection sequencing analysis, yielding a highly reliable set of inhibitors decreasing the probability of selecting unspecific binders or false positives.

2.2. Results and Discussion

2.2.1 - Phage Display I

A commercially available M13 library PhD-12 (NEB E8111L) was used for initial selection against DXS. After three rounds of panning, a small sample of the elute was sequenced using the Sanger method. The sequencing-data analysis showed clear evidence of selection as several sequences were repeated indicating their enrichment (Table 2).

Sequence	ID	Sequence	ID
PVNKQHTSLQNN	**P1**	ERLMTPPKLFRN	NA
TAELYPDLQSSQ	**P2**	MTHKQMHKHHGL	NA
DDTYPSRPVYLK	NA	LVSLTPPWINVD	NA
DLYLSHGAPPQH	NA	SSAQMNLNTFLN	**P13**
HVTHNITNESNS	NA	ELQIGSWRMPPM	NA
ARMTFSQMSPHT	NA	LGSHNIRLGEGS	NA
TGSIRPKLHASP	NA	YPHPIRQNFFAY	NA
MSSRSRPHINSL	**P3**	KSHTENSFTNVW	NA
QLARMSSLHVPM	NA	KLPPMNSDSMVW	NA
EDARRPPTSTEH	**P4**	HMNAHLTFQSAI	NA
SHEISRITAVSK	NA	DAVKTHHLKHHS	NA
VDMVTKQLLEYP	NA	VNHEYKLHSIKY	NA

Table 2. ***Peptide sequences selected after phage display I****. Peptide sequences were generated by translating the sequenced DNA considering the "amber mutation" wherein the codon TAG was translated with the amino acid Q. Repeated sequences are highlighted in color. Sequences in bold were subjected to in-vitro biochemical evaluation against D. radiodurans DXS. Peptide IDs (P1, P2, P3, P4) are assigned to the tested sequences.*

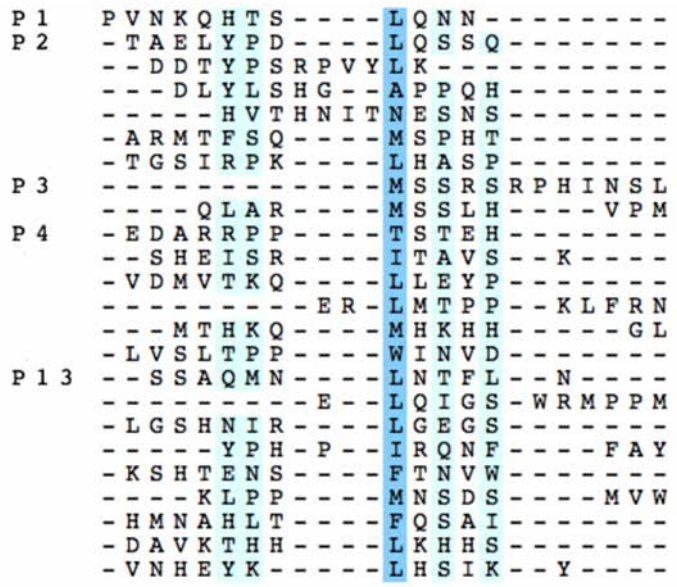

Figure 4. *Sequence alignment of the peptides selected in the first step. The software Kalign (http://msa.sbc.su.se/cgi-bin/msa.cgi) was used to perform the alignment. No common motif was detected. The alignment is visualised using the software specific option "Color by Conservation" that highlights the conserved residues with a range from white (no conservation) to dark blue (conserved).*

We took the four most prevalent sequences (P1−P4, Table 2) and tested the chemically synthesized peptides for their inhibitory activity against *D. radiodurans* DXS.

2.2.2 - Biochemical evaluation of selected peptides - I

DXS catalyzes the rate limiting step of TDP-dependent decarboxylative condensation of pyruvate and D-glyceraldehyde 3-phosphate to 1-deoxy-D-xylulose-5-phosphate. In the MEP pathway, this reaction is immediately followed by the conversion of 1-deoxy-D-xylulose-5-phosphate into 2-C-methyl-D-erythritol-4-phosphate mediated by IspC and with NADPH as proton donor.

Since neither D-glyceraldehyde 3-phosphate nor 1-deoxy-D-xylulose-5-phosphate absorb or emit photons in the UV/Vis range, the direct measurement of DXS activity via spectrophotometric assay is not possible. However, the next step of the MEP pathway

results in the conversion of NADH to NAD^+. Both strongly absorb ultraviolet light at different and well resolved peacks, 259 nm for NAD^+ and 340 nm for NADH. As a conseguence, a two enzymes assay was employed to determine the activity of DXS (the first enzyme) by calculating the consumption of NADPH using IspC as an auxiliary enzyme. This is an indirect assay as the activity of a second enzyme (IspC) is measured and linked to the activity of the target enzyme (DXS). However, since the formation of 1-deoxy-D-xylulose-5-phosphate is the rate-limiting step, the rate of consumption of NADPH can be directly employed to estimate the activity of DXS. Ideally, all peptides should have been dissolved in the same buffer. However, some of the peptides were poorly soluble in water, which necessiated the use of dimethyl sulfoxide (DMSO) as cosolvent for such peptides. Peptides P1 and P2 were dissolved in DMSO and peptides P3 and P4 were dissolved in water and their *D. radiodurans* DXS inhibition was monitored photometrically at 340 nm. To not miss out on potential slow binders, we investigated the influence of incubating the peptides with *D. radiodurans* DXS in Tris-HCl buffer (pH = 7.6) for 30 hours both at room temperature and at 4 °C. Given that the activity of the enzyme is unchanged in the presence of up to 3% of DMSO, we performed both the direct measurements and the incubation studies with 2.5% of DMSO.

Pept.ID	Solvent	Percentage of inhibition
P1	DMSO	30% at 1000 μM[a]
P2	DMSO	50% at 1000 μM[a]
P3	H_2O	47% at 250 μM[a]
P4	H_2O	30% at 1000 μM[a]

Table 3. ***List of peptides selected from the first phage display and their inhibitory activities against D. radiodurans DXS.*** *P1–P4 are amidated at the C-terminus . [a] Values obtained after pre- incubation of the peptide in Tris-HCl buffer (pH = 7.6) with D. radiodurans DXS for 30 hours at room temperature and/or at 4 °C.*

The best results were obtained for P2 (50% of inhibition at 1000 μM after 30 hours incubation at 4 °C) and particularly P3 (47% of inhibition at 250 μM, after 30 hours incubation at room temperature) (Table 3). Both P2 and P3 contain two adjacent Ser residues in the sequence: this Ser-Ser motif might function as a fingerprint for the recognition of the TDP-binding pocket of *D. radiodurans* DXS.

This prediction was further supported by preliminary docking studies (Figure 5). The analysis of docking experiments showed that the active site for peptide docking is close to the two serine residues that interact with a region of DXS lying in close proximity to the TDP-binding site.

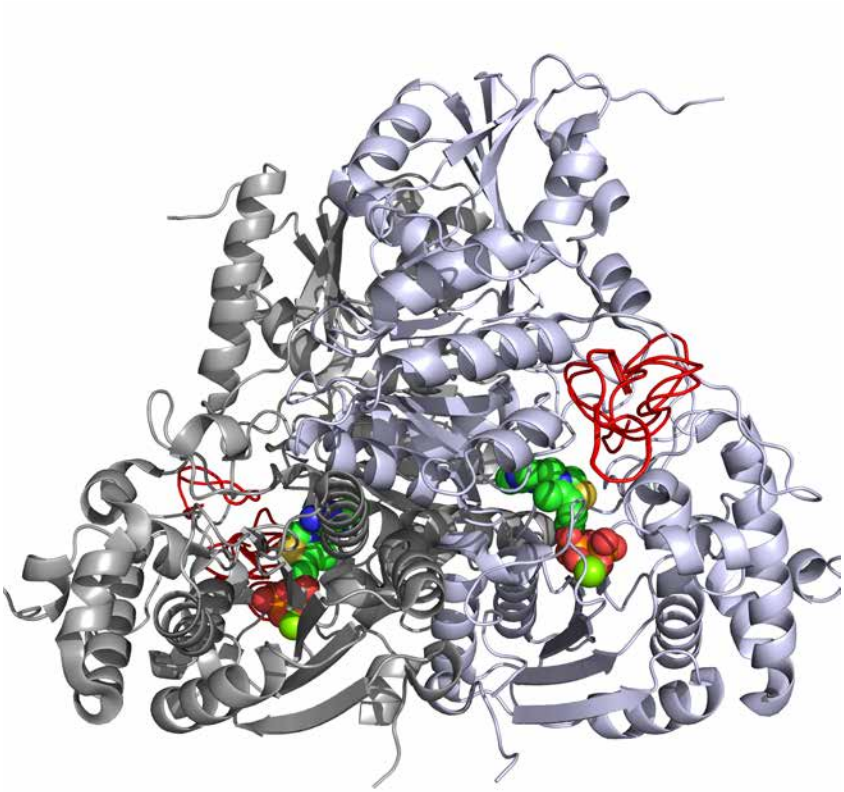

Figure 5. ***Docking of peptides on DXS.*** *Several peptide conformers (in red) were docked on the same DXS (PDB 2O1X, cartoon representation in grey, TDP as space space-filling model). For some peptides, like the one depicted (P3), the best conformers resulted in proficient docking in proximity to the enzyme's active site.*

Although these resuts are yet to be supported by crystallography, they are useful in visualizing the interaction of peptides and DXS. A clear understanding of the reltionship

between the size of the target enzyme, its active site and the selected peptides is also essential for further development of inhibitors. Though not deterministic, computer-based folding and docking models of small petpides provides an opportunity for gaining further structural insights on how both partners interact. Figure 5 shows the computer-generated models obtained by in-silico docking of folded petides and DXS struture obtained by X-ray crystallography.

2.2.3 - Phage Display II

We performed a second phage-display selection protocol using a custom-made library taking into account the Ser-Ser motif (see experimental section for further details). The procedure was similar to that explained in the first step but in this case DXS was incubated simultaneously with phages from the new library, phages from the original PhD-12 library were added to increase sequence complexity and wild-type phages were supplemented to screen for non-specific binders. The eluted phages were identified through Sanger sequencing after the selection (Table 4).

Important observations were that the peptide ALWPPNLHAWVP was a contaminant that was detected several times and seems to bind non-specifically; the peptide P12 (MAIPTRGKMPQY) was sequenced several times as it may be a DXS binder that was not identified during the first phage display step; and the peptides KAIRTRGKRPQY and THPSTKVPGTPA were found only once so they may be contaminants rather than real binders.

Focusing on the sequences containing the serine motif, we can see that some of them are repeated, *e.g.* P9, while others are not repeated but contain some recurrent motifs like the presence of extra serine residues and multiple aromatic amino acids within the sequence (in bold and underlined in Table 4).

Sequence	Library	Pept.ID
YSSTI**Y**TPTAVG	Custom	**P5**
GSSLL**YS**G**S**GPA	Custom	**P6**
SSSPVA**W**ALAMR	Custom	**P7**
DSS**S**GL**Y**LRPL**S**	Custom	**P8**
HSSPVQTD**W**ITV	Custom	**P9**
HSSPPFP**W**LLVT	Custom	**P10**
VSS**S**I**F**PIALPD	Custom	**P11**
MAIPTRGKMPQY	PhD-12	**P12**
ALWPPNLHAWVP*	PhD-12	NA
KAIRTRGKRPQY	PhD-12	NA
THPSTKVPGTPA	PhD-12	NA
ASSVI**S**PR**W**LL**W**	Custom	NA
DSST**W**L**F**L**SSY**R	Custom	NA
TSSAAAP**YYS**PP	Custom	NA
VSSMKGPTL**S**TN	Custom	NA

Table 4. ***Peptides selected after the second phage display step.*** *Peptide sequences were generated by translating the sequenced DNA considering the "amber mutation" wherein the codon TAG was translated with the amino acid Q. Repeated sequences are highlighted in color. Extra serines and aromatic residues are highlighted in bold. * Indicates a contaminant sequence which non-specifically recognises any protein.*

2.2.4 - Biochemical evaluation of selected peptides - II

Some of the new peptides obtained from the second phage display plus the peptide P13 coming from the first phage display were purchased from commercial sources and tested for *D. radiodurans* DXS inhibitory activity (Table 5, P5−P13). Biochemical evaluation without pre-incubation gave a successful result only for peptide P7, which had an IC_{50} of

13 ± 3 μM. All the other peptides either did not show inhibition or very weak if any; for instance peptide P10 had 30% inhibition at 1000 μM.

After accurate estimation of the peptide P7 concentration in solution using ultraviolet spectrophotometry on the basis of its single tryptophan residue, the IC_{50} value was recalculated to be 9.5 ± 2 μM. Considering the observation from the first step that the peptides in DMSO show higher activity at lower temperatures and those in water are active at ambient temperature, incubation experiements were conducted for all the peptides using the best possible conditions. The peptides P5 and P6 produced a weak inhibition of 30% and 47%, respectively at 1000 μM after incubation for 30 hours at 4 °C. The in vitro *D. radiodurans* DXS inhibition activity of peptide P7 was confirmed through the biochemical assay; however, the incubation period had no apparent influence on its inhibitory potential. The peptide P13 was inactive during direct measurements; however, on incubation at 4° C for 30 hours, its IC_{50} was 49 ± 11 μM.

Pept.ID	Solvent	IC_{50} (μM)
P5	DMSO	>1000
P6	DMSO	>1000
P7	H_2O	**13 ± 3 (9.5 ± 2.0)[a]**
P8	H_2O	>500
P9	H_2O	>500
P10	DMSO	>1000
P11	DMSO	>1000
P12	H_2O	>1000
P13	DMSO	**49 ± 11[b]**

Table 5. ***List of peptides selected from the second phage display and their respective D. radiodurans DXS inhibitory activities.*** *P5–P13 are not amidated at the C-terminus. [a] The value in parentheses corresponds to the re-calculated IC_{50} value based on the concentration of the peptide determined by absorbance, as described in the Experimental Section. [b] IC_{50} values obtained after pre-incubation of the peptide in Tris-HCl buffer (pH = 7.6) with D. radiodurans DXS for 30 hours at room temperature and/or at 4 °C.*

Unfortunately, owing to the absence of either tryptophan or tyrosine residues, it was not possible to determine the accurate solution concentration of peptide P13 by absorbance measurements. Comparison of the sequences of the two best peptides P7 and P13, a C-terminal serine motif was found to be a striking similarity. It is likely that this motif underlies the DXS inhibitory effect. It must be also noted that the serine motif is located at the C-terminus of the sequence. Furthermore, peptides bearing a different amino acid at the C-terminus, preceding the serine motif (e.g., P5, P6, P8), had either a very weak or no *D. radiodurans* DXS inhibition properties.

The biochemical assays were based on the measurement of the second enzyme of the MEP pathway, the DOXP reductase (IspC). It was possible to use this auxiliary enzyme as it produces a UV-detectable product during catalysis. In particular, the rate of NADPH consumption by IspC was monitored for this assay. The use of a coupled spectrophotometric assay requires a follow-up assay with the auxiliary enzyme, IspC. Therefore we tested P7 for its inhibitory potency against *E. coli* IspC and found that it has an IC50 value of 490 ± 60 μM. The fact that P7 acts both as an inhibitor of DXS and of IspC can be considered an advantage. In fact, the possibility of targeting multiple enzymes of the MEP pathway with one compound looks very appealing for the development of novel drugs, potentially less prone to the emergence of drug resistance.[5]

2.2.5 - Rationalization of the binding mode – *Alanine scanning*

Comparing the sequences of the two most successful peptides, P7 (containing a Ser-Ser-Ser motif) and P13 (containing a Ser-Ser motif), it is clear that the Ser residues at the N-terminus are essential for their inhibitory potency. In fact, peptides bearing a different amino acid at the N-terminus, right before the Ser motif, (e.g., P5, P6 and P8), display no inhibition or very weak inhibition of *D. radiodurans* DXS.

To elucidate the contribution of each amino acid residue, we performed alanine scanning of P7, which displays low micromolar activity against *D. radiodurans* DXS also without pre-incubation. Nine peptides (P7b−l), obtained by serial substitution of any non

Ala residue with an Ala, were purchased and tested *in vitro* against *D. radiodurans* DXS without pre-incubation (Table 6). Moreover, to understand the influence of the free C-terminus in particular, the peptide P7 with a C-amidated terminus (P7a) was also tested.

ID	Sequence	Solvent	IC_{50} (μM)
P7 (ref)	SSSPVAWALAMR	H_2O	13 ± 3
P7 (ref)	SSSPVAWALAMR	DMSO	93 ± 17
P7a	SSSPVAWALAMR-$CONH_2$	H_2O	>300
P7b	**A**SSPVAWALAMR	DMSO	>500
P7c	S**A**SPVAWALAMR	DMSO	>500
P7d	SS**A**PVAWALAMR	DMSO	>500
P7e	SSS**A**VAWALAMR	DMSO	43 ± 13
P7f	SSSP**A**AWALAMR	H_2O	>300
P7g	SSSPVA**A**ALAMR	DMSO	420 ± 100
P7h	SSSPVAW**A**AAMR	H_2O	250 ± 20
P7i	SSSPVAWALA**A**R	H_2O	170 ± 20
P7l	SSSPVAWALAM**A**	DMSO	47 ± 13

Table 6. ***Results of the alanine scanning of P7.*** *Upon replacing the proline at the fourth position with an alanine, the inhibitory activity was improved, indicating that a small hydrophobic residue at this position is important for its activity. However, rigidity due to proline can hinder the interaction between P7 and D. radiodurans DXS.*

Given that some derivatives of P7 were insoluble in water even at very low concentrations, they were tested in DMSO. The peptide P7 was tested in DMSO to have a reference for its inhibitory activity in both solvents. We verified the activity of this peptide on *D. radiodurans* DXS by using a direct NMR-based assay in which the reaction velocity of DXS was evaluated by monitoring the appearance of the product of the reaction DXP, resulting in an IC_{50} value of 92 ± 17 μM.

Replacement of one of the three serine residues at the C-terminus of P7 (derivatives P7b−d) resulted in a dramatic loss of the inhibitory activity. Amidation of the C-terminus (P7a) produced the same result. Taken together, these results suggest that a non-amidated SSS motif at the C-terminus of the peptide chain plays an essential role in the protein-recognition process and in the inhibitory activity observed for peptide P7. Modification of the first residue at the N-terminus provides room for improvement of the inhibitory potency of peptide P7 while amidation of the C-terminus (P7a) resulted in a complete loss of the inhibitory potency (IC_{50} > 300 μM). The presence of an alanine rather than an arginine (P7l) almost doubled the inhibitory potency. This suggests that different, small hydrophobic residues might be suitable in this position to improve the inhibitory potency of peptide P7. Moreover, we noticed that the replacement of the hydrophobic core of the peptide, up to the C-terminus (P7f−i) leads to a loss in inhibitory activity. In general, replacement of the hydrophobic core of the peptide, up to the N-terminus leads to 10-20 fold loss of inhibitory activity. Even the presence of Ala instead of Val or Leu (P7f and P7h, respectively) causes substantial loss in activity (P7f: IC_{50} > 300 μM; P7h: IC_{50} = 250 ± 20 μM), showing how important inter- or intramolecular hydrophobic interactions seem to be for the inhibitory activity of P7.

2.3. Conclusions

In this chapter, the succesful identification of the first peptide inhibitor for the MEP pathway's first rate-limiting enzyme DXS is reported. DXS is a suitable target as it is also involved in vitamin B1 and vitamin B6 biosynthesis. However, it has not been intesively explored as a target for antibacterial drug discovery as indicated by the availability of only a few small organic DXS inhibitors. The phage display selection helped in the rapid identification of efficient peptide DXS inhibitors with a comparable activity to the best available small organic molecules. Furthermore, using alanine scanning, the significance of the N-terminal serine-rich motif was revealed. In this way, we were able to bypass the need for crystallography. However, we would like to note that the findings of the present work are just the first step in a promising development of peptide inhibitors as new generation antibacterials. Further studies are required involving optimisation of the binding affinity and delivery process of the peptide to achieve desired levels of *in vivo* DXS inhibition.

2.4. Final notes

A few months after having written this chapter, new results came from collaborators in the Hirsch group that are investigating the activity of the discovered peptides. Last updates (data not shown), report a sharp decrease in the inhibitory activity when the peptides are added to the enzyme in presence of 1% Triton-X, suggesting that the peptides may form aggregates, lately confirmed also by TEM images (data not shown).

These last results are now calling into question the mechanism of inhibition as well the specificity toward the target. This fact underlines once more the challenges hidden behind the selection of a proper inhibitor and its validation.

2.5. Experimental section

Media and solutions

Liquid Broth (LB) Medium

10 g of Bacto-Tryptone, 5 g yeast extract and 5 g NaCl were mixed in ultra-pure water to prepare a volume of one liter. The solution was autoclaved and stored at room temperature.

Tetracycline Stock

20 mg/mL of Tetracycline hydrochloride was dissolved in 70% ethanol and stored at –20°C. This solution was vortexed before each use.

IPTG/Xgal

1.25 g of IPTG (isopropyl-β-D-thiogalactoside) and 1 g of Xgal (5-bromo-4-chloro-3-indolyl-β-D-galactoside) were mixed in 25 mL of DMF (dimethyl formamide) and stored at –20°C.

LB/Tet/IPTG/Xgal Plates

15 g of agar was added to prepare one liter of LB medium. The solution was autoclaved and cooled below 55°C. Then, 1 mL of Tetracycline stock and 1 mL of IPTG/Xgal stock were added per liter. The solution was mixed gently and poured into petri dishes. The plates were allowed to dry for 30 minutes and stored at 4°C in the dark till used.

SOC Medium

0.5 mL of 2M $MgCl_2$ and 2 mL of 1M glucose (both sterile) were added to 100 mL of LB medium and stored at 4°C.

Phosphate Buffered Saline (PBS)

A solution of 50 mM sodium phosphate and 150 mM of NaCl was prepared and pH was adjusted to 7.5. The solution was stored at room temperature after autoclaving.

PEG/NaCl Solution

A solution of 20% (w/v) polyethylene glycol–8000 and 2.5M NaCl was prepared and autoclaved. This was mixed well while still warm to combine separated layers and filtered. The solution was stored at room temperature until further use.

Bacterial strain

The cloning and expression of the phage library, titering and inoculation of the sequencing plates was conducted using *E. coli* ER2738 (NEB E4104S) (Genotype: *F´proA+B+ lacIq Δ (lacZ) M15 zzf::Tn10 (TetR)/ fhuA2 glnV Δ (lac-proAB) thi-1 Δ (hsdS-mcrB) 5)*. The ER2738 is a male *E. coli* in which the F´can be selected for by using tetracycline in the growth medium. This strain allows Blue/White screening and it is an amber mutant strain.

Expression and purification of *D. radiodurans* DXS

Gene expression and protein purification of *D. radiodurans* DXS were performed as described in earlier literature.[15] Briefly, E. coli BL21 (DE3) carrying the HisTag-DXS expressing vector pET22b-H6TEVEKDRDXS was inoculated into LB medium and supplemented with ampicillin (100 mg/mL). This mixture was incubated in a shaking flask at 37° C until OD_{590} of 0.4 was reached. Expression of DXS was initiated by adding IPTG at a final concentration of 0.5 mM, and the culture was further incubated at 20° C for 20 h. Cells were harvested, resuspended (5 mL per 1 g of cells) in 50 mM Tris-HCl pH 8.0 supplemented with 300 mM NaCl, 15 mM imidazole and 0.02% NaN_3 (buffer A) and disrupted using a French-Press. The cell debris was removed by centrifugation, and the supernatant was loaded to a Ni-chelating sepharose column (1 cm x 15 cm) equilibrated with buffer A. The retained proteins were eluted with imidazole and resuspended in buffer B (50 mM Tris-HCl pH 8.0, 100 mM NaCl, 5 mM DTT, 0.02% NaN_3) using desalting

column HiPrep 26/10 (GE Healthcare) and finally concentrated to 19 mg/mL using Amicon Stirred Ultrafiltration Cell (Amicon) equipped with polyether sulfone ultra-filtration membrane (pore size 10 kDa, Pall Life Sciences). Aliquots were frozen at −80° C for long-term storage. Isolated and purified DXS showed no measurable DXS activity unless enough external TDP was added.

General M13 protocols

To avoid contamination with environmental bacteriophages, all the procedures described were performed under a sterile flow bench. Disposable gloves and aerosol-resistant micropipette tips were used to avoid contaminants. Throughout the study, a single phage M13KE derived from the common cloning vector M13mp19 was used to avoid deviations. It carries the lacZα gene, which will turn blue infected colonies of *E. coli* ER2738 when plated in Xgal and IPTG containing media. This differentiates environmentally derived phages, which typically yield colorless plaques.

Phage titering:

20 mL of LB supplemented with Tetracycline was inoculated with a single white colony of ER2738 grown on a LB/Tet/IPTG/XGal plate. The plates were incubated on a shaker rotating at 200 RPM at 37°C for 4-5 hours till mid-log phase ($OD_{600}\sim0.5$) growth was obtained. During the incubation phase, fresh 10 to 1000 fold serial dilutions of phages in sterile LB were prepared. 10 µl of each of these phage dilutions were used to infect 0.9 mL of ER2738 grown at mid-log phase and previously aliquoted in a sterile 2 mL round bottomed tube. The mixture was briefly vortexed and incubated at 37°C for approximately 5 minutes. The contents were poured in prewarmed LB/Tet/IPTG/XGal labeled plates and allowed to dry under a sterile flow bench followed by overnight incubation at 37°C. This procedur results in blue plaques on the plates. By multiplying the number of blue plaques by the dilution factor of the plates, the phage titer, expressed as plaque forming units (pfu) per 10 µl, is obtained.

Library amplification

20 mL of LB supplemented with Tetracycline was inoculated with a single white colony of ER2738 grown on a LB/Tet/IPTG/XGal plate. This plate was incubated on a shaking incubator (200 RPM) at 37°C for 4-5 hours till the growth reaches early-log phase (OD_{600}～ 0.05). After infection of the culture with the input phages (usually the elution fraction coming from a selection protocol), the culture was incubated at 37° C for approximately 5 minutes. Then the plates were transferred to a shaking incubator at 200 RPM set at 37° C to allow the growth for 4 hours. This stage is critical as extended incubation leads to accumulation of recombinant or wild-type M13KE phages (always present even in commercial libraries) that will interfere with the selection process.

Phage purification

The phage-production-culture was transferred into a centrifuge tube, and the cells were pelleted down by spinning for 15 minutes at 7000g at 4°C. The supernatant was transferred to a fresh tube and re-spun to remove any residual cells. The upper 80% of the supernatant was transferred to a fresh sterile tube. To this tube, $1/6^{th}$ volume of 20% PEG-8000 in 500 mM NaCl was added. The tube was incubated on ice after proper mixing for 4 hours to overnight. This allows the phage to precipitate. Following the incubation, the tubes were spun at 12,000g for 15 minutes at 4°C. The supernatant was discarded and the tube was respun followed by removal of the residual supernatant with a pipette. The phage pellet looks like a white smear on the bottom side of the tube.

After suspending the pellet in 1 or 2 mL of TBS, the suspension was filtered into a microcentrifuge tube through a syringe equipped with a 0.2 μm filter. 10 μl of this phage soultion was used for titering and the remainder was stored at 4°C. This solution was used within one week. For experiments planned over periods longer than a week, the phage suspension was diluted with sterile 50% glycerol at 1:1 ratio and stored at -20 or -80°C.

Sequencing

All the sequences were determined by Sanger sequencing performed by GATC Biotech, Germany. The samples were shipped as ssDNA (M13 genome) or as M13-infected *E. coli* colonies. The primer p3-CS-R: GTACAAACTACAACGCCTGT, a M13 specific custom primer was used for all the sequencing. All the peptide sequences were predicted by translating the sequenced DNA considering the "amber mutation" wherein TAG was translated as glutamine (Gln, Q).

Sequence alignment

The translated sequences were converted to FASTA format and aligned using the software Kalign2[43,44] available at the Stockolm Bioinformatic Center website (http://msa.sbc.su.se/cgi-bin/msa.cgi). Following settings were used for the alignments: Gap open penalty 9.0; Gap extension penalty 0.85; Terminal gap penalties 0.45; Bonus score 0.0. The results were visualised using the software specific option "Color by Conservation" that highlights the conserved residues with a range from white (no conservation) to dark blue (conserved). Pale colors indicate partial conservation i.e. the chemical properties of the residues are similar without sequence correlation.

Folding and docking: 3D structures of the peptides were modeled using PEP-FOLD, a de-novo structure prediction software optimized for short peptides (9 to 36 residues).[45-47] The official server (http://bioserv.rpbs.univ-paris-diderot.fr/services/PEP-FOLD/) was used for submission of the input sequences.

The de-novo-folded peptides were docked against the crystallography-derived structure of *D. radiodurans* DXS (PDB entry: 2O1X) using PatchDock[48] available at http://bioinfo3d.cs.tau.ac.il/PatchDock/ for initial docking and FireDock[49,50] available at http://bioinfo3d.cs.tau.ac.il/FireDock/ for refining. The results were downloaded locally as PDB files and were analyzed using PyMol[51,52].

Phage Display I

The first phage display selection protocol was carried out using a commercially available M13 library (NEB E8111L) consisting of M13 phages expressing a 12aa peptide at the N-terminus of each p3 coat protein. A small linker Gly-Gly-Gly-Ser was introduced between the peptide and the coat protein to increase the degree of freedom of the protruding peptides and to minimize the contribution of the p3 protein to the overall binding. The library can be represented schematically as N-term-X_{12}-GGGS-p3-C-term.

Three rounds of selection were performed in 1 mL of PBS buffer. In each round 10^{10} phages were incubated with 1mg of His-tagged DXS in a low-protein-binding tube for 30 min on ice.

The DXS functionalized with NHS-desthiobiotin was used during round I and II, and Dynabeads MyOne Streptavidin C1 (Invitrogen 65001) were chosen to capture the enzyme from the solution during the washing steps.

During the third round MagneHis Ni-Particles (Promega V8560) were used to capture the target enzyme and in order to remove the phages selected against streptavidin during the previous rounds.

After the incubation, 0.1 mL of beads were added to the solution and mixed in a thermo-shaker for 15 minutes at 4° C, followed by insertion of the tube into a magnetic rack to facilitate adhesion of the magnetic beads on one side of the tube. Phages expressing DXS-binders were retained on the beads. The buffer with unbound phages was gently pipetted out and discarded. The unbound or weakly bound phages were further cleaned by ten times washing in 1 mL of PBST (PBS with 0.05% Tween 20), keeping the tube in magnetic rack during the process. The strongly bound phages were eluted by suspending the beads with 1 mL of elution buffer (1 mM Biotin in PBS for round 1 and 2, and 500 mM imidazole in PBS for round 3). The beads were discarded and the elution fraction was titered and amplified as described above. The finally eluted phages were used to infect a fresh culture of *E. coli* ER2738. The cells were plated on LB-agar supplemented with Tetracycline, IPTG and XGal. Blue colonies resulting from phage infection were sequenced.

Library design and cloning

A custom library was designed in order to include the motif Ser-Ser at the N-terminus of the peptides. Two oligonucleotides, one coding for the library itself and one used for cloning purpose were designed. The sequences were as shown below:

Library:

CATGTTTCGGCCGA(MNN)$_9$GGAGGAMNNAGAGTGAGAATAGAAAGGTACCCGGG

Extension Primer: CATGCCCGGGTACCTTTCTATTCTC

The first oligo (Library) codes for the reverse strand of the library and it includes two flanking regions that contain the restriction site for KpnI/Acc651 and EagI that is needed for cloning into the M13KE vector. The random part of the peptide sequence is coded by NNK codons (reverse complement of MNN) where N is any of the bases while K represents G or T (thus, M represent C or A). An NNK codon can code for all the 20 amino acids but only for one stop-codon i.e., TAG. Combining the use of NNK codons together with amber mutant strains like *E. coli* ER2738 ensures that the whole library encodes for full length peptides.

The "Extension Primer" was partially complementary with the library-coding oligo and it was used to generate the dsDNAs for cloning. The library duplex and cloning were performed as per the instructions of the manufacturer's manual (NEB E8111L).

Phage Display II

In the second phage display step, two rounds of selection were performed using a custom made phage library. This library can be schematically represented as N-term-XSSX9-GGGS-p3-C-term. Incubation was done using TBS buffer, washing was carried out using TBST (TBS with 0.05% Tween 20), proteins were recovered using MagneHis Ni-Particles (Promega V8560), and elution was achieved using 1 mM TPP in TBS. TPP was chosen to competitively elute peptides interacting with the TPP binding site on DXS.

1mg of DXS was incubated simultaneously with phages from the new library and the original PhD-12 library, added to increase the sequence complexity. Additionally, wild

type phages were added to compete with non-specific binders from the libraries. The different phage pools were mixed at 1:1:1 ratio prior to incubation with the targets.

Sequencing: Blue colonies resulting from phage infection were picked and sent for Sanger sequencing (at GATC Biotech) using the custom made primers specified above.

Biochemical evaluation of inhibitory activity

Biochemical evaluation of inhibitory activity of peptide P7 against *E. coli* IspC was performed according to standard protocol reported in the literature. [53]

Photometric assays were conducted in transparent flat-bottomed 96-well plates (Greiner Bio-One). Assay mixtures contained 100 mM Tris-HCl (pH 7.6), 4 mM $MnCl_2$, 5 mM dithiothreitol (DTT), 0.5 mM NADPH, 1.2 μM TDP, 0.5 mM sodium pyruvate, 1.0 mM glyceraldehyde 3-phosphate, 8.3 μM IspC and 0.41 μM D. radiodurans DXS.

The tolerance of DXS with respect to DMSO concentration was determined by measurement of the reaction velocity in the presence of different concentrations of DMSO. The activity of the enzyme was found to be stable in presence of up to 3% DMSO.

To determine the inhibitory activity of the peptides after incubation, solutions containing 300 μL of 100 mM Tris-HCl (pH 7.6), 0.41 μM of *D. radiodurans* DXS, and serial 1:2 dilutions of each peptide starting with 2000 μm were prepared. The peptides were solubalised either in water or DMSO as solvent. The water solutions were incubated at room temperature for 30 hours, whereas DMSO solutions were incubated at 4°C for 30 hours. After incubation, 95 μL of each solution was put into a 96-well plate, to which 47.5 μL of a buffer containing 100 mM of Tris-HCl (pH 7.6) and 2 mM of glyceraldehyde 3-phosphate were added. This step initiates the reaction. Control experiments, same conditions as describe above but without peptides, were run parallel with all the tests at similar temperatures for the same duration as the test experiments. However, no potential loss of enzyme activity was observed in any of the control experiements conducted.

The exact concentration of peptide P7 in solution was calculated using the formula:

[Peptide concentration] mg/mL = (A_{280} x DF x MW) / ε

Where A_{280} was the absorbance of the peptide solution at 280 nm in a 1 cm cell; DF was the dilution factor; MW was molecular weight of the peptide and ε was the molar extinction coefficient of Tryptophan at 280 nm (5690 $M^{-1}cm^{-1}$).

2.6 - References

1. World Health Organization. *Global Tuberculosis Report 2012*. (2012).
2. World Health Organization. *Tuberculosis control in the South-East Asia Region 2013*. (searo.who.int, 2013).
3. Wongsrichanalai, C., Varma, J. K., Juliano, J. J., Kimerling, M. E. & MacArthur, J. R. Extensive Drug Resistance in Malaria and Tuberculosis. *Emerging Infectious Diseases* 16, 1063–1067 (2010).
4. Hale, I., O'Neill, P. M., Berry, N. G., Odom, A. & Sharma, R. The MEP pathway and the development of inhibitors as potential anti-infective agents. *Medicinal Chemistry Communications* 3, 418–433 (2012).
5. Rohmer, M. The discovery of a mevalonate-independent pathway for isoprenoid biosynthesis in bacteria, algae and higher plants†. *Natural Product Reports* 16, 565–574 (1999).
6. Arigoni, D. *et al.* Terpenoid biosynthesis from 1-deoxy-d-xylulose in higher plants by intramolecular skeletal rearrangement. *Proceedings of the National Academy of Sciences of the United States of America* 94, 10600–10605 (1997).
7. Brown, A. C. & Parish, T. Dxr is essential in Mycobacterium tuberculosis and fosmidomycin resistance is due to a lack of uptake. *BMC Microbiology* 8, 78 (2008).
8. Odom, A. R. & Van Voorhis, W. C. Functional genetic analysis of the Plasmodium falciparum deoxyxylulose 5-phosphate reductoisomerase gene. *Molecular and Biochemical Parasitology* 170, 108–111 (2010).
9. Lynen, F. Biosynthetic pathways from acetate to natural products. *Pure and Applied Chemistry* 14, (1967).
10. Katsuki, H. & Bloch, K. Studies on the Biosynthesis of Ergosterol in Yeast FORMATION OF METHYLATED INTERMEDIATES. *Journal of Biological Chemistry* 242, 222–227 (1967).
11. Rodriguez-Concepcion, M. The MEP Pathway: A New Target for the Development of Herbicides, Antibiotics and Antimalarial Drugs. *Current pharmaceutical design* 10, 2391–2400 (2004).
12. Hunter, W. N. The Non-mevalonate Pathway of Isoprenoid Precursor Biosynthesis. *Journal of Biological Chemistry* 282, 21573–21577 (2007).
13. Evaluation of Fosmidomycin and Piperaquine in the Treatment of Acute Falciparum Malaria.
14. Xiang, S., Usunow, G., Lange, G., Busch, M. & Tong, L. Crystal Structure of 1-Deoxy-d-xylulose 5-Phosphate Synthase, a Crucial Enzyme for Isoprenoids Biosynthesis. *Journal of Biological Chemistry* 282, 2676–2682 (2007).
15. Hayashi, D., Kato, N., Kuzuyama, T., Sato, Y. & Ohkanda, J. Antimicrobial N -(2-chlorobenzyl)-substituted hydroxamate is an inhibitor of 1-deoxy- d -xylulose 5-phosphate synthase. *Chemical Communications* 49, 5535–5537 (2013).
16. Mueller, C., Schwender, J., Zeidler, J. & Lichtenthaler, H. K. Properties and inhibition of the first two enzymes of the non-mevalonate pathway of isoprenoid biosynthesis. *Biochemical Society Transactions* 28, 792–793 (2000).

17. Mao, J. *et al.* Structure–activity relationships of compounds targeting mycobacterium tuberculosis 1-deoxy-d-xylulose 5-phosphate synthase. *Bioorganic & Medicinal Chemistry Letters* 18, 5320–5323 (2008).
18. Smith, J. M., Vierling, R. J. & Meyers, C. F. Selective inhibition of E. coli 1-deoxy- d -xylulose-5-phosphate synthase by acetylphosphonates. *Medicinal Chemistry Communications* 3, 65–67 (2012).
19. Smith, J. M. *et al.* Targeting DXP synthase in human pathogens: enzyme inhibition and antimicrobial activity of butylacetylphosphonate. *The Journal of Antibiotics* 67, 77–83 (2014).
20. Masini, T. & Hirsch, A. K. H. Development of inhibitors of the 2C-methyl-D-erythritol 4-phosphate (MEP) pathway enzymes as potential anti-infective agents. *Journal of Medicinal Chemistry* 57, 9740–9763 (2014).
21. Hyde-DeRuyscher, R. *et al.* Detection of small-molecule enzyme inhibitors with peptides isolated from phage-displayed combinatorial peptide libraries. *Chemistry & Biology* 7, 17–25 (2000).
22. Devlin, J. J., Panganiban, L. C. & Devlin, P. E. Random peptide libraries: a source of specific protein binding molecules. *Science* 249, 404–406 (1990).
23. Glee, P. M. *et al.* Peptide ligands that bind IgM antibodies and block interaction with antigen. *Journal of Immunology* 163, 826–833 (1999).
24. Markwardt, F. in *Proteolytic Enzymes* 19, 924–932 (Elsevier, 1970).
25. Vale, W., Rivier, C. & Brown, M. Regulatory peptides of the hypothalamus. *Annual review of physiology* (1977).
26. Ghatei, M. A. *et al.* Regulatory peptides in the mammalian respiratory tract. *Endocrinology* 111, 1248–1254 (1982).
27. Wright, N. A. *et al.* Epidermal growth factor (EGF/URO) induces expression of regulatory peptides in damaged human gastrointestinal tissues. *The Journal of Pathology* (1990). doi:10.1002/path.1711620402
28. Brubaker, P. L. & Drucker, D. J. Minireview: Glucagon-like peptides regulate cell proliferation and apoptosis in the pancreas, gut, and central nervous system. *Endocrinology* 145, 2653–2659 (2004).
29. Simonson, M. S. & Dunn, M. J. Cellular signaling by peptides of the endothelin gene family. *The FASEB Journal* (1990).
30. Jimenez-Porras, J. M. Pharmacology of peptides and proteins in snake venoms. *Annual Review of Pharmacology* (1968).
31. SHAFQAT, J., BEG, O. U., YIN, S. J. & ZAIDI, Z. H. Primary structure and functional properties of cobra (Naja naja naja) venom Kunitz-type trypsin inhibitor. *European Journal of Biochemistry* 194, 337–341 (1990).
32. Shen, G. S., Layer, R. T. & McCabe, R. T. Conopeptides: From deadly venoms to novel therapeutics. *Drug discovery today* 5, 98–106 (2000).
33. Li, J. *et al.* Trypsin inhibitory loop is an excellent lead structure to design serine protease inhibitors and antimicrobial peptides. *The FASEB Journal* (2007).
34. Young, T. S. *et al.* Evolution of cyclic peptide protease inhibitors. *Proceedings of the National Academy of Sciences* 108, 11052–11056 (2011).
35. Schlesinger, M. J., Collier, N. C., Adams, S. P. Washington University. Antiviral

peptides. (1992).
36. Jenssen, H., ANDERSEN, J., Mantzilas, D. & GUTTEBERG, T. A wide range of medium-sized, highly cationic, ?-helical peptides show antiviral activity against herpes simplex virus. *Antiviral Research* 64, 119–126 (2004).
37. Bai, F. *et al.* Antiviral peptides targeting the west nile virus envelope protein. *Journal of Virology* 81, 2047–2055 (2007).
38. Slocinska, M., Marciniak, P. & Rosinski, G. Insects Antiviral and Anticancer Peptides: New Leads for the Future? *Protein and Peptide Letters* 15, 578–585 (2008).
39. Vlieghe, P., Lisowski, V., Martinez, J. & Khrestchatisky, M. Synthetic therapeutic peptides: science and market. *Drug Discovery Today* 15, 40–56 (2010).
40. Peczuh, M. W. & Hamilton, A. D. Peptide and protein recognition by designed molecules. *Chemical Reviews* (2000).
41. Stanfield, R. L. & Wilson, I. A. Protein-peptide interactions. *Current opinion in structural biology* 5, 103–113 (1995).
42. Smith, G. P. & Petrenko, V. A. Phage display. *Chemical Reviews* (1997).
43. Lassmann, T. & Sonnhammer, E. L. Kalign – an accurate and fast multiple sequence alignment algorithm. *BMC Bioinformatics* 6, 298 (2005).
44. Lassmann, T., Frings, O. & Sonnhammer, E. L. L. Kalign2: high-performance multiple alignment of protein and nucleotide sequences allowing external features. *Nucleic Acids Research* 37, 858–865 (2009).
45. Maupetit, J., Derreumaux, P. & Tufféry, P. PEP-FOLD: an online resource for de novo peptide structure prediction. *Nucleic Acids Research* 37, gkp323–W503 (2009).
46. Maupetit, J., Derreumaux, P. & Tufféry, P. A fast method for large-scale De Novo peptide and miniprotein structure prediction. *Journal of Computational Chemistry* 31, 726–738 (2010).
47. Thevenet, P. *et al.* PEP-FOLD: an updated de novo structure prediction server for both linear and disulfide bonded cyclic peptides. *Nucleic Acids Research* 40, W288–W293 (2012).
48. Schneidman-Duhovny, D., Inbar, Y., Nussinov, R. & Wolfson, H. J. PatchDock and SymmDock: servers for rigid and symmetric docking. *Nucleic Acids Research* 33, W363–W367 (2005).
49. Andrusier, N., Nussinov, R. & Wolfson, H. J. FireDock: Fast interaction refinement in molecular docking. *Proteins: Structure, Function, and Bioinformatics* 69, 139–159 (2007).
50. Mashiach, E., Schneidman-Duhovny, D., Andrusier, N., Nussinov, R. & Wolfson, H. J. FireDock: a web server for fast interaction refinement in molecular docking. *Nucleic Acids Research* 36, W229–W232 (2008).
51. DeLano, W. L. Pymol: An open-source molecular graphics tool. *CCP4 Newsletter On Protein Crystallography* (2002).
52. Delano, W. L. The PyMOL Molecular Graphics System. *(2002)* (2002). doi:10.1234/12345678
53. Masini, T. *et al.* De novo fragment-based design of inhibitors of DXS guided by spin-diffusion-based NMR spectroscopy. *Chemical Science* 5, 3543–3551 (2014).

Chapter,3

Probing,peptide,libraries,on,CB8

Abstract

Cucurbit[n]urils are macrocyclic molecules made of glycoluril (=$C_4H_2N_4O_2$=) monomers linked by methylene bridges (-CH_2-). These compounds are particularly useful as they are suitable hosts for an array of neutral and cationic species, and selectively bind specific amino acid side chains. In particular, CB8 and CB8-Methyl viologen (CB8-MV) complex can form high-affinity host-guest interactions specifically with the aromatic amino acids tryptophan, phenylalanine and tyrosine at the N-terminus. This has made CB8 an important tool for the development of recognition systems involving peptides and proteins. In this study, we perform phage display on CB8 using different types of libraries to get a better insight into the selectivity of CB8 toward different amino acids. Moreover, for the first time we report on the formation of a complex involving cyclic peptides and non-N-terminal aromatic amino acids binding in the context of CB8.

3.1 - Introduction

In recent years, supramolecular host-guest chemistry is developing into a promising method to control the interactions between biomolecules such as peptides and proteins.[1-4] In particular, the combination of macrocyclic molecules such as cucurbiturils and aromatic amino acids like phenylalanine and tryptophan have proven to be very effective to achieve dimerisation of peptides and proteins, and their functionalisation in a reversible and non-covalent fashion.[5-7] Peptide and protein dimers are important building blocks in biological processes with interesting theoretical and practical implications for materials science.[8,9] Protein dimerisation is a ubiquitous mechanism for regulation of vital biological activities of proteins including receptor clustering, signal transduction, and apoptosis.[10,11] Hence, understanding of these processes might have tremendous implications in the medical field as well. Moreover, the reversible functionalisation of enzymes opens up a whole new range of possibilities in basic biochemical research, in the separation of protein mixtures, and possibly in the diagnosis and treatment of human diseases.[12]

In this regards, pioneering work from Nguyen and collaborators[6,13] showed that control over protein dimerisation by means of an encoded peptide is feasable. This was achieved by using a very short, genetically incorporated, N-terminal phenylalanine–glycine–glycine (FGG) peptide motif and a cucurbit[8]uril molecule.

3.1.1 - CB8

Cucurbit[n]urils are macrocyclic molecules made of glycoluril (=$C_4H_2N_4O_2$=) monomers linked by methylene bridges (-CH_2-) (Figure 1). These compounds are particularly useful as they are suitable hosts for an array of neutral and cationic species.[14,15] Cucurbit[n]urils have already been shown to selectively bind specific amino acid side chains.[6,13,16]

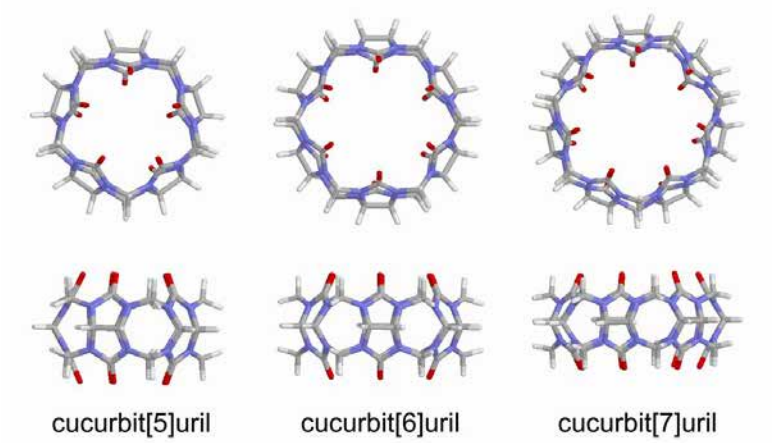

Figure 1. ***Computer models of CB5, CB6, and CB7.*** *Top row presents the view into the cavity and the bottom is the side view. ("Models of cucurbiturils" by M. Stone at English Wikipedia)*

Among this family of molecules, CB8 has become an important compound as it can simultaneously accommodate two aromatic guests[17,18] (Figure 2). The binding scope as well as its mode of binding have been extensively investigated.[16] In particular, it has been shown that CB8 and CB8-methyl viologen (CB8-MV) complexes undergo host-guest interactions with the aromatic amino acids tryptophan, phenylalanine and tyrosine.[16]

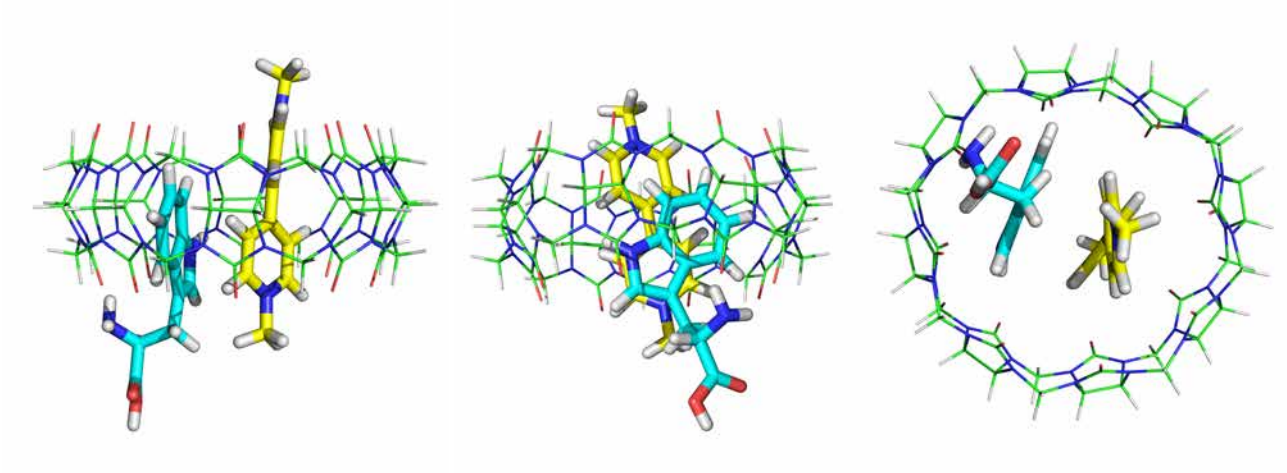

Figure 2. ***Models of CB8 complexed with MV and tryptophan.*** *CB8 is rendered as line-model and colored green, Trp and MV are rendered as stick-model and colored cyan and yellow, respectively.*

While these interactions are of high affinity, especially when a ternary complex is formed, no interaction has been observed for any of the other genetically encoded amino acids (Table 1).[16] This selectivity qualifies CB8 for the development of binding motifs and supramolecular complexes involving peptides and proteins.

Amino acid (AA)	Q8-MV+AA K_a (M^{-1})[a]	Q8+AA K_{ter} (M^{-2})[b]
Trp	4.3 (±0.3) x 10^4	6.9 (±1.3) x 10^7
Phe	5.3 (±0.7) x 10^3	1.1 (±0.2) x 10^8
Tyr	2.2 (±0.1) x 10^3	< 10^3 [b]
All 17 others	No binding observed	No binding observed

Table 1. ***Binding constant of CB8 and CB8-MV with natural amino acids.*** *[a] Values are from Reference [19]; [b] Thermodynamic data for the overall formation of the ternary complexes (K_{ter}) that has units of M-2, values are from Reference [16]; [c] The units given here assume a 1:1 host:guest stoichiometry*

Previous studies on the strength of CB[8] binding with aromatic amino acids were carried out by several groups [20,21] that have highlighted the importance of having the guest residue Phe or Trp at the N-terminal position. However, most of these studies have never dealt with the possibility of ternary complex formation when the guest residues are located within the peptide sequence. In fact, the contrary was even proposed, "*Sequence-specific recognition is most likely the result of close proximity between the aromatic group and the N-terminal ammonium group, where inclusion of an N-terminal aromatic side chain forces the proximal ammonium group (which is otherwise well solvated in water) into close proximity to Q8, thus promoting chelation by the carbonyl groups to stabilize the complex.*".[21]

Scherman's group was the first one to demonstrate the possibility of strong complex formation between CB8 and non terminal phenylalanine in short linear peptides[7]. In this chapter, we would like to extend the search for new binding motifs involving internal aromatic amino acids and CB8. In particular, we focus on exploiting large peptide libraries

that are produced by phage display. The current work is a collaborative effort between the Herrmann group and the laboratory of Prof. Oren Scherman in Cambridge.

3.1.2 - Selection strategy

Phage display was chosen as method to screen large peptide libraries in order to detect strong CB8 binders. The following selection strategy was conceived considering few important facts. First of all, CB[8] complexes are unstable at low concentration of NaCl, so standard buffers like PBS must be avoided. Second, no beads, plates or other commercial supports are available to retain CB[8], thus the choice was limited to MV-functionalised silica and glass surfaces made in the Scherman group. Third, no information is available about the interaction between CB[8] and phage libraries. To the best of our knowledge, this work is the first attemp to perform phage display on such a supramolecular target. For this reason, two different libraries were tested.

It was decided to perform three rounds of selection using surfaces functionalised with MV and pre-incubated with CB8 to obtain the solid support configuration depicted in Figure 3.

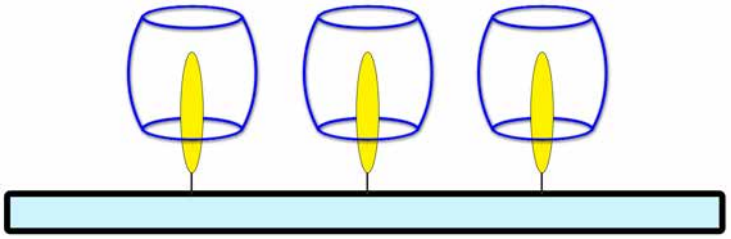

Figure 3. ***Schematic view of the solid support used for the selections.*** *CB8 molecules (blue barrels) are kept in place by their interaction with methyl viologen (yellow ellipse) that is covalently linked on the glass/silica surface.*

To avoid selection bias against the blank support, glass and silica surfaces were alternated during the selection. Two different phage libraries PhD-7 and PhD-C7C were used. The PhD-7 library is composed of seven amino acid long linear peptides followed by a GGGS linker fused with the capsid protein p3. The sequence of this library is NH_2-X_7GGGS-p3-COOH where X represents any of the 20 natural amino acids. In contrast, the PhD-7C7 library is composed of cyclic peptides containing 7 random amino acids between two cysteines and, similarly to PhD-7, followed by a GGGS linker fused with the capsid protein p3. An extra N-terminal Ala is also present leading to the following sequence: NH2-ACX_7CGGGS-p3-COOH. To explore the effect of neighbouring residues, each library was selected under two different buffer conditions, acidic (10 mM KH_2PO_4 - pH 5.0) and basic (10 mM K_2HPO_4 - pH 8.0). In total, four different phage display selections were conducted (Table 2).

Display N°	Library	Buffer
1	PhD-7 (linear peptides)	10 mM KH_2PO_4 - pH 5.0
2	PhD-C7C (cyclic peptides)	10 mM KH_2PO_4 - pH 5.0
3	PhD-7 (linear peptides)	10 mM K_2HPO_4 - pH 8.0
4	PhD-C7C (cyclic peptides)	10 mM K_2HPO_4 - pH 8.0

Table 2. ***Phage display overview.*** *Libraries and incubation buffer combinations.*

The input and output phages were titered following the selection. Phages eluted at the end of the third round of selection were sequenced. The sequences were analysed for the presence of a selected motif or change in amino acid composition compared to an unbiased library.

3.2 - Results and Discussion

3.2.1 - Phage Display

The panning of the libraries on the functionalised surfaces worked as expected. The slection process and enrichment of target-binders in the phage library was monitored through all rounds (Figure 4). In view of the same number of input phages used (10^9 pfu/μL), the titer of the elution fractions increased round after round, as expected in case of selection. The recovered phages were 10^3-10^4pfu/μL during the first round increasing to 10^5-10^6pfu/μL in the third round.

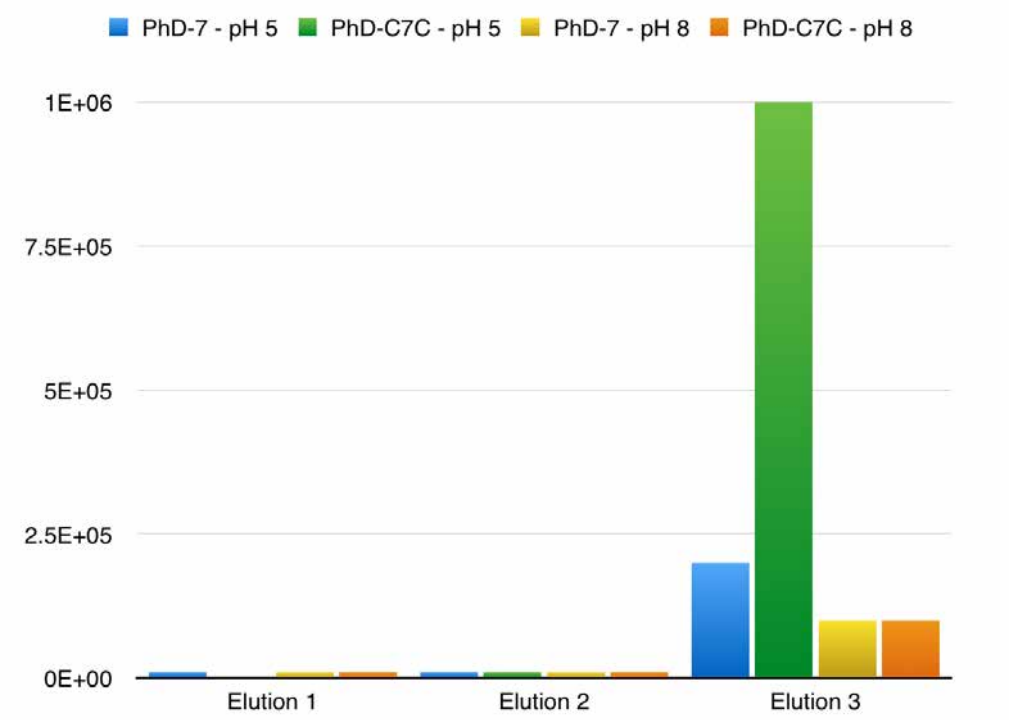

Figure 4. ***Titering of the eluted phages.*** *The titering was estimated after each round of selection and it is represented as number of phages per μL. The numbers are indicative only for the order of magnitude and prone to a large error. However, it is possible to appreciate that all the libraries have undergone a selection process that leads to increased retention of phages during the third round of selection. Selection 2 showed the best trend as it retained the lowest number of phages during first round and highest number during the last round.*

In particular, "Selection 2"(PhD-C7C incubated with acidic buffer) showed the best trend: the phages eluted after the first, second and third rounds were 10^3, 10^4 and

10^6pfu/μL respectively, an increase in binder-to-non-binder ratio significantly higher than the ones obtained with the other selections.

Around 50 colonies from the elution fraction of each selection were picked and sequenced. The corresponding peptide sequence was derived by translation. The analysis of amino acid composition showed some differences only for the samples from Selection 2 when compared with the expected sequence composition of an unselected library. Particularly, this pool was significantly enriched in Gly, His, Phe, Pro and Ser while poor in Ile and Trp compared to reference pools (Figure 5). In other selections, no difference in amino acid composition compared to the starting libraries was detected.

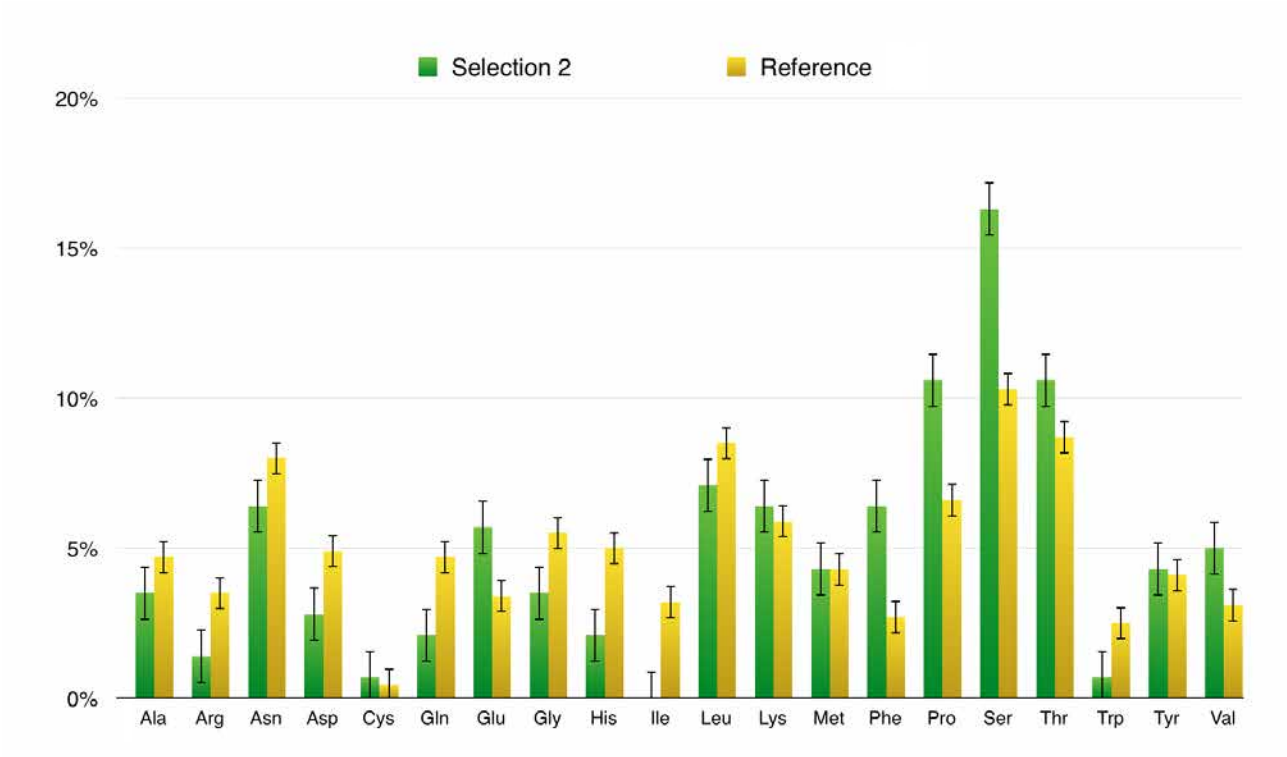

Figure 5. ***Total amino acid composition of the library.*** *The data obtained after Selection 2 are shown in green while the amino acid composition before selection (as reference) is shown in yellow.*

Of particular note is the over-representation of the Phe residue, that is known to form host-guest interaction with CB8-MV. Encouraged by these results, we explored a larger pool of the selected sequences through sequencing. A total of 93 complete sequences (651

residues) from Selection 2 were compared to 97 sequences (679 residues) from the original library (Table 3).

Residue	Reference	Selection 2	Difference
Ala (A)	4.70%	4.90%	4.3%
Arg (R)	3.50%	4.80%	37.1%
Asn (N)	8.00%	8.40%	5%
Asp (D)	4.90%	3.80%	-22.5%
Cys (C)	0.44%	0.44%	0%
Gln (Q)	4.70%	4.50%	-4.3%
Glu (E)	3.40%	4.50%	32.3%
Gly (G)	5.50%	5.80%	5.5%
His (H)	5.00%	4.00%	-20%
Ile (I)	3.20%	1.50%	-53.1%
Leu (L)	8.50%	7.50%	-11.7%
Lys (K)	5.90%	6.00%	1.7%
Met (M)	4.30%	3.80%	-11.6%
Phe (F)	2.70%	3.80%	40.7%
Pro (P)	6.60%	7.70%	16.7%
Ser (S)	10.30%	12.00%	16.5%
Thr (T)	8.70%	9.70%	11.5%
Trp (W)	2.50%	1.10%	-56%
Tyr (Y)	4.10%	2.50%	-39%
Val (V)	3.10%	3.70%	19.3%

Table 3. ***Values of amino acids composition of Selection 2.*** *The table is showing the relative abundance of each residue in a pool of 93 sequences from the last elution of Selection 2 and 97 sequences from the reference library. Significant differences in amino acid composition (|difference| > 30%) are highlighted.*

Repeated sequences	Repeated times
NTGSPYE	4
QNPNQKF	3
LKLGEKW	3
NNGSPYE	2
Motifs of length 2aa	**Repeated times**
PY	6
KF	6
FS	5
YE	5
SF	4
PF	3
FN	3
KW	3
TY	3
RW	2
YP	2
YS	2
TF	2
Motifs of length 3aa	**Repeated times**
SPY	5
PYE	5
EKW	3
QKF	3

Table 4. ***Repeated sequences and common motifs.*** *Few sequences were found multiple times, all containing either one of the aromatic amino acids Tyr, Phe or Trp. Motifs containing one aromatic residue were also found multiple times among the sequenced samples, among them proline-containing motifs are higlited in green, serine-containing motifs in blue and lysine- or arginine-containing motifs in yellow.*

The sequencing results allowed a new judgment of the amino acid distribution. The relative increase in Phe residues was lower as compared to the first result, but the difference was still significant. The under-representation of Trp and Ile and the overrepresentation of the Glu residues was also confirmed.

In-depth analysis of the sequences revealed repeated sequences and small motifs (Table 4). An important observation was that all the repeated sequences contained an aromatic residue, and Trp and Tyr residues occured in repeated sequence. However, the overall abundance of Trp and Tyr residues was low. The analysis of the small repeated motifs aids in understanding whether specific residues were selected around the aromatic ones. Table 4 shows that Pro and Ser residues were selected as these were most represented followed by positively charged residues like Lys and Arg.

These results highlight the importance of obtaining high-throughput sequencing data for the analysis of residue distribution.

3.2.2 - Interaction studies

In order to verify the data obtained by phage display, we synthesized the three most repeated sequences, ACNTGSPYEC (Seq.1), ACQNPNQKFC (Seq.2), and ACLKLGEKWC (Seq.3), and analysed their binding with CB8-MV complex by fluorescence spectrophotometry (Figure X1) and isothermal titration calorimetry (ITC) (Figure 6).

All of the sequences showed quenching of the aromatic residue emission upon addition of the CB8-MV complex with a plateau at 1:1 molar ratio. This spectroscopic behaviour suggests that both partner bind each other at an equimolar ratio.

The results were confirmed by ITC that shows the binding at a 1:1 ratio for all of the sequences . Moreover, Seq2 exhibited a binding constant of $2.0 \cdot 10^5$ M^{-1} , much higher than the one obtained for N-terminal Phe ($5.3 \cdot 10^3$ M^{-1}).[16]

Notably, the binding of Seq.1 was strongly influenced by the pH. At pH 4.5, the glutamic acid E9 (Figure 7) gets protonated and the interaction between the aromatic residue and CB8 becomes stronger, while at pH 7.4, the host-guest interaction was weaker. This observation is consistent with the existing literature[16] that the N-terminus of linear

peptides stabilises the host-guest interaction. Here, we propose that a similar effect might be mediated by the neighbouring side chains of aromatic amino acids.

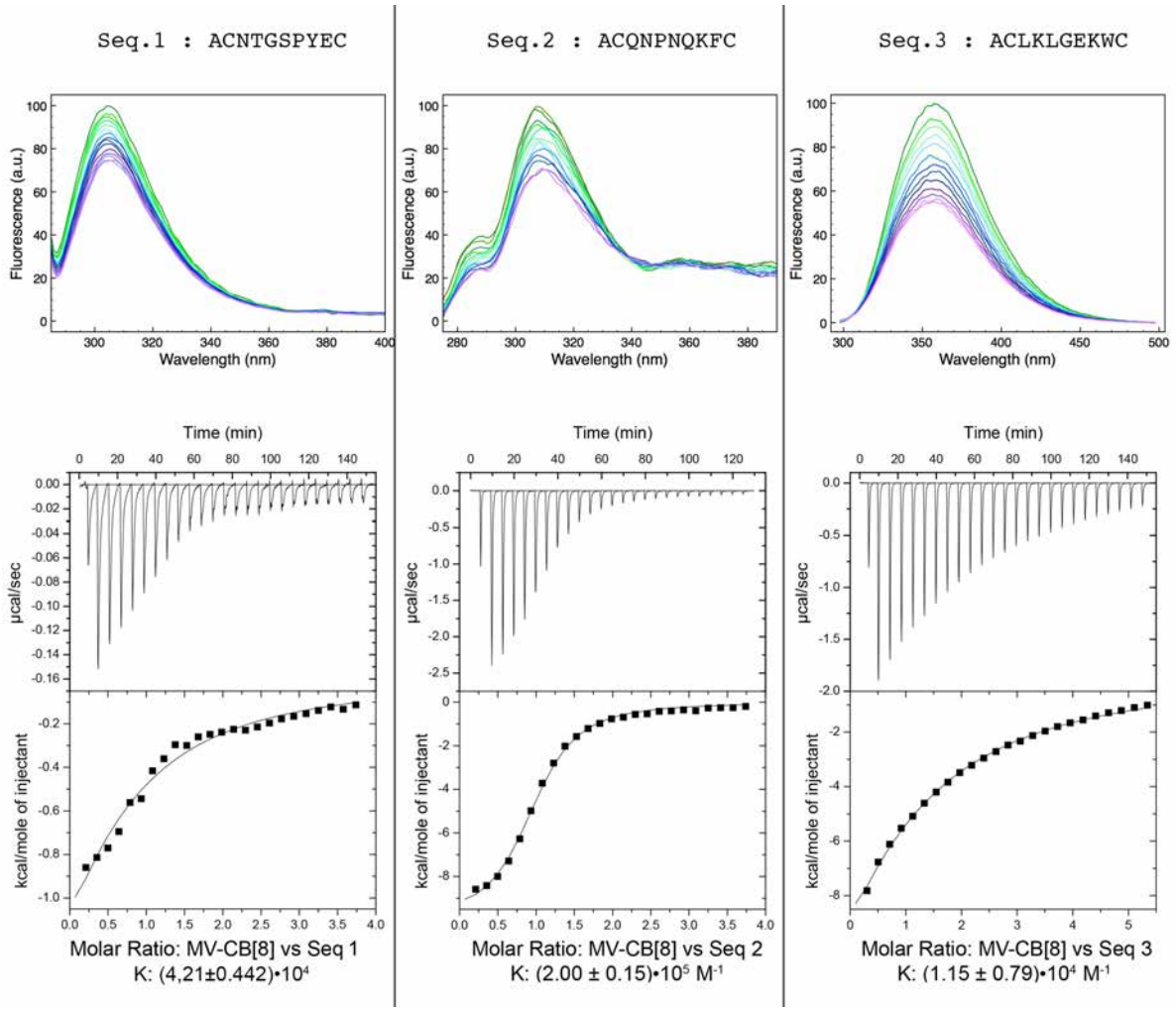

Figure 6. ***Results of the interaction studies of CB8-MV using the cyclic peptides.*** *The interaction was characterized by fluorescence measurements (top) and ITC (bottom). A clear binding event was detected with both methods.*

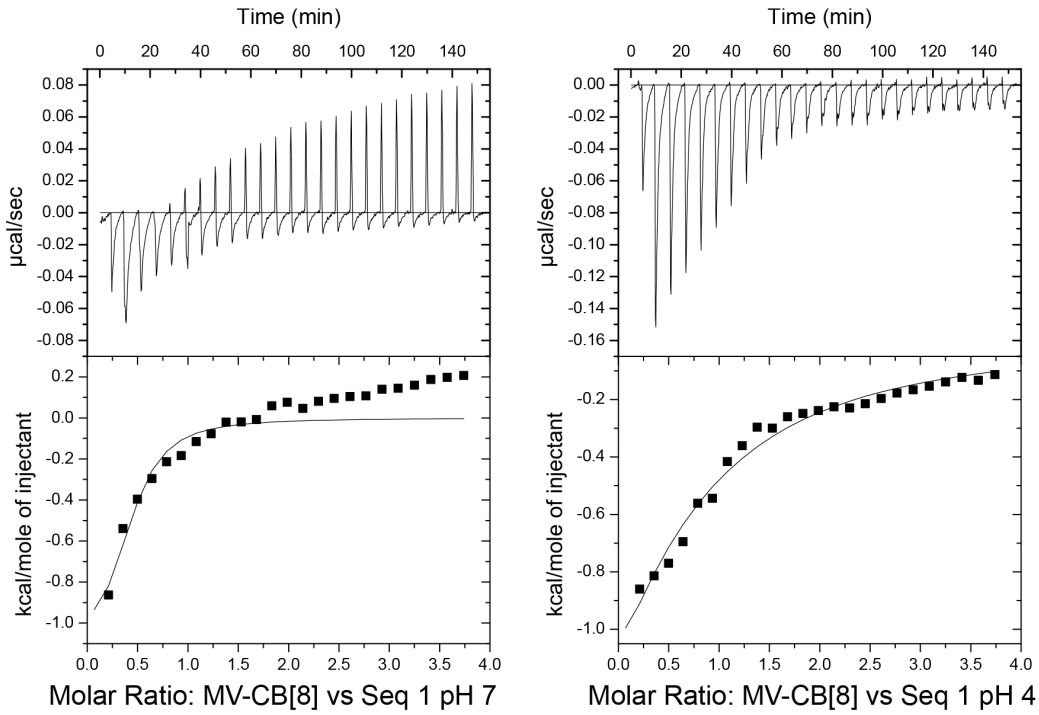

Figure 7. ***Influence of pH on Seq.1/CB8-MV interaction.*** *The protonation of the Glu residue of Seq.1 influences the host-guest complexation. At pH 7.4, the Glu is negatively charged, lowers the interaction with CB8-MV. The opposite occurs when the pH drops and the net charge is positive. Then, the Glu residue stabilises the interaction with CB8-MV.*

3.3 - Conclusions

With this work we were able to demonstrate for the first time that cyclic peptides form complxes with CB8 and non-terminal aromatic amino acids are suitable for such host-guest interactions.

Our data are in agreement with previous findings and underline the importance of having an aromatic residue in the sequence that is *per se* responsible for the formation of the complex. Also in line with previous findings is the observation that a positive charge is needed for the stabilisation of the complex at the portal of CB8. In general, the N-terminal group of a linear peptide was reported to be responsible for the charge stabilisation needed to form the peptide-CB8 complex. However, we showed that other factors like the protonation state of the neighbouring residues, may play a role as well allowing the effective formation of a complex between CB8 and non-terminal aromatic residues. We

think that this study opens up new possibilities of forming CB8 protein complexes going beyond the constriction of having only the N-terminus as anchoring point.

, ,

3.4 - Experimental section

Chemicals

All the amino acids, 2-(6-chloro-1H-benzotriazole-1-yl)-1,1,3,3-tetramethylaminium hexafluorophosphate (HCTU), dichloromethane (DCM) and dimethyl formamide (DMF) were peptide-synthesis-grade and were procured from AGTC Bioproducts Ltd (UK). The following compounds were of analytical grade and were purchased from Sigma–Aldrich (USA): N,N'-dimethylviologen (MV), dimethylsulfoxide (DMSO), diisopropylethylamine (DIPEA), trifluoroacetic acid (TFA), phenol, thioanisole, monobasic potassium and dibasic sodium phosphate. HPLC-grade acetonitrile and N–methylpyrrolidone (NMP) and analytical-grade piperidine and ethanedithiol (EDT) were aquired from Fisher Scientific (USA). Cucurbit[8]uril (CB[8]) was synthesized in our laboratory according to the protocol of an earlier publication.[22] Ultra pure water was obtained from Synergy UV Ultrapure water system (18.2 M Ω·cm at 25° C). A stock solution of 0.5 M phosphate buffer was adjusted to pH 7.4 and sterile filtered. A 10 mM phosphate buffer was prepared as and when required by diluting the 0.5M stock with pH adjusted to 7.4. The concentration of CB[8] was standardised by calorimetric titration with methyl viologen, using binding constants reported in literature.[21]

Surfaces

We used silica and glass surfaces (of 1cm^2 area) functionalized with methyl viologen to bind CB8. The substrates were functionalized by spreading 1 mL of 150mM CB8 in ultra-pure water on the surface. After 5-10 minutes the solution was removed and the surfaces were gently washed 3 times with 1mL of ultra pure water.

Phage Library

Commercial libraries of recombinant phages were purchased from NEB (E8100S and E8120S). Since the binding of CB8 toward MV is negatively influenced by the presence

of salts, the libraries, originally in TBS buffer, were dialyzed against ultra-pure water before use.

Phage display

500 µl of phage library with a concentration of 10E9 pfu/mL (5ul of 10E9 pfu/µl diluted in 5 mL) was gently pipetted on top of the CB8-functionalized surfaces and incubated at room temperature for 5 minutes. The phage suspension was then gently removed and discarded. The same procedure was repeated 10 times. The surfaces were washed 5 times by gently pipetting 1mL of ultra pure water. On top of the substrates, different elution buffers were used resulting in 4 selections.

CB8-MV complex is disrupted by high sodium ion concentration, so LB medium containing 172 mM NaCl was used as elution buffer. 500 µl of LB was deposited on the surface. After 30 minutes the LB was recovered and stored. This LB contains the phages that remained on the surfaces after the washing steps. Two different incubation buffers were tested. One was acidic (10 mM KH_2PO_4 - pH 5) and the other was basic (10 mM K_2HPO_4 - pH 8).

Peptide synthesis

Fmoc solid–phase peptide synthesis (SPPS) was carried out in Cambridge by Silvia Sonzini, a Ph.D. student in the Scherman group, on the CEM Liberty Automated Microwave Peptide Synthesiser using MBHA rink amide resin (0.6 mM/g) as solid support for a 0.1 mmol scale synthesis. Fmoc deprotection was accomplished by a solution of 20% piperidine in DMF using a power of 45 W, at a temperature of 75 °C over 180 seconds. The peptide coupling was performed using a double coupling strategy and 5 equivalents of amino acids and HCTU both dissolved in DMF, and 10 equivalents of base (DIPEA solution 2M in NMP). The coupling was run with 25W power, at 75 ◦C over 600 s. Microwave irradiation was not used with Pro and Cys residues. The Fmoc deprotection and coupling were run at room temperature for 900 s and 1 h, respectively. The cleavage cocktail contained a high percentage of TFA. The

mixture of TFA/water/thioanisol/phenol/EDT at a ratio of 82.5:5:5:5:2.5 was added to the dry resin and shaken over 3 h at room temperature. After the cleavage procedure, peptides were precipitated in diethyl ether and centrifuged for 4 up to 6 times at 4◦C at 4000 rpm over 5 min before being lyophilised and stored as a white powder at -20◦C. Peptide purity was verified by HPLC analysis and ESI-MS. The peptides, dissolved at a concentration of 1 mg/mL, were cyclised in a solution of 5% DMSO in water for 16 h and the reaction was monitored by MS-ESI. On completion, the reaction solutions were freeze-dried and the residues obtained re-dissolved and purified by semi-preparative HPLC. The purity of the final cyclised peptides was confirmed by analytical HPLC and MS-ESI. Fresh peptide solutions were prepared for each experiment and their concentration was established by UV-Vis absorbance before use. The linear sequences, on account of their good purity, were used for other analyses without any further purification.

Fluorescence Titrations

The titrations were accomplished by measuring the fluorescence emission of filtered solutions in 10 mM phosphate buffer at pH 7.4. The peptide concentrations were maintained constant (12.5 to 30 μM depending on the sequence), while the concentration of MV-CB[8] was increased by small volume additions of a concentrated solution (1 mM). The sequences feature different aromatic residues with fluorescent properties. Therefore, sequence 1 was excited at 275 nm and emission was analyzed at 300 nm; sequence 2 was excited at 257 nm and fluorescence was analyzed at 285 nm; and sequence 3 was excited at 280 nm and emission was analyzed at 355 nm. The ratio between the fluorescence intensity at each addition of MV-CB[*8*] over the initial intensity was plotted against the ratio of (MV-CB[*8*]):peptide concentration to obtain an indicative stoichiometry of the complexes. All the plots were average of three independent replications of the assays.

ITC Titrations

The conditions applied were 25°C, 1000 rpm stirring speed, 60 s initial delay and 20 injections of 2 μL delayed by 90 seconds. The ITC titrations were carried out using MV-CB[8] at 1 mM and sequences 1-3 at 0.1 mM in a 10 mM phosphate buffer solution at pH 7.4. Sequence 1 was dissolved in a 10 mM phosphate buffer solution at pH 4 for the ITC experiments at low pH. The filtered solutions were kept at 23°C and degassed for 10 min prior to the experiments. All the titrations were replicated three times. Data were analysed with MicroCal Origin software. The data were fitted with the"one binding site"model.

3.5 - References

1. Han, X. & Tamm, L. K. A host-guest system to study structure-function relationships of membrane fusion peptides. *Proceedings of the National Academy of Sciences of the United States of America* 97, 13097–13102 (2000).
2. Boas, U., Söntjens, S. H. M., Jensen, K. J., Christensen, J. B. & Meijer, E. W. New Dendrimer–Peptide Host–Guest Complexes: Towards Dendrimers as Peptide Carriers. *ChemBioChem* 3, 433–439 (2002).
3. Heo, S. W. *et al.* Host–Guest Chemistry in the Gas Phase: Selected Fragmentations of CB[6]–Peptide Complexes at Lysine Residues and Its Utility to Probe the Structures of Small Proteins. *Analytical Chemistry* 83, 7916–7923 (2011).
4. Jiao, D. *et al.* Supramolecular Peptide Amphiphile Vesicles through Host–Guest Complexation. *Angewandte Chemie International Edition* 51, 9633–9637 (2012).
5. Molecular recognition of insulin by a synthetic receptor. 133, 8810–8813 (2011).
6. Dang, D. T., Nguyen, H. D., Merkx, M. & Brunsveld, L. Supramolecular control of enzyme activity through cucurbit[8]uril-mediated dimerization. *Angew. Angewandte Chemie International Edition* 52, 2915–2919 (2013).
7. Sonzini, S., Ryan, S. T. J. & Scherman, O. A. Supramolecular dimerisation of middle-chain Phe pentapeptides via CB[8] host–guest homoternary complex formation. *Chemical Communications* 49, 8779–8781 (2013).
8. Kim, B.-K. *et al.* Homodimeric SV40 NLS peptide formed by disulfide bond as enhancer for gene delivery. *Bioorganic & Medicinal Chemistry Letters* 22, 5415–5418 (2012).
9. Aggarwal, S., Singh, P., Topaloglu, O., Isaacs, J. T. & Denmeade, S. R. A dimeric peptide that binds selectively to prostate-specific membrane antigen and inhibits its enzymatic activity. *Cancer Research* 66, 9171–9177 (2006).
10. Marianayagam, N. J., Sunde, M. & Matthews, J. M. The power of two: protein dimerization in biology. *Trends in Biochemical Sciences* 29, 618–625 (2004).
11. Matthews, J. M. *Protein Dimerization and Oligomerization in Biology*. (2012).
12. Peczuh, M. W. & Hamilton, A. D. Peptide and protein recognition by designed molecules. *Chemical Reviews* (2000).
13. Nguyen, H. D., Dang, D. T., van Dongen, J. L. J. & Brunsveld, L. Protein Dimerization Induced by Supramolecular Interactions with Cucurbit[8]uril. *Angewandte Chemie International Edition* 49, 895–898 (2010).
14. Huang, W. H., Liu, S. & Isaacs, L. *Modern supramolecular chemistry* 113–142 (2008).
15. Isaacs, L. Cucurbit[n]urils: from mechanism to structure and function. *Chemical Communications* 0, 619–629 (2009).
16. Rajgariah, P. & Urbach, A. R. Scope of amino acid recognition by cucurbit[8]uril. *Journal of Inclusion Phenomena and Macrocyclic Chemistry* 62, 251–254 (2008).
17. Kim, H. J. *et al.* Selective Inclusion of a Hetero-Guest Pair in a Molecular Host: Formation of Stable Charge-Transfer Complexes in Cucurbit[8]uril. *Angewandte Chemie International Edition* 40, 1526–1529 (2001).

18. Jeon, W. S., Kim, H. J., Lee, C. & Kim, K. Control of the stoichiometry in host–guest complexation by redox chemistry of guests: Inclusion of methylviologen in cucurbit[8]uril. *Chemical Communications* 1828–1829 (2002). doi:10.1039/B202082C
19. Bush, M. E., Bouley, N. D. & Urbach, A. R. Charge-Mediated Recognition of N-Terminal Tryptophan in Aqueous Solution by a Synthetic Host. *Journal of the American Chemical Society* 127, 14511–14517 (2005).
20. Lagona, J., Mukhopadhyay, P., Chakrabarti, S. & Isaacs, L. The Cucurbit[n]uril Family. *Angewandte Chemie International Edition* 44, 4844–4870 (2005).
21. Heitmann, L. M., Taylor, A. B. & Hart, P. J. Sequence-specific recognition and cooperative dimerization of N-terminal aromatic peptides in aqueous solution by a synthetic host. *Journal of the American Chemical Society* 128, 12574-12581 (2006).
22. Day, A., Arnold, A. P., Blanch, R. J. & Snushall, B. Controlling factors in the synthesis of cucurbituril and its homologues. *The Journal of Organic Chemistry* 66, 8094–8100 (2001).

Chapter,4

M13,as,biomaterial

Abstract

Apart from phage display, M13 has unique characteristics that make it appealing for material science. Its regular structure, genetically determined, and the fact that its capsid is almost entirely formed by the self assembly of a single protein, p8, qualify M13 to be a suitable building block for the fabrication of new nano biomaterials. Here, we show how to unleash the potential of M13 as genetically tunable material by direct mutagenesis of its major capsid protein. For the first time, we report the fabrication of thermotropic liquid crystals by the complexation of a mutant phage particle and cationic surfactants.

4.1 - Introduction

The prime application of phage display, as described in the previous section, is the development of aptamers as evidenced by a large body of literature. This technique of selection of the peptides against a desired target from complex libraries is one of the easiest methods available for this purpose.

The application we pursued here, i.e., phage display for the development of new materials, though conceptually similar to regular phage display, is much less explored. As in phage display, this method is based on exposing peptides on the surface of a phage capsid. However, it differs by the fact that selection is not driven by evolution. The rationale behind it is that a single modification of the major capsid protein p8 drives a substantial change of the physical and chemical properties of the whole phage capsid, which can be extremely advantageous in materials science if the phage particle itself is used as a building block to study and develop new materials.

This chapter will provde an overview of how phages are transformed into innovative new materials. Special focus will be on the realization of phage-derived liquid crystals and tuning of their physical properties by means of genetic engineering.

4.1.1 - Phages and liquid crystals

The state of matter intermediate of conventional liquid and that of solid crystals are called liquid crystals (LCs). LCs are broadly classified in three types; thermotropic LCs that exhibit a phase transition into the liquid-crystal phase as temperature is changed, lyotropic LCs in which the phase transitions is dependent on both temperature and concentration of the liquid-crystal molecules in a solvent, and metallotropic LCs that are composed of both organic and inorganic molecules whose liquid-crystal transition depends on the ratio of the inorganic and organic composition. LCs play an important role in biological processes as their properties like mobility and order are vital in self-organization and structure formation in cells.[1-3] Lyotropic liquid-crystalline phases are especially abundant in living systems. Most of the cell membranes can be considered as LCs. Liquid crystalline phases can be derived from many other bimolecules, including

nucleic acids,[4,5] proteins,[6,7] and viruses.[8,9] These LCs are mostly of lyotropic nature as these are formed in water and are stabilised by the amphiphilic partitioning of hydrophilic and hydrophobic molecular components. However, technological applications of LCs have been limited mostly to the thermotropics (TLCs). These are weakly amphiphilic and are ordered by virtue of steric molecular shape, flexibility, and/or van der Waals and dipolar forces,[10] which allows TLCs to adopt a wide variety of phases that exhibit dramatic and useful responses to external forces. For instance, one of the most common applications is associated to opto-electronic effects that have been used in the fabrication of LC displays.

The distinction between lyotropic and TLCs suggests that there may be interesting possibilities in the development of biomolecular or bio-inspired LC systems in which the importance of amphiphilicity is reduced and the LC phases obtained are more thermotropic in nature. Applications for such biological TLC materials still need to be fully explored and their solvent-free properties and functions could be investigated in a state where no or only traces of water are present.[11-14] Indeed some studies have already proven that a two-component (water-free) mixture of nucleic acid and surfactant forms solid-state materials that exhibit a variety of interesting and potentially useful propoerties.[15-19] However, examples of solvent-free TLCs based on biological building blocks such as nucleic acids, proteins, and multi-protein complexes are scarce.[20,21] This fundamental lack of knowledge of fabrication and superstructure formation of TLCs based on bimolecular, inspired my colleague Kai Liu to explore this concept. As filamentous bacteriophages are an attractive building block for the development of new LCs, I was involved in developing phage mutants that can be transformed into thermotropic LCs.

4.1.2 - Phages as a biomaterial

In a quest for development of novel liquid crystalline materials, phages have become promising and important building blocks. Such an endeavour usually brings together researchers from various fields. A marriage of physical, biological, and chemical sciences has helped in the past for the development of many novel materials with tremendous potentials. However, when it comes to the development of introduction of biological

organisms into materials science, collaborations have been scarce untill recent times. This is most likely due to a complete lack of commonalities between these two fields.

The recent advent of nanotechnology has provided a common ground for bridging the interactions between material scientists and biologists. Nanomaterials have been fundamentally present everywhere, inside and ouside of every organism. However, these have been hard to make ever since first conceptualised by Richard Feynman in his famous talk "There's Plenty of Room at the Bottom" at the annual meeting of the American Physical Society in Pasadena, California, on December 29th, 1959. Such difficult to make materials, usually have ordinated arrays of functional molecules of precise length, thickness, a degree of functionalization, and absolute monodispersity. Such a regularity and orderliness palys a vital role in the development of LCs as well.

Viruses are an excellent example of unbelievably precise and complex structure and symmetry.[22] One such example are filamentous bacteriophages. Their monodisperse length is genetically controlled. The high aspect ratio of their capsids drives their self-assembly into microstructures without the need for micro-fabrication. Moreover, one of the main characteristic that makes filamentous phages like M13 so appealing for material science is their capsid structure. The M13 capsid is composed of a single protein p8, which forms 99% of the capsid.[23] Hence, each phage can be considered as an extremely versatile protein nanotube exposing a peptide array uniformly spaced at 2.7 nm in the axial direction and 2 nm in the lateral direction.[24] The functionality of each phage depends on its shape, charge, and displayed peptide. All of these properties can be changed through chemical or genetic modifications to obtain a nano filament with very densely displayed functional peptides (1.5×10^{13} epitopes/cm^2).[25]

As mentioned above, the genetic modification of M13 is a powerful approach to tune the capsid properties. Since the phage body is composed of 2700 copies of p8, alterations in this protein lead to drastic changes in the chemical and physical properties of the entire capsid. The N-termini of these proteins are flexible, hydrophilic domains, located on the outer surface of the phage and can be altered by up to eight amino acids appended on every p8 unit.[26] Their ability to display peptide-based information on surfaces, coupled

with replication and self-assembly into long-range ordered nanofilamentous structures, make M13, an ideal and attractive building block for many potential applications. These possibilities have been explored with filamentous bacteriophages in the past few years by various groups, including approaches in energy storage materials, and high performance memory and computing devices. [27-31]

Combinations of biomolecules and inorganic components provide a new paradigm for synthesizing nanoscale or larger structures with tailored physical properties. The synthesis techniques for designing such materials leverage on the molecular recognition properties of many biological molecules and their ability to nucleate the growth of inorganic nanostructures. For example, peptides isolated for binding to inorganic surfaces have been used to trigger the nucleation and growth of nanocrystals of metals[28] or semiconductors. While still displayed on the phage, these peptides have also been used as templates for the oriented growth of nanowires.[30,32] Peptide binders evolved against Ag particles[31] using a phage-displayed 12-mer combinatorial library yielded two sequences that could direct Ag precipitation from an aqueous solution of Ag ions. Similar experiments have been performed for ferromagnetic systems such as L10 CoPt and FePt,[33] which are of interest as ultrahigh-density memory devices. The selection of such peptides is similar to that occurring in a typical affinity selection experiment where the inorganic surface to which a peptide ligand is bound, is exposed to a phage-displayed combinatorial peptide library; followed by the enrichment of the phage exposing surface binding peptides during three or more rounds of selection.

4.1.3 - Mutagenesis of M13

The Polymersae Chain Reaction (PCR) was used to realise mutagenesis in M13. PCR is a very versatile molecular biology tool, which uses a synthetic DNA primer containing the desired mutation complimentary to the template DNA around the mutation site so that it can hybridize to generate mutant copies. The mutation may be a single base change (a point mutation), multiple base changes, a deletion, or an insertion.[34,35] The single-stranded primer is then extended using an enzyme, the DNA polymerase, which copies the rest of

the gene. The gene thus copied contains the mutated site, and is then introduced into a host-cell vector for cloning. Finally, mutants are selected by DNA sequencing to check for the presence of the desired mutation. Several variations of this procedure exist (Figure 1), all of which are well established methods that easily produce the desired mutations especially when working with plasmids as templates.

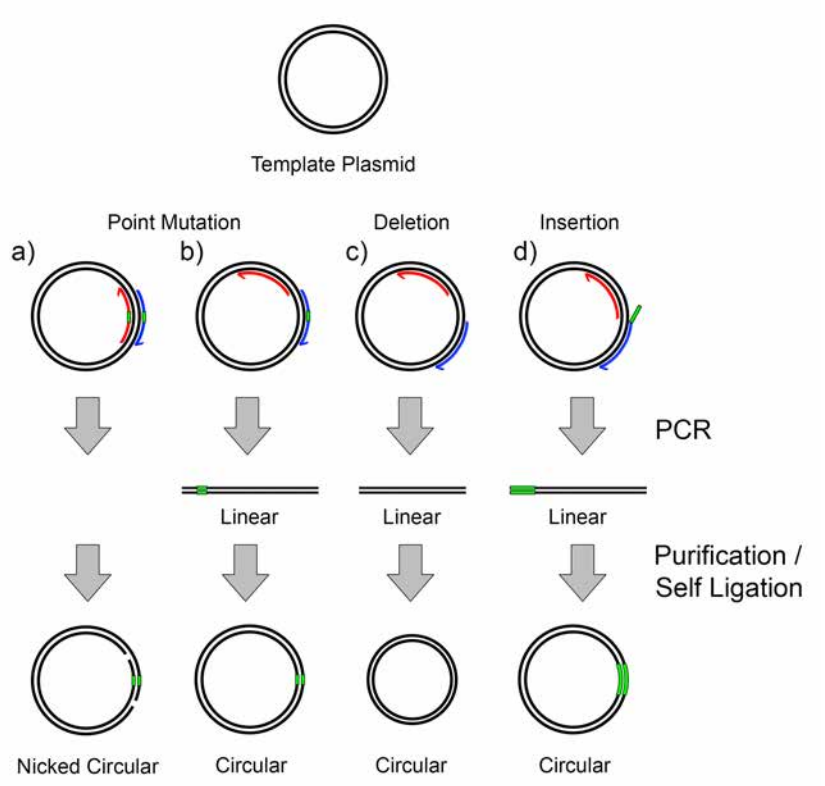

Figure 1. ***PCR-based mutagenesis methods.*** *Starting from a plasimd as template, there are different methods that allow to introduce various types of genetic alterations with the help of PCR and appropriate primers. Point mutations can be introduced by using a) two primers carrying a single base or single codon mismatch in the middle of their sequence and that anneal in the same region of the plasmid. PCR amplification of the whole template using such primers leads to the formation of a double nicked circular plasmid that can be diretly transformed into host cells. One mutagenic primer and one normal primer can be used to introduce small b) or larger d) insertions. In this case, the primer-annealing regions on the template do not overlap leading to the formation of a linear mutated dsDNA that can be circularized and transformed. Finally, deletions c) can be accomplished by using normal primers flanking the region to be deleted. In this case, the PCR product is linear dsDNA that needs to be circularised by self-ligation prior to transformation.*

However, when dealing with bacteriophages, the successful implementation of such a technique becomes unexpectedly tricky. The main reason that makes the editing of M13 not trivial is its genome. Viruses are not like other organisms, as their genome (including M13) is extremely compact; little or no space is available between the coding regions. Furthermore, many proteins are coded by overlapping genetic sequences, which restricts the possibilities for insertion of foreign DNA segments.

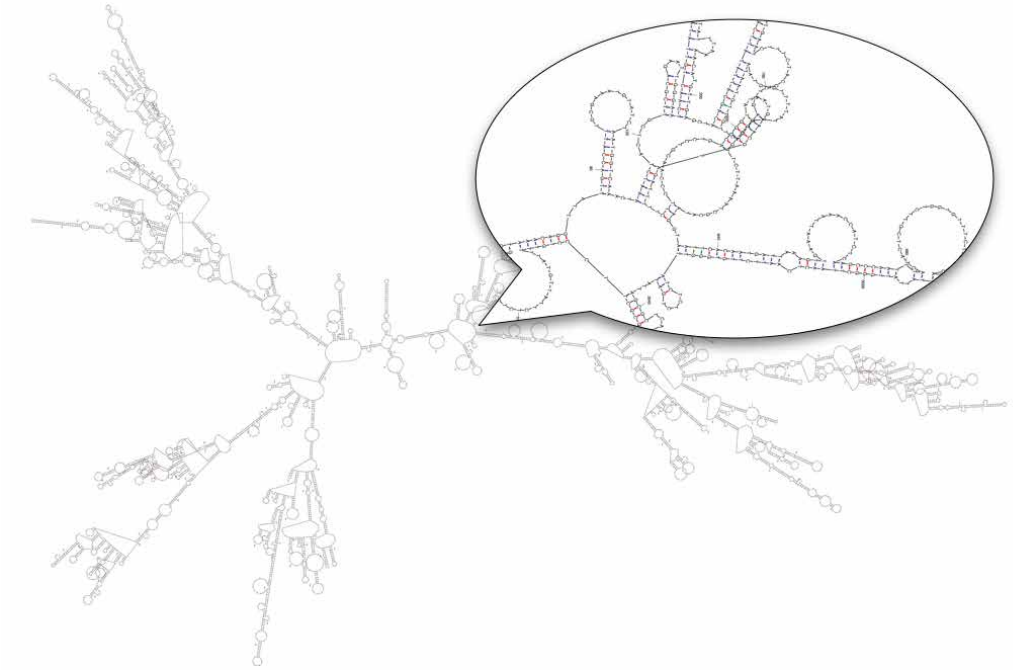

Figure 2. ***Structure of M13 genome.*** *Overview of secondary structure of the M13 genome that has been determined using mfold software.*[36] *The balloon zooms into one of the numerous complex structural arrangements formed in the genome.*

Furthermore, M13 has a circular ssDNA genome, most of which, contrary to being a true single strand, is complicated by interspersed base-paired regions, and formation of stems and loops (Figure 2). The secondary genome structure is vital for proper development of the mature phage particle, which can be easily affected by insertion, deletion or modification of the genome sequence. Hence, though M13 genome seems to

bear similarity with plasmid DNA, it is very difficult to work with reguar PCR-based mutagenesis methods that are available for plasmids. Moreover, as we aim at modifying the protein p8, which will eventually influence its structure and surface-charge distribution, the phage may end up losing its ability to form a stable capsid or infect the host.[37] As a consequence, even if the mutagenesis is acheived, the stability of the genome or the viability of the phage is most likely to be jeopardised. Even though the phage particles propagate, a reduction in their viability will give an upperhand for wild-type phages that will eventually end up naturally selected and get enriched during amplification. To overcome these difficulties, the phage stability is verified at each stage of the selection through DNA sequencing and analysis of the exposed peptide by mass spectrometry.[33] Last but not least, in addition to the viability, the mutated phasges may react differently to the solvents and solutes employed in the fabrication protocols. Thus, efforts will be required to optimise every step of the production and purification of each new phage variant to obtain the mutants in sufficient quantities as required for the studies, especially when material properties are characterised.

4.2 - Results and Discussion

4.2.1 - Mutagenesis

Several M13 mutants have been produced by applying different mutagenesis protocols; two of these are as follows.

M13-K8A. The first mutant, called M13-K8A, is a variant of M13 in which lysine 8 has been mutated to alanine; leading to the halving of positive surface charge on the phage particle. The wild-type p8, once assembled into the phage capsid, exposes two primary amino groups: the one at the N-terminus and the one of lysine 8 (Figure 3). These primary amino groups can be modified by chemical modification in an aqueous buffer under mild

pH conditions like the one used for NHS-ester coupling. Such reactions open up the possibility for the functionalisation of M13 phage particles; allowing to link up to 5400 and 2700 functional units per particle in the wild type and mutant M13-K8A, respectively.

Successful mutagenesis was achieved using the QuickChange protocol (Figure 1a). Two complementary oligonucleotides were designed in order to anneal to a region of 30 bp of the p8 gene with the designed mutation, AAA to GCA, inserted in the middle of the sequence, mismatching the template DNA for two bases. A PCR reaction was performed using ssDNA purified from M13 phages as template. Upon transformation of *E. coli* with the PCR product, several blue colonies were picked and sequenced. As shown in Figure 4, some of the seqenced clones were succesfully mutated showing the codon GCA, that codes for alanine instead of the codon AAA that codes for lysine in the wild type phages. These clones were further amplified for few generations and sequenced once more to determine the stability of the mutants. An unstable mutant could revert to wild-type after few generations, if the newely introduced mutation is particularly disadvantageous. However, this was not the case. We were able to grow the mutants for several generations obtaining similar yield of phage particles compared to the original M13. Overall, the mutation introduced was shown to be stable after several generations and culture periods up to 24 hours (Figure 4c).

To prove that a single K to A amino acid substitution allowed us to tune the degree of functionalisation of the viral particle, we decided to anchor a fluorescent dye to the exposed primary amino groups using NHS chemistry. Having fewer amines available, the mutant phage M13-K8A is expected to have fewer anchor points on the surface than the wild type.

For the coupling reaction, 10^{10} M13KE and M13-K8A phages were resuspended in 500 μL of PBS at pH 8.0 containing 3 mg of the dye Atto 565 NHS ester (SIGMA). After an overnight reaction carried out at 4°C, the reaction was stopped using diethylamine and dialysed against PBS. The recovered phages were visualised *via* wide-field microscopy using a LED light of wavelength 570 nm to excite the dye while the emission between 625-725 nm was measured with an acquisition time of 1 second. As shown in Figure 5, a clear

difference in brightness was observed between the wilde type and the mutant phage. Notably, the phages mantained their infectivity after functionalisation. This simple experiment showed that it is indeed possible to tune the degree of functionalisation of a filamentous bacteriophage by genetic engineering of the p8 gene.

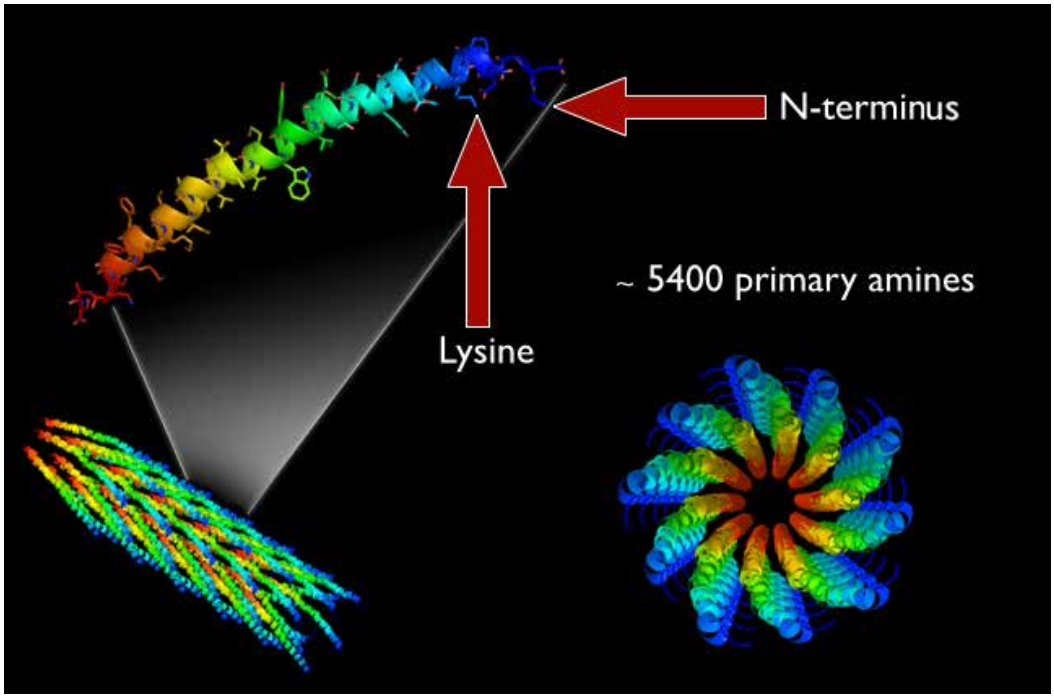

Figure 3. Structure of *wild type p8 assembly.* *The 3D structure was rendered with PyMol (http://pymol.org/) and PDB file obtained from Protein Data Bank (PDB ID: 2C0W). The exposed amino groups are indicated by the arrows.*

M13-ELA. While M13-K8A was developed to tune the degree of chemical functionalisation of the viral particle, the next mutant was developed for direct tuning of liquid crystalline phase by means of genetic engineering through changes in particle thickness and hydrophobicity. Rodlike viruses are ideal building blocks for lyotropic LC materials due to their monodisperse and anisotropic shape. M13 in particular offers another feature, it has several negatively charged amino acids exposed on the capsid that could interact with cationic surfactants.

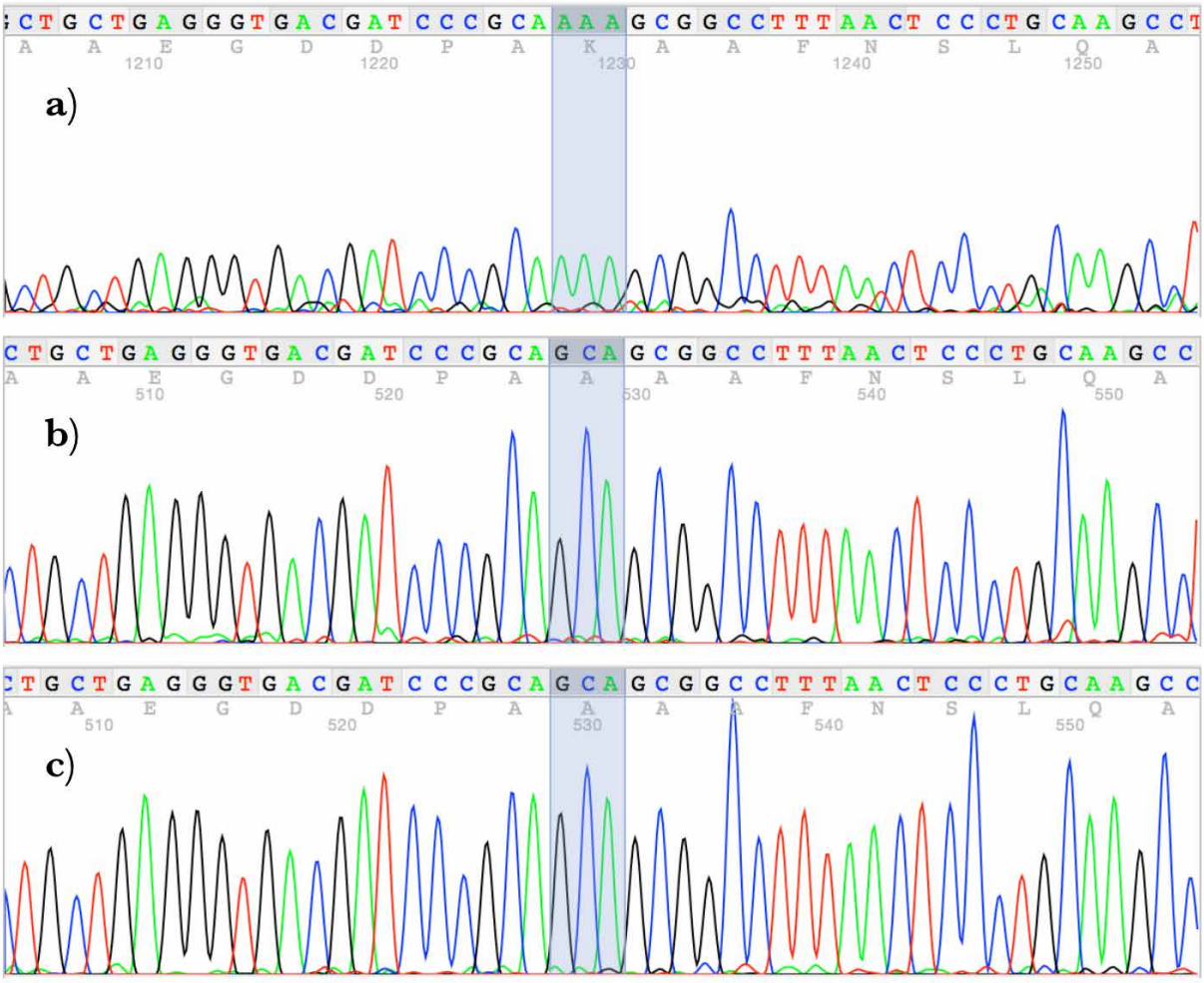

Figure 4. ***Sequencing results of various M13 phages.*** *M13 nucleotide sequence of wild type (a), of M13-K8A post-mutagenesis (b) and of M13-K8A after 24 hours culture. The post-culture sequencing was conducted to demonstrate the stability of the mutant over time. The substituted amino acid (K to A) is highlighted in the picture.*

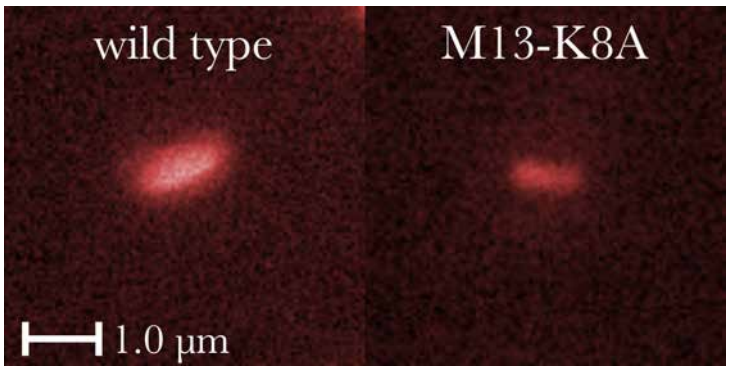

Figure 5. ***Functionalization of wild type and mutant phage with an NHS-ester dye.*** *The red spots are 1 µm long, as expected from the structure of the phage particle. Note the difference in brightness due to the lower degree of functionalisation of the mutant phage (M13-K8A).*

These characteristics have been leveraged to produce TLCs in which the phage act as rigid part and cationic surfactants make up the flexible units. Similar TLCs were achieved with negatively charged DNA and supercharged polypeptides.[38] Electrostatic interactions couple these rigid and flexible components into hybrid assemblies, which then order into lamellar phases of alternating rigid and flexible layers stabilized by the tendency in TLCs for rigid and flexible to spatially segregate. The next step was to produce TLCs from much bigger building blocks, *i.e.*, filamentous phages.

However, preliminary experiments involving wild-type M13 complexed with cationic surfactancts in absence of water resulted in crystalline rather then liquid-crystalline phases. Reasoning on the cause of these results, we speculated that the packing between the surfactants and the virion was too tight and could possibly be solved by lowering the charge density or the thickness of the phage capsid. For this reason we decided to modify the p8 protein more extensively by adding five extra amino acids at its N-terminus. Specifically, the elastin motif VPGVG amino acid sequence was added. Elastin is an intriguing protein that imparts elastomeric properties to vertebrate tissues. The elasticity of this protein is known to hinge on a complex interaction with the solvent. Elastin becomes elastic only upon hydration and the elastic properties depend on the solvent polarity. [39,40] An interesting feature of elastin is that it undergoes an inverse temperature transition at approximately 20 °C to 40 °C; a process that results in reduction of protein gyration radius, expulsion of water and formation of a complex network of hydrogen bonds.[41-44] In a nutshell, all these characteristics have made it a good candidate for realisation of a liquid crystalline material building block.

A two-step PCR approach (see experimental section) was used to accomplish the mutagenesis of wild type M13 into the ELA variant. This variant carries the VPGVG coding sequence at the N-terminus of the p8 coding region between the leader peptidase signal and the first alanine of the mature protein. The leader peptidase sequence is responsible for the delivery of a newly synthesised p8 to the bacterial membrane where it is then cleaved by a bacterial peptidase in order to form the mature protein p8.

The DNA sequence was validated firstly by sequencing, the results reported in Figure 6, which show the right insertion of the nucleotide sequence coding for the motif VPGVG

exactly in between the leader peptidase signal of the protein p8 (highlighted in green in the picture), and the N-terminus of the mature p8 (highlighted in red). To prove that the elastin motif is efficiently produced and incorporated into the phage particles, we used mass spectrometry to determine the mass of wild type and mutant p8.

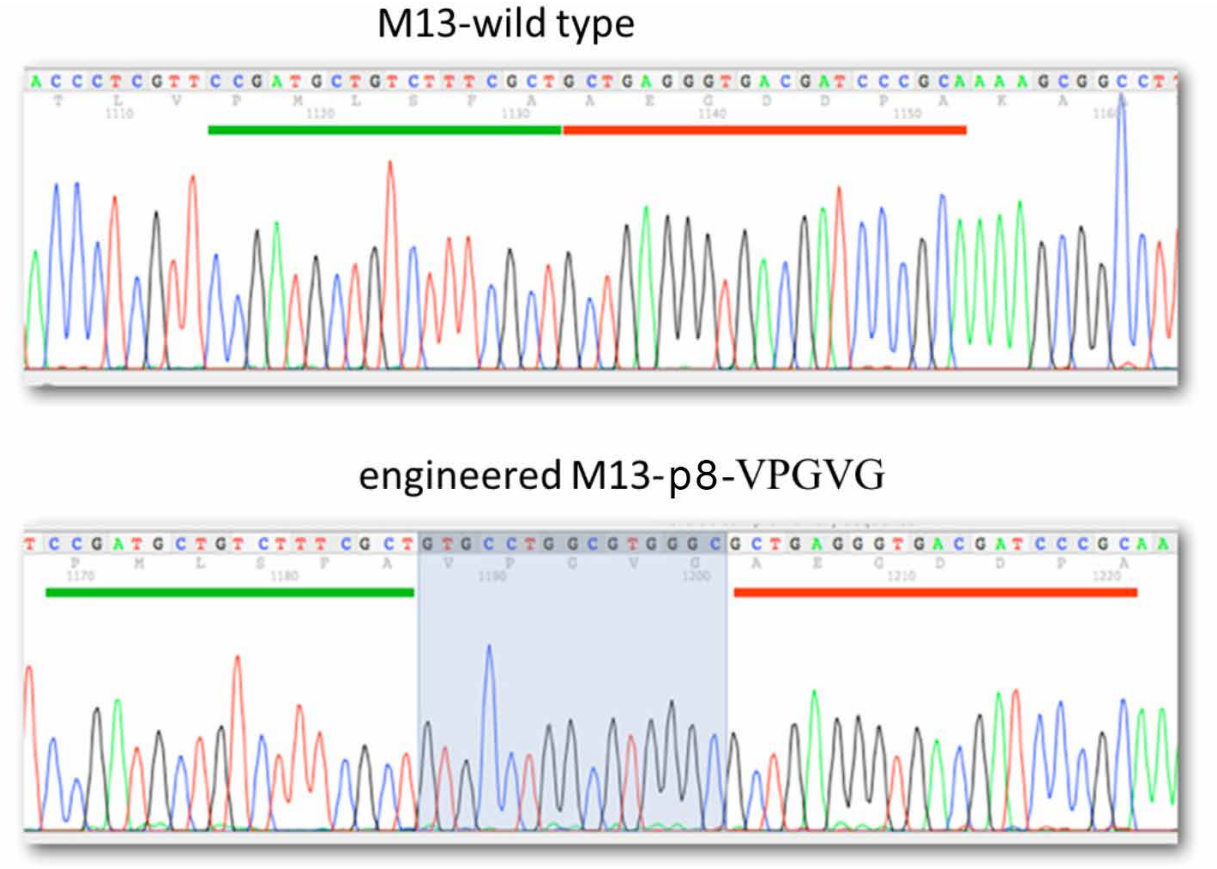

Figure 6. ***Validation of the mutagenesis of M13-ELA through sequencing.*** *The VPGVG coding sequence was inserted between the peptidase signal (underlined in green) and the N-terminus of the mature p8 (underlined in red).*

As shown in Figure 7, we were able to succesfully measure the mass of VPGVG-p8 5658 Da (calculated 5648 Da) and of the wild type p8, 5245 Da (calculated 5238 Da). From the comparison of the two masses (ΔMw = 413 Da, calculated 410 Da), we confirmed the expression of the mutated coat protein and its integration into viable phages.

The filamentous structure of the phages was finally confirmed by TEM imaging (Figure 8) that showed particles of 1 μm in lenght and 7 nm in diameter, exactly as expected.

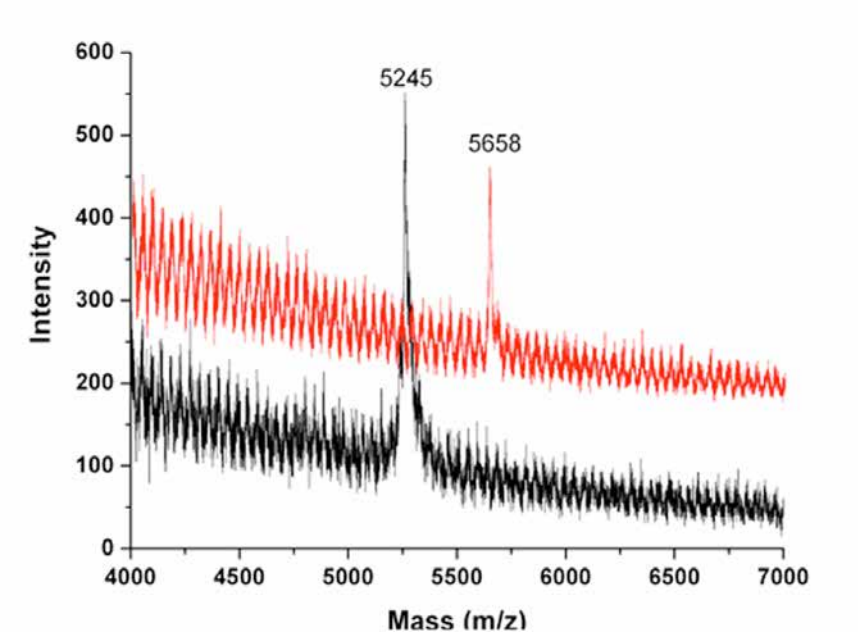

Figure 7. ***Characterisation of M13-ELA by MALDI-TOF mass spectrometry.*** *The mass spectra of the major coat protein p8 of wild type (black line) and engineered M13-phage (red line) are shown.*

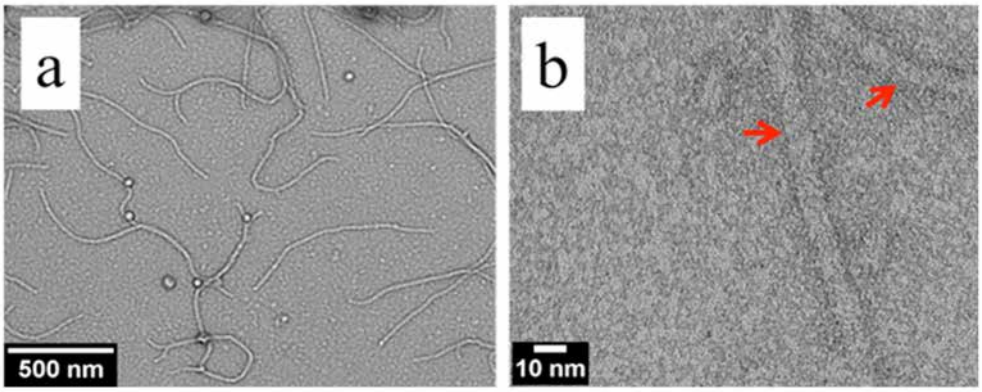

Figure 8. ***Characterisation of M13-ELA by TEM.*** *The TEM images of engineered phage, indicating that the obtained phage exhibits a length of 1 μm (a) and a diameter of around 7 nm (b). The helical arrangement of the p8 protein on the surface of phage is clearly visible in the magnified image (red arrows).*

4.2.2 – Phage-based Liquid Crystals

After determining the viability of M13-ELA phage in culture, several milligrams of pure viral particles were produced and used to synthesize LCs. Particular efforts have been made to ensure the purity of each batch of phages. To dilute residual protein contaminants, the pahge pellet was resuspended in PBS and recovered using the already described PEG precipitation method and dialized extensively with ultra pure water. Finally, the pahge suspension was freeze-dryed.

In the next step, my collegue, Kai Liu was transforming the phage particles into LCs. Briefly, two surfactants: dimethyldioctylammonium bromide (DOAB) and didodecyldimethylammonium bromide (DDAB) were used to form ionic complexes with the phage particles. In fact, the N-terminal glutamate and aspartate residues of the p8 protein (NH2-VPGVGAEGDDPA···-COOH; negatively charged residues are underlined) electrostatically interact with the cationic head groups of the surfactants.

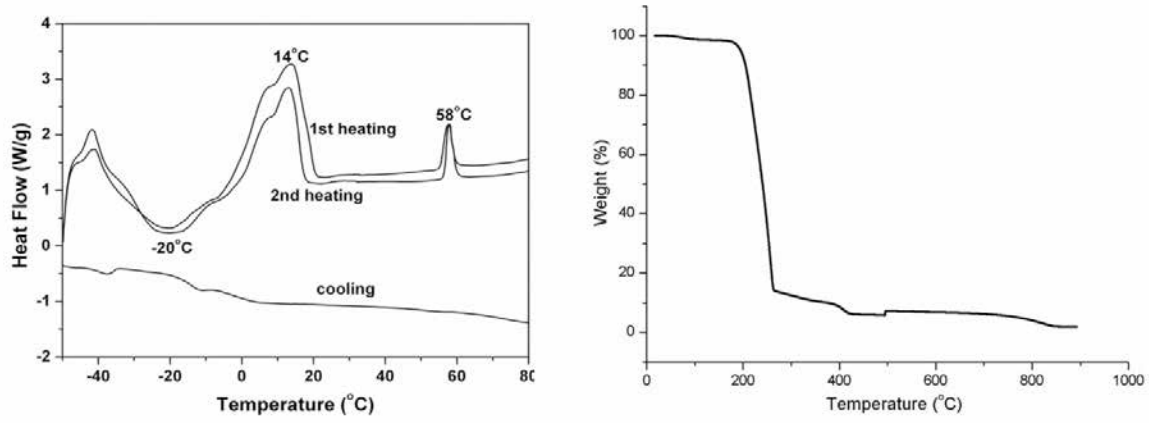

Figure 9. ***Characterisation of phage-DOAB-DDAB complex.*** *On the left, differential scanning calorimetry (DSC) traces are shown (at a heating/cooling rate of 5 °C/min) with two phase transitions of the phage-DOAB-DDAB complex, detected at 14 and 58 °C, corresponding to crystalline– smectic and smectic–isotropic transitions, respectively. The graph on the right shows the results of thermogravimetric analysis (TGA) of phage-DOAB-DDAB complexes. The water content was very low (less than 2%) and the thermal degradation started as the temperature reached 200 °C.*

It was found that complexation of the phage particles with mixed surfactants of DOAB and DDAB, leads to a smectic mesophase with typical focal-conic birefringence at a temperature range of 14–58 °C (Figure 9).

Moreover, SAXS and WAXS measurements (Figure 10) showed smectic layer reflection (q = 0.0686 $Å^{-1}$) and its harmonics (q = 0.1371, 0.208 $Å^{-1}$) with a periodicity of 91.5 Å. The layer spacing corresponds to a bilayer structure made of a sublayer of phage (~70 Å) and an interdigitated sublayer of surfactants (DOAB and DDAB; ~21.5 Å). Each repeating layer consists of tail-to-tail interacting surfactants that protrude from the phage particle.

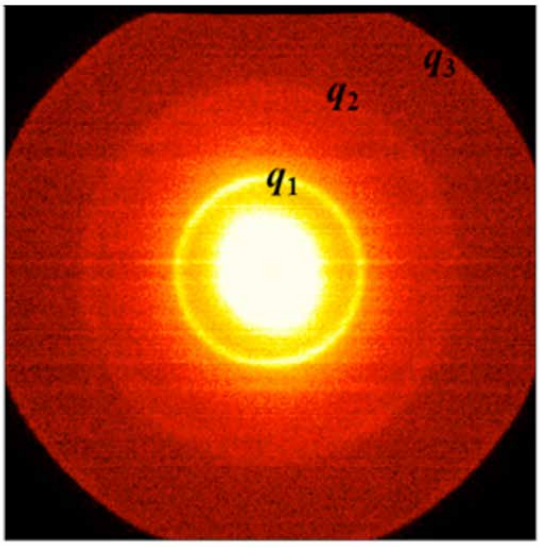

Figure 10. ***Characterisation of phage-DOAB-DDAB complex by SAXS.*** *The picture shows pattern of oriented phage-DOAB-DDAB complex at 25 °C upon cooling. The diffraction rings at q_1, q_2, and q_3 are the first, second, and third orders of the 91.54 Å layer spacing.*

Long-range periodic layer structures in the mesophase were confirmed by freeze-fractioned (FF)-TEM studies (Figure 11). The fractured plane revealed individual phages globally, along a preferred direction. Nematic orientational ordering had developed between different phages within the sublayer as a result of the rigidity and large length-to-diameter aspect ratio of phage.

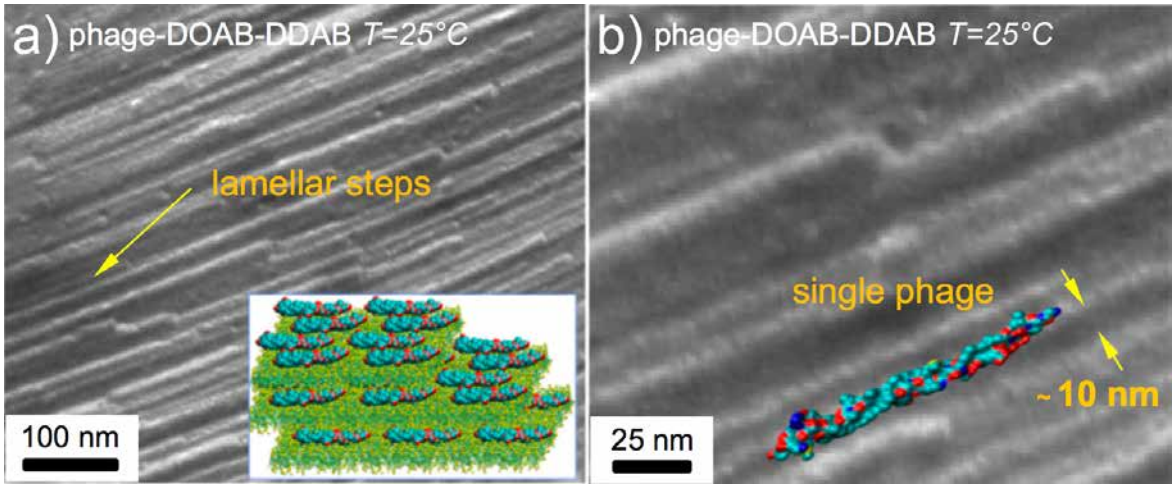

Figure 11. ***FF-TEM images of the mesophases formed by the phage–surfactant complexes.*** *Periodicities of 12 nm; and 50 nm are evident in the FF-TEM images (a), and its zoomed version (b). Long-range ordered lamellar structure of the phage–DOAB– DDAB-complexes, where individual phages were identified at the layer edges, indicating the orientational order of phages within the sub layer. The layer spacing matches well with the SAXS data.*

4.3 – Conclusions

With this work, we were able to demonstrate how little modifications on the protein p8 can lead to great changes in the chemical and physical properties of the complete capsid. A simple amino acid sobstitution, for example, allowed us to control the degree of chemical functionalisation of the capsid. Finally, we showed that phages can be effectively used as building blocks for the fabrication of new hybrid materials like thermotropic liquid crystals.

Given the stability of such a particle, their wide degree of functionalisation and the ease of engineering their surfaces using simple PCR methods; M13 phages have enormous potential to serve as versatile bulding blocks in materials science.

4.4 – Experimental section

Two steps mutagenesis

The vector M13-pVIII-VPGVG, that produces M13-ELA phages, was obtained by two-step PCR mutagenesis of M13-wild type DNA (New England Biolab). The VPGVG coding sequence was added at the N-terminus of the pVIII coding region between the peptidase signal and the first alanine of the mature protein. The following oligonucleotides (Sigma) were used for cloning.

p8 Elastin Forward Primer:

3′-GTTCCGATGCTGTCTTTCGCTGTCCCAGGTGTTGGTGTGCCTGGCGTGGGCGCTGAGGG
TGACGATCCCGCAAAAG-5′

p8 Elastin Reverse Primer:

3′-CTTTTGCGGGATCGTCACCCTCAGCGCCCACGCCAGGCACACCAACACCTGGGACAGCGA
AAGACAGCATCGGAAC-5′

The oligos were phosphorylated using polynucleotide kinase (PNK; Fermentas) following the manufacturer's protocol. In the first step, PCR was performed using only the reverse primer to generate the mutated reverse strand that was used as template for the second PCR in which the forward primer was employed to form a circular double nicked dsDNA that carried the mutated p8 gene. The PCR procedure consisted of 25 cycles of 8° C for 3 min, 55° C for 1 min, and 72° C for 8 min. Phusion HD DNA Polymerase (Thermo Scientific) was employed for amplification.

The resulting PCR product was purified by the Wizard SV Gel, PCR Clean-Up System (Promega), and transformed by electroporation into electrocompetent E.coli ER2738. The transformed cells were incubated for 1 h at 37° C and then plated on agar plates containing X-gal/isopropyl-β-D-1-thiogalactopyranoside (IPTG)/tetracycline. The plates were incubated at 37° C overnight. Single colonies were amplified and DNA was purified from supernatant using QIAprep Spin M13 Kit (QIAGEN). The insertion of the VPGVG coding sequence was confirmed by DNA sequencing (GATC Biotech, Germany)

Analysis of mutant phage particles by MALDI TOF mass spectometry

The genetically modified viruses were amplified using *E. coli* ER2738 in LB medium supplemented with tetracycline (10 g BactoTM tryptone, 5 g BBLTM yeast extract, 5 g NaCl per liter), purified twice by standard PEG/NaCl precipitation method, resuspended in water, to obtain at a final concentration of 10^{12}-10^{13} pfu/. One milliliter aliquots of the phage in water suspension were frozen in liquid nitrogen, lyophilized and stored at -20° C until further use. PEG-purified phages were analyzed through matrix-assisted laser desorption/ionization time-of-flight (MALDI-TOF) mass spectrometry. Therefore, 2,5-dihydroxybenzoic acid (DHB) was used as matrix.

Microscopy

Wild type M13 and M13K8A functionalized with a fluorescent dye were visualized by fluorescence microscopy. A LED light (wavelength 570 nm) was used to excite the dye (Atto 565 NHS ester, SIGMA #72464) and the emission between 625-725 nm was measured with an acquisition time of 1 second. The objective used was a 63x and the magnification in the ocular was10x leading to a total magnification of 630x.

TEM characterisation

Phage solutions (10-100 nM) were placed on glow discharged plain carbon grids. These were subsequently stained with 2% uranyl acetate.

Preparation of phage-DOAB-DDAB complex

A volume of 100 μL of approximately 1 μM engineered phage aqueous solution was added to 100 μL of approximately 100 mM aqueous mixture of cationic lipids (final molar ratio DOAB:DDAB = 1:1). This mixture was shaken at room temperature till a precipitate was observed. The precipitate was collected by centrifugation and the supernatant was discarded. After lyophilization, further characterization of the material was carried out.

4.5 - References

1. Nakata, M. *et al.* End-to-End Stacking and Liquid Crystal Condensation of 6 to 20 Base Pair DNA Duplexes. *Science* 318, 1276–1279 (2007).
2. Koltover, I. An Inverted Hexagonal Phase of Cationic Liposome-DNA Complexes Related to DNA Release and Delivery. *Science* 281, 78–81 (1998).
3. Hamley, I. W. Liquid crystal phase formation by biopolymers. *Soft Matter* 6, 1863–1871 (2010).
4. Strzelecka, T. E., Davidson, M. W. & Rill, R. L. Multiple liquid crystal phases of DNA at high concentrations. *Nature* 331, 457–460 (1988).
5. Livolant, F. Ordered phases of DNA in vivo and in vitro. *Physica A: Statistical Mechanics and its Applications* 176, 117–137 (1991).
6. Livolant, F. & Bouligand, Y. Liquid crystalline phases given by helical biological polymers (DNA, PBLG and xanthan). Columnar textures. *Journal de Physique* 47, 1813–1827 (1986).
7. Yu, S. M. *et al.* Smectic ordering in solutions and films of a rod-like polymer owing to monodispersity of chain length. *Nature* 389, 167–170 (1997).
8. Dogic, Z. & Fraden, S. Ordered phases of filamentous viruses. *Current Opinion in Colloid & Interface Science* 11, 47–55 (2006).
9. Chung, W.-J. *et al.* Biomimetic self-templating supramolecular structures. *Nature* 478, 364–368 (2011).
10. Ramamoorthy, A. *Thermotropic Liquid Crystals*. (2007).
11. Briman, M., Armitage, N. P., Helgren, E. & Grüner, G. Dipole Relaxation Losses in DNA. *Nano Letters* 4, 733–736 (2004).
12. Yamahata, C. *et al.* Humidity dependence of charge transport through DNA revealed by silicon-based nanotweezers manipulation. *Biophysical Journal* 94, 63–70 (2008).
13. Lewis, F. D. *et al.* Distance-dependent electron transfer in DNA hairpins. *Science* 277, 673–676 (1997).
14. Hamad-Schifferli, K., Schwartz, J. J., Santos, A. T., Zhang, S. & Jacobson, J. M. Remote electronic control of DNA hybridization through inductive coupling to an attached metal nanocrystal antenna. *Nature* 415, 152–155 (2002).
15. Tanaka, K. & Okahata, Y. A DNA-Lipid Complex in Organic Media and Formation of an Aligned Cast Film. *Journal of the American Chemical Society* 118, 10679-10683 (1996).
16. Okahata, Y., Kobayashi, T. & Tanaka, K. Anisotropic electric conductivity in an aligned DNA cast film. *Journal of the American Chemical Society* 120 (1998).
17. Neumann, T., Gajria, S., Bouxsein, N. F., Jaeger, L. & Tirrell, M. Structural responses of DNA-DDAB films to varying hydration and temperature. *Journal of the American Chemical Society* 132, 7025–7037 (2010).
18. Gajria, S., Neumann, T. & Tirrell, M. Self-assembly and applications of nucleic acid solid-state films. *Wiley Interdisciplinary Reviews: Nanomedicine and Nanobiotechnology*

(2011).
19. Kwon, Y.-W., Choi, D. H. & Jin, J.-I. Optical, electro-optic and optoelectronic properties of natural and chemically modified DNAs. *Polymer Journal* 44, 1191–1208 (2012).
20. General, S. & Antonietti, M. Supramolecular organization of oligopeptides, through complexation with surfactants. *Angewandte Chemie International Edition* 41, 2957–2960 (2002).
21. Perriman, A. W., Cölfen, H., Hughes, R. W., Barrie, C. L. & Mann, S. Solvent-free protein liquids and liquid crystals. *Angewandte Chemie International Edition* 48, 6242–6246 (2009).
22. Mateu, M. G. Assembly, stability and dynamics of virus capsids. *Archives of Biochemistry and Biophysics* 531, 65–79 (2013).
23. Henry, T. J. & Pratt, D. THE PROTEINS OF BACTERIOPHAGE M13. *Proceedings of the National Academy of Sciences of the United States of America* 62, 800–807 (1969).
24. Chung, W.-J., Merzlyak, A., Yoo, S. Y. & Lee, S.-W. Genetically Engineered Liquid-Crystalline Viral Films for Directing Neural Cell Growth. *Langmuir : the ACS journal of surfaces and colloids* (2010). doi:10.1021/la100226u
25. Petrenko, V. A., Smith, G. P., Gong, X. & Quinn, T. A library of organic landscapes on filamentous phage. *Protein Engineering.* 9, 797–801 (1996).
26. Malik, P. *et al.* Role of Capsid Structure and Membrane Protein Processing in Determining the Size and Copy Number of Peptides Displayed on the Major Coat Protein of Filamentous Bacteriophage. *Journal of Molecular Biology* 260, 9–21 (1996).
27. Szardenings, M. Phage display of random peptide libraries: applications, limits, and potential. *J Recept Signal Transduct Res* 23, 307–349 (2003).
28. Nam, K. T. *et al.* Virus-enabled synthesis and assembly of nanowires for lithium ion battery electrodes. *Science* 312, 885–888 (2006).
29. Nam, K. T. *et al.* Stamped microbattery electrodes based on self-assembled M13 viruses. *Proceedings of the National Academy of Sciences of the United States of America* 105, 17227–17231 (2008).
30. Merzlyak, A., Indrakanti, S. & Lee, S.-W. Genetically engineered nanofiber-like viruses for tissue regenerating materials. *Nano Letters* 9, 846–852 (2009).
31. Naik, R. R., Stringer, S. J., Agarwal, G., Jones, S. E. & Stone, M. O. Biomimetic synthesis and patterning of silver nanoparticles. *Nature Materials* 1, 169–172 (2002).
32. Sweeney, R. Y., Park, E. Y., Iverson, B. L. & Georgiou, G. Assembly of multimeric phage nanostructures through leucine zipper interactions. *Biotechnology and Bioengineering* 95, 539–545 (2006).
33. Kriplani, U. & Kay, B. K. Selecting peptides for use in nanoscale materials using phage-displayed combinatorial peptide libraries. *Current Opinion in Biotechnology* 16, 470–475 (2005).
34. Heckman, K. L. & Pease, L. R. Gene splicing and mutagenesis by PCR-driven overlap extension. *Nature Protocols* 2, 924–932 (2007).
35. Innis, M. A., Gelfand, D. H., Sninsky, J. J. & White, T. J. *PCR protocols: a guide to methods and applications*. (2012).
36. Zuker, M. Mfold web server for nucleic acid folding and hybridization prediction.

Nucleic Acids Research 31, 3406–3415 (2003).
37. Li, Z., Koch, H. & Dübel, S. Mutations in the N-terminus of the major coat protein (pVIII, gp8) of filamentous bacteriophage affect infectivity. *Journal of Molecular Microbiology and Biotechnology* 6, 57–66 (2003).
38. Liu, K. *et al.* Thermotropic liquid crystals from biomacromolecules. *Proceedings of the National Academy of Sciences* 111**,** 18596–18600 (2014).
39. Lillie, M. A. & Gosline, J. M. The effects of hydration on the dynamic mechanical properties of elastin. *Biopolymers* 29, 1147–1160 (1990).
40. Mistrali, F., Volpin, D., Garibaldo, G. B. & Ciferri, A. Thermodynamics of elasticity in open systems. Elastin. *The Journal of Physical Chemistry* 75, 142–149 (1971).
41. Urry, D. W. Entropic elastic processes in protein mechanisms. I. Elastic structure due to an inverse temperature transition and elasticity due to internal chain dynamics. *Journal of Protein Chemistry.* 7, 1–34 (1988).
42. Urry, D. W., Shaw, R. G. & Prasad, K. U. Polypentapeptide of elastin: temperature dependence of ellipticity and correlation with elastomeric force. *Biochemical and Biophysical Research Communications* 130, 50–57 (1985).
43. Urry, D. W., Trapane, T. L. & Prasad, K. U. Phase-structure transitions of the elastin polypentapeptide-water system within the framework of composition-temperature studies. *Biopolymers* 24, 2345–2356 (1985).
44. Urry, D. W., Trapane, T. L., Iqbal, M., Venkatachalam, C. M. & Prasad, K. U. Carbon-13 NMR relaxation studies demonstrate an inverse temperature transition in the elastin polypentapeptide. *Biochemistry* 24, 5182–5189 (1985).

Chapter 5

Evaluation of new aminoglycoside antibiotics

Abstract

Several new antibiotics have been produced by functionalisation of Neomycin B using a new technology called "aptameric protective groups" whereby a RNA aptamer is used as non covalent protective group for the modification of aminoglycosides. The derivatives obtained have been tested on Escherichia coli to determine their antimicrobial activities. The results we report in this chapter show that several new aminoglycoside derivatives are highly active antibiotics.

5.1 - Introduction

During my PhD adventure I had the fortunate chance of being involved in an already running and very promising project centered on functionalization of antibiotics by supramolecular chemistry. The project was initiated by Prof. Herrmann and carried out by my colleague Dr. Andreas Bastian. The idea behind this project was simple and yet innovative: leverage the host-guest complex formed by aptamers and complexed molecules to perform site-specific reactions with only few steps and high yield.

By non-covalently interacting with a complex natural product, the aptamers block the reactivity of several functional groups. The chemical functionalities not in contact with the aptamers can be regioselectively transformed in a chemical reaction.

This kind of approach resulted extremely advantageous in cases in which one has compounds that exhibit several chemical equivalent groups and the goal is to modify only one of these groups. The case study selected to demonstrate the efficacy of such an approach was focused on the functionalisation of a special class of antibiotics, the aminoglycosides (Figure 1), which are complex carbohydrates containing multiple amino and hydroxy groups.

As many natural products, this class of antibiotics is difficult to synthesise from scratch or to functionalise in a specific and effective manner and for this reason it is hard to come up with new promising derivatives. In the meantime, the world is facing the rise of antibiotic resistant bacteria and pharmaceutical companies struggle to bring new active molecules to the market. One main problem they face is the efficient production of derivatives of already known compounds because, as stated before, the modification of complex natural products can be extremely costly and time-consuming. However, Dr. Bastian produced a multitude of new antibiotic derivatives by employing the aptameric protective group (APG) technology.

This chapter illustrates just the key concepts of the aptameric protective groups since this work has been already extensively covered by Dr. Bastian's thesis (Bastian, A. A. 2012) and pubications.[1,2]

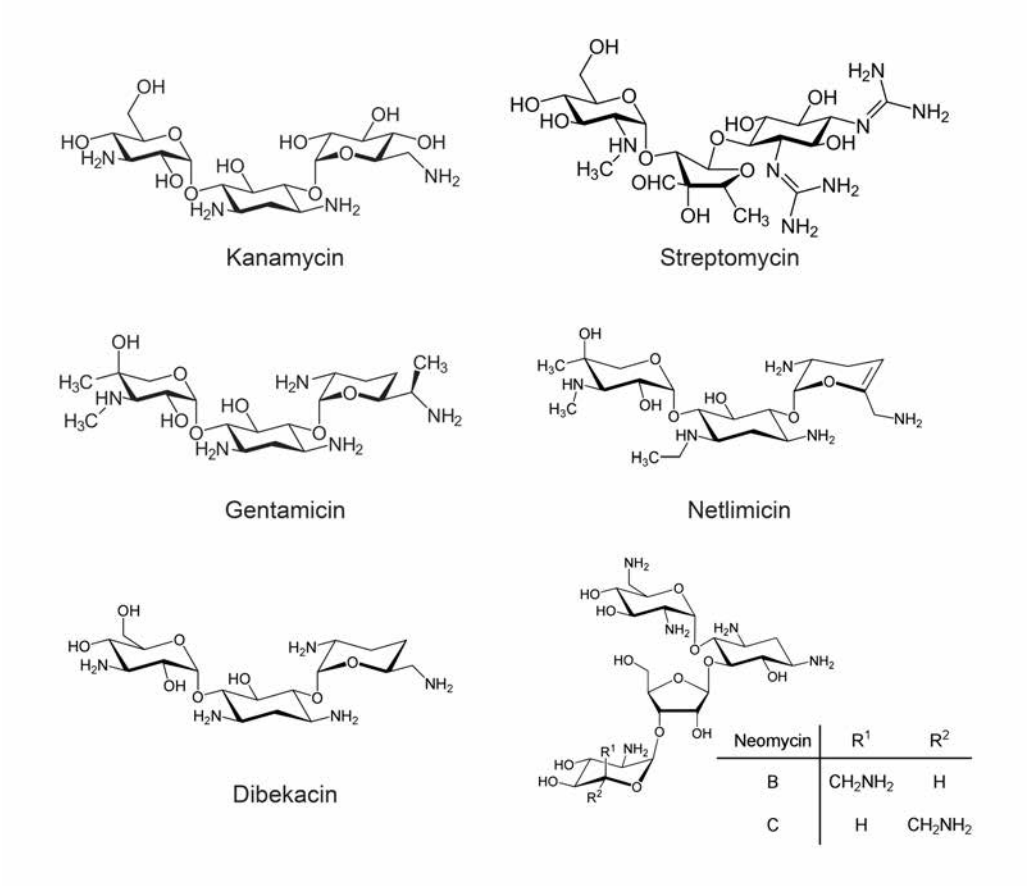

Figure 1. *Overview of the structure of the most used aminoglycosides antibiotics. Characteristic of this class of carbohydrates is the presence of two or more amino sugars connected by glycosidic bonds*

The majority of this work will focus instead on the antimicrobial activity of the aminoglycoside antibiotics and on the potency of their derivatives obtained in the Herrmann lab. Hopefully, the reader will be convinced about the power of the new aptameric protective group technology and its utility for the derivatisation of complex natural products.

5.1.1 - Aminoglycoside antibiotics

Aminoglycosides are highly potent, broad-spectrum class of antibiotics chemically composed by two or more amino sugars connected by glycosidic bonds. Their history begins in 1944, when Streptomycin was discovered by Selman Abraham Waksman who derived it from actinobacterium *Streptomyces griseus* and received for it the Nobel Prize in Physiology and medicine in 1951.[3,4] Remarkably, Streptomycin (Fig. 1.1) was the first antibiotic remedy for tuberculosis[5,6] and it was followed by a series of milestone compounds (Fig 1) like Neomycin,[7] Kanamycin, Gentamicin, and Tobramycin, with many advantageous properties for the treatment of life-threatening infections establishing the utility of aminoglycosides for the treatment of bacterial infections.

The therapeutic history of aminoglycoside antibiotics is characterised by cycles of positive and negative opinions on their effects and their usage for treatment of bacterial infections.[8,9] The main point against their usage is the occurrence of nephrotoxicity and ototoxicity, however, a strong argument for their application is the fact that aminoglycosides do retain activity against the majority of Gram-negative clinical bacterial isolates in many parts of the world. [10,11]

Bacteria developed several resistance mechanisms to overcome the effects of aminoglycoside antibiotics [12].

Three distinct mechanisms are known:

- alteration of the ribosomal binding sites
- decreased uptake and/or accumulation of the drug in bacteria
- expression of enzymes, which modify the antibiotic and thereby inactivate it

Resistance to Streptomycin that binds to a single site on the 30S subunit of the ribosome, can occur as consequence of a single alteration of the ribosomal binding site. The same mechanism is uncommon for other aminoglycosides since they bind to multiple sites on both ribosomal subunits and high-level resistance cannot be selected in a single step. The other two resistance strategies affect the whole class of aminoglycoside antibiotics. Changes in membrane permeabilisation due to a transport defect is the cause

of reduced drug uptake. Even if the underlying molecular mechanisms are largely unknown, this phenomenon has been frequently observed in *Pseudomonas aeruginosa* and other gram-negative bacteria where it confers moderate resistance.

In contrast, enzymatic modification is the most common type of aminoglycoside resistance and often the action of a single enzyme results in a high level of resistance.

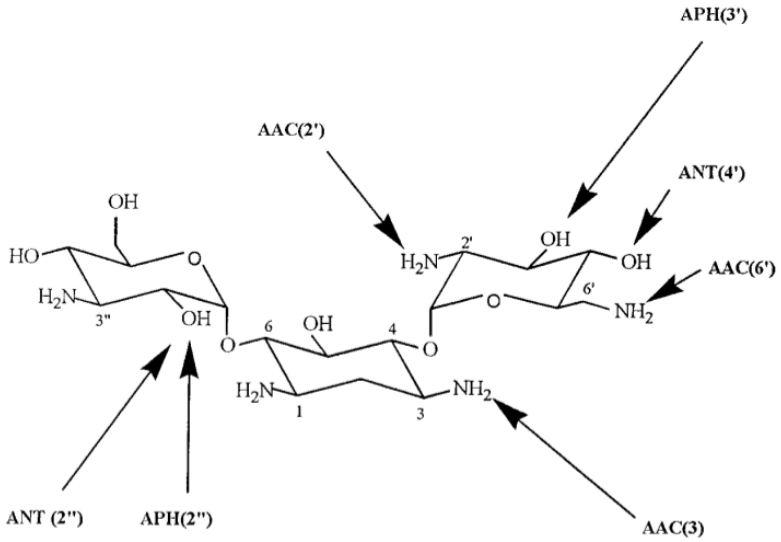

Figure 2. Structure of the aminoglycoside susceptible functions. *The functional groups affected in typical aminoglycosides (kanamycin and gentamicin derivatives) are on positions 3, 2′, and 6′ for AAC, positions 4′ and 2′′ for ANT; and positions 3′ and 2′ for APH.* [13]

Bacteria have evolved more than 50 different enzymes divided in three main groups (Table 1) including N-acetyltransferases (AAC), O-adenyltransferases (ANT) and O-phosphotransferases (APH). AAC enzymes catalyse the acetyl CoA-dependent acetylation of an amino group. ANTs facilitate ATP-dependent adenylation of hydroxyl groups. APH enzymes catalyse the ATP-dependent phosphorylation of specific aminoglycoside hydroxyl groups (Fig 2). [13]

The following table (Table 1, adapted from [14]) lists common genes encoding for aminoglycoside-modifying enzymes (this table is not complete).

Enzyme	Genes	Aminoglycoside Substrates
Acetylation		
AAC(3)-I	aac(3)-Ia aac(3)-Ib	Gm
AAC(3)-II	aac(3)-IIa aac(3)-IIb aac(3)-IIc	Gm, Tob
AAC(3)-III	aac(3)-IIIa aac(3)-IIIb aac(3)-IIIc	Gm, Tob, Km, Neo, Prm
AAC(3)-IV	aac(3)-Iva	Gm, Tob
AAC(3)-VI	aac(3)-Via	Gm
AAC(6′)-I	aac(6′)-Ia … aac(6′)-Ii	Tob, Amk
AAC(6′)-II	aac(6′)-IIa aac(6′)-IIb	Gm, Tob
AAC(6′)-APH(2″)	aac(6′)-aph(2″)	Gm, Tob, Amk
AAC(2′-I)	aac(2′)-Ia	Gm, Tob
Adenylylation		
ANT(2″)-I	ant(2″)-Ia ant(2″)-Ib ant(2″)-Ic	Gm, Tob, Km
ANT(3″)-I	ant(3″)-Ia	Sm, Spcm
ANT(4′)-I	ant(4′)-Ia	Tob, Amk
ANT(4′)-II	ant(4′)-IIa	Tob, Amk
ANT(6)-I	ant(6)-Ia	Sm
Phosphorylation		
APH(2″)-I	aph(2″)-Ia	Gm, Tob, Amk
APH(3′)-I	aph(3′)-Ia aph(3′)-Ib aph(3′)-Ic	Km, Neo, Prm
APH(3′)-II	aph(3′)-IIa	Km, Neo, Prm, GmB
APH(3′)-III	aph(3′)-IIIa	Km, Neo, Prm, Amk, GmB
APH(3′)-IV	aph(3′)-Iva	Km, Neo, Prm
APH(3′)-V	aph(3′)-Va aph(3′)-Vb aph(3′)-Vc	Neo, Prm
APH(3′)-VI	aph(3′)-Via aph(3′)-Vib	Km, Neo, Prm, Amk, GmB
APH(3′)-VII	aph(3′)VIIa	Km, Neo

Enzyme	Genes	Aminoglycoside Substrates
APH(3″)-I	aph(3″)-Ia aph(3″)-Ib	Sm
APH(6)-I	aph(6)-Ia aph(6)-Ib aph(6)-Ic aph(6)-Id	Sm

Table 1. Aminoglycoside resistance genes and respective aminoglycoside-modifying enzymes. *Abbreviation key: Amk, Amikacin; Gm, Gentamicin; GmB, Gentamicin B; Km, Kanamycin; Neo, Neomycin; Pm, Paromomycin; Spcm, Spectinomycin; Sm, Streptomycin; Tob, Tobramycin. The Roman numerals and letters that follow stand for unique resistance profiles and protein designations, respectively. The nomenclature is defined as follows: AAC, ANT, or APH for the type of enzymatic modification, followed by a number in parentheses designating the site of modification.*

5.1.2 - Aptamers as supramolecular protective groups

Regioselective modification of complex molecules, like natural products, is a very complex task that often requires dozens of consecutive reactions leading to a very poor yield. The modification of aminoglycoside antibiotics is a very good example of these limitations. Since a molecule like Neomycin contains several —almost equally reactive— primary amino groups, the realization of its derivatives requires a labour-intensive semi- or total synthesis.

One approach that aims to solve this issue is the use of supramolecular protective groups able to selectively shield all primary amines except the one that is modified. These supramolecular protective groups consist of nucleic acids and are termed aptamers since they strongly bind to its target. Very similar to phage display, the SELEX (Systematic evolution of ligands by exponential enrichment) [15,16] method allows for the selection of RNA aptamers. Aptamers with high selectivity and specificity towards aminoglycoside antibiotics were already reported in the literature and my colleague Dr. A. Bastian focused his PhD work on exploring the applicability of such RNA aptamers as supramolecular

protective groups for an efficient and fast derivatisation of several aminoglycoside antibiotics (Figure 3, from [1]).[1,17]

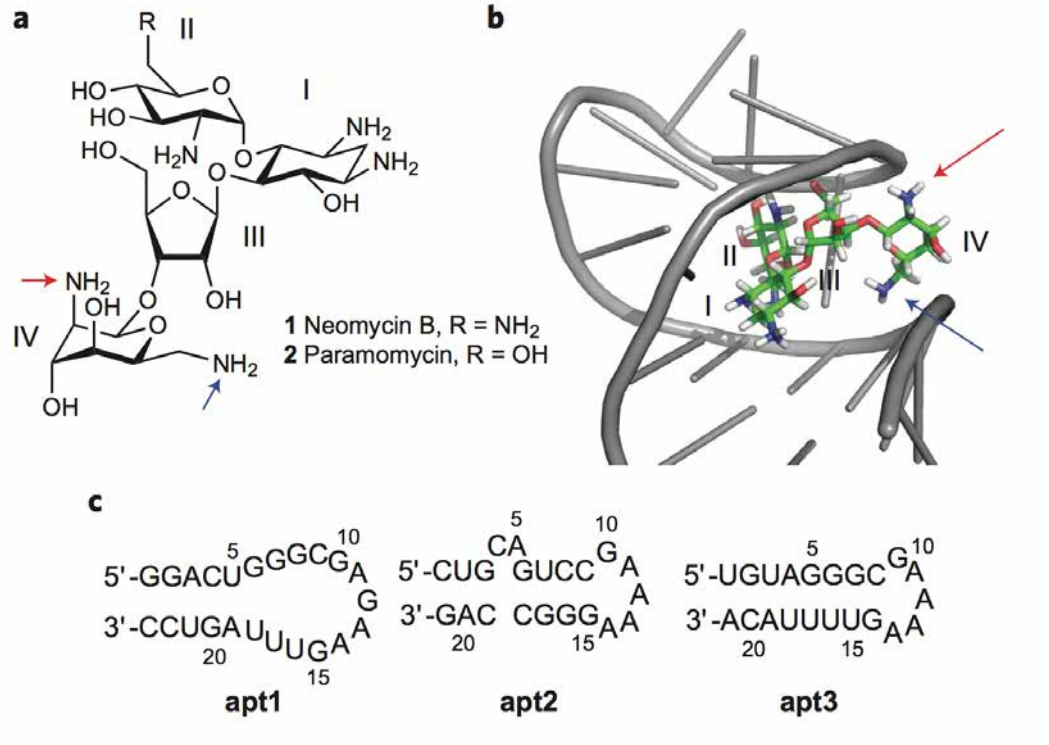

Figure 3. Structures of aminoglycosides, protection mode and sequences of APGs.

a) Structure of two aminoglycoside antibiotics. b) Apt1 selectively protecting neomycin B (ref. 16) (green, carbon; red, oxygen; blue, nitrogen; white, hydrogen). c) Sequences of applied APGs apt1, apt2 and apt3. The arrows indicate accessible amino groups of neomycin B ring IV for derivatisation by applying acylation (blue arrows) and urea bond formation (red arrows).

5.1.3 - Antimicrobial susceptibility tests

The evaluation of the antimicrobial activity of antibiotics is generally carried out following standard procedures, which can be divided in dilution method and disk diffusion methods. In dilution tests, microorganisms are tested for their ability to produce visible growth on a series of agar plates (agar dilution) or in microplate wells of broth (broth microdilution) containing dilutions of the antimicrobial agent. Dilutions methods are considered very accurate and are often used as reference for others antimicrobial susceptibility tests like the disk diffusion. The aim of a dilution test is to determine the

minimal inhibitory concentration (MIC), a concentration at which a target antimicrobial agent inhibits the visible growth of a specific microbe.

In contrast, the disk diffusion method, also called Kirby-Bauer diffusion test or agar diffusion test, relies on paper disks impregnated with antibiotics. The disks are deposited on top of a agar plate previously inoculated with bacteria and the plate is incubated to allow bacterial growth. If an antibiotic stops the bacteria from growing or kills the bacteria, there will be an area around the disks where the bacteria have not grown enough to be visible. This is called a zone of inhibition and its diameter depends on the antibiotic potency and can be directly correlated with the MIC. The larger the area of the inhibition zone is, the greater is the antibiotic potency and lower is the MIC value.

At the beginning of this study, the disk diffusion method was used to evaluate the efficiency of the first few derivatives. Later on, since the number of samples to test increased significantly, the dilution method proved to be a faster way to compare the efficiency of many antibiotics at once. In terms of the results obtained, both methods proved to be reliable and interchangeable.

It is important to note that the MIC value of a specific agent also depends on the growth medium of choice. In this work the medium of choice was Muller Hinton II (MH) that is the most widely used medium internationally and also recommended as reference medium by the Clinical and Laboratory Standards Institute (http://clsi.org). The overall goal of this study is to determine whether the new aminoglycoside derivatives produced in the Herrmann group are effective against a variety of different bacterial strains and different resistance enzymes. A first set of experiments was carried out on *E. coli* ATCC 25922, a standard laboratory strain, and two different resistance enzymes: acc(3')-IV and aph(3')-I.

5.2 - Results and Discussion

After the successful synthesis of novel neomycin B derivatives employing the aptameric protective group technology, compounds 4a, 5 and 8a–8c (Figure 4) were investigated for their antimicrobial activities against *E. coli* ATCC 25922.Two methods, the Kirby-Bauer disc test and the determination of the minimal inhibitory concentration (MIC) were employed for this purpose. As shown in Table 2, all of the derivatives tested remained highly active antibiotics. Therefore, we can exploit the APG technology directly to gain new structure–property relationships. From inspection of the structures, one can conclude that larger residues at the amino groups of ring IV are well tolerated and do not significantly decrease antimicrobial activity.

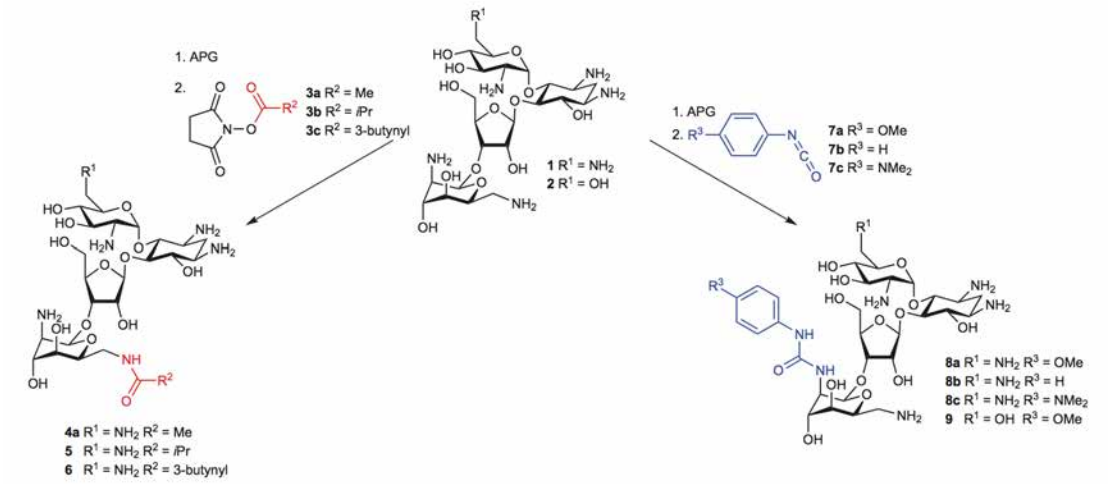

Figure 4. Structures of Nomycin derivatives. *a) Structure of representative aminoglycoside antibiotics. b) apt1 selectively protecting neomycin B (ref. 16) (green, carbon; red, oxygen; blue, nitrogen; white, hydrogen). c) Sequences of applied APGs apt1, apt2 and apt3. The arrows indicate accessible amino groups of neomycin B ring IV for derivatisation by applying acylation (blue arrows) and urea bond formation (red arrows).*

After these first promising results new derivatives were produced (Figure 5) by Eliza Warszawik who is also a PhD student in the Herrmann group. These new compounds have been obtained using a different approach that does not require the use of aptameric protective groups but that leads to the functionalization of the C3-position of the 2-desoxystreptamine ring of neamine antibiotics.[2] A comparative MIC test for all the

compounds on *E. coli* expressing two differt resistance genes has been executed in order to verify the effects of the different derivatives. Our final goal is to find a suitable functional group that helps to reduce the affinity of the derivative toward the resistance enzyme while keeping reasonable antibacterial activity meaning still able to bind to the bacterial ribosomal subunit.

Compound	Diameter† (mm)	MIC (μM)
1	16.8	3.1
1‡	16.1	3.1
2‡	13.2	12.5
4a	13.9	6.3
5	11.5	12.5
8a	12.7	6.3
8b	12.9	6.3
8c	15.1	6.3

Table 2. Antimicrobial activity of modified aminoglycosides. *All compounds were used as heptafluorobutyric acid (HFBA) salts, except for neomycin B sulfate 1 (Sigma Aldrich). †The zones of inhibition of E. coli ATCC 25922 as determined by the Kirby–Bauer disc method are given. For all compounds, the molar amount was kept constant at 17.5 nmol. ‡Antibiotic HFBA salt, purified by HPLC using the same conditions as those for neomycin B derivatives 4a, 5 and 8a–8c.*

Of course, due to the vast number of different resistance enzyme, some modifications may work for specific classes of enzymes but not for others. At the moment we focused on two resistance genes vastly spread among gram negative bacteria: aph(3')-I and acc(3')-IV.

The results (Figure 6) show that at least one compound, 148, is able to retain a significant antibaterial activity even in presence of two of the most spread aminoglicoside resistance enzymes. Indeed, the MIC value for this compound resulted to be around 0.06 μM, comparable with Amikacin and stronger than Kanamycin. Compound 446, showed a

strong antibacterial activity at higher concentration than Neomycin but comparable with Amikacin and Kanamycin, however, the effects of these compound are severely reduced, but not nullified, upon presence of resistance enzymes aph-3 or acc-3-4. All other new derivatives of Neomycin B did not show an antibacterial activity against *E. coli*. These results indicate that the epimerisation of the hydroxy group of ring II at position 3 only slightly diminishes binding of 446 to the ribosome evidenced by the lower activity compared to non-modified Neomycin B.

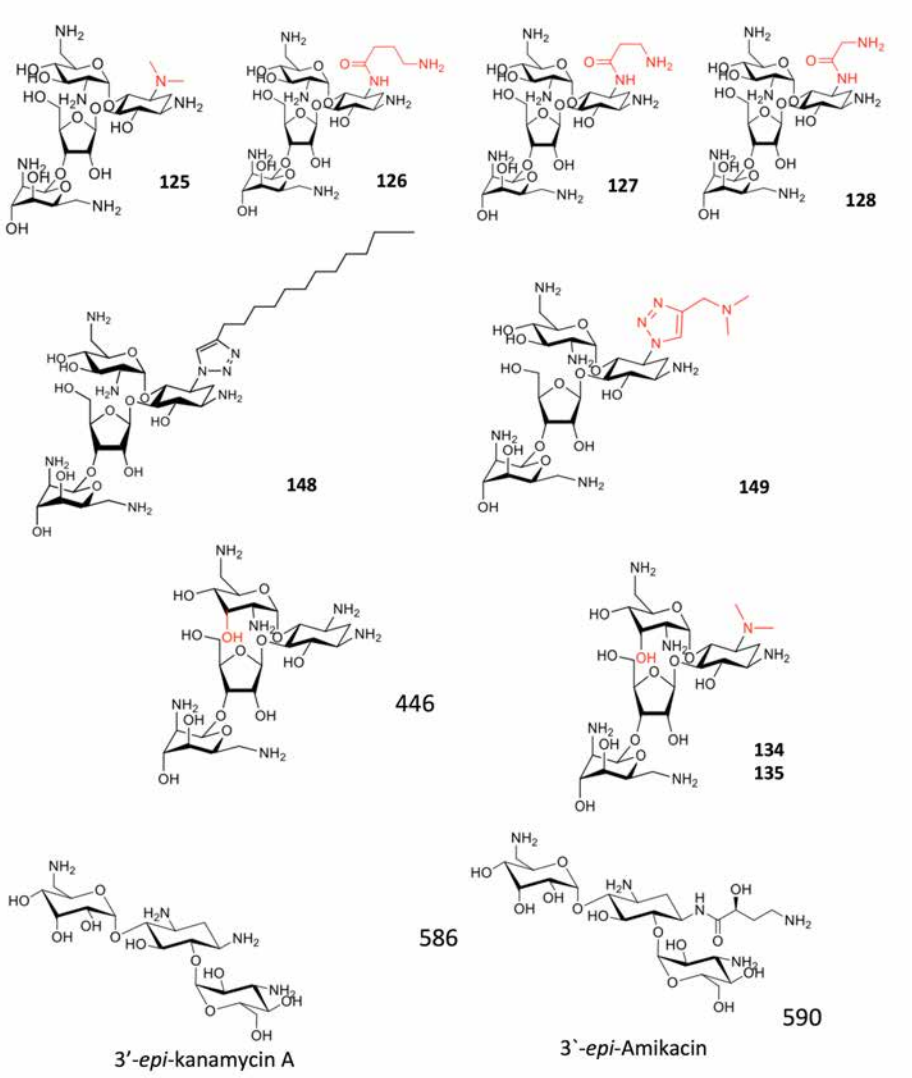

Figure 5. ***Structures of novel Nomycin derivatives functionalized ot the position 3 of the 2-desoxy streptamine ring (compounds 125, 126, 128, 134, 148 and 149).*** *Moreover, compound 446 is not modified at ring I but rather at ring II. In this compound the hydroxy group at position 3 is in an axial position while in Neomycin B it is in an equatorial configuration. Compound 134 is modified at ring I and ring II.*

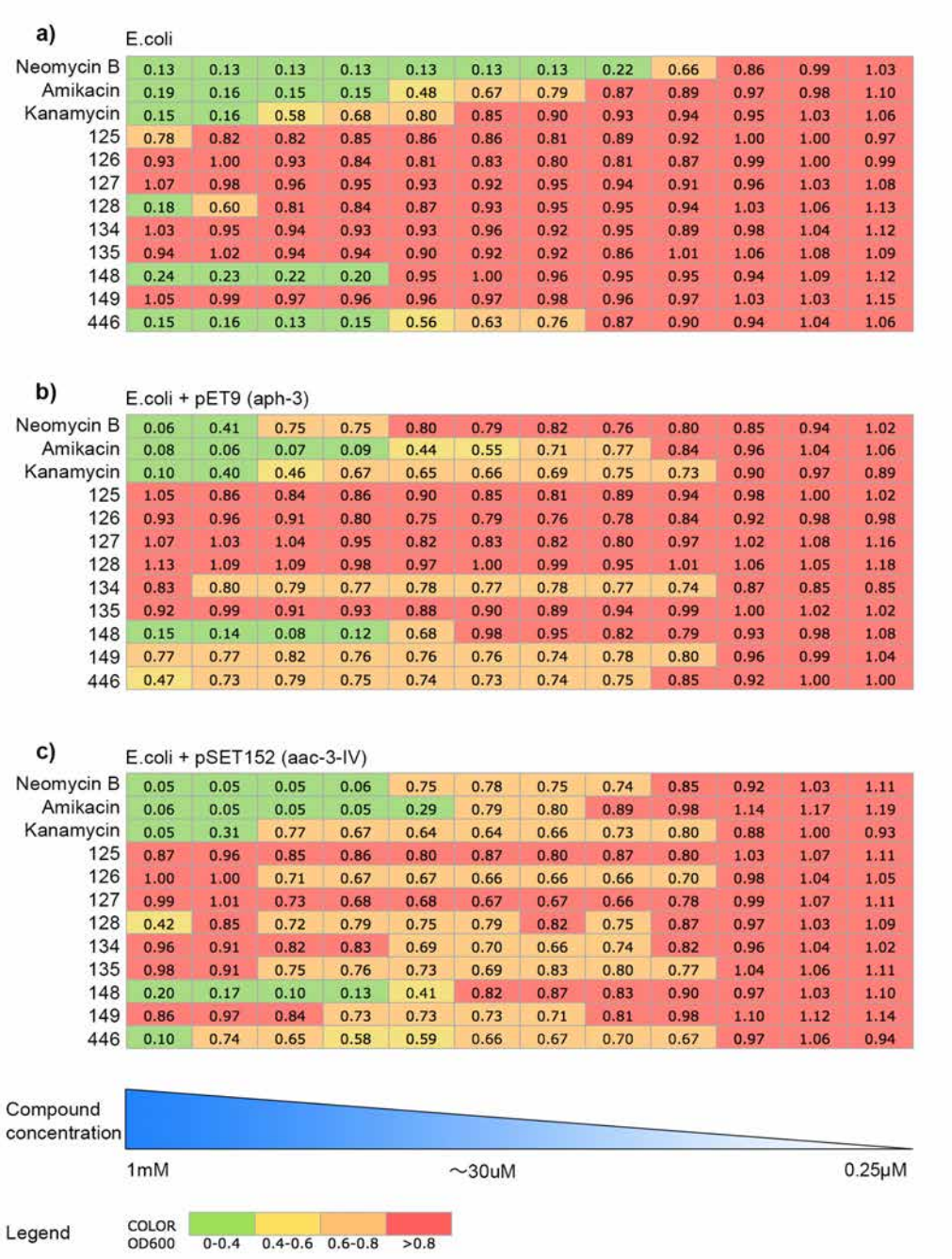

Figure 6. MIC test of novel aminoglycoside derivatives. *The OD_{600} of E.coli ATCC 25922 expressing a) no resistance enzyme , b) aph(3')-I resistance enzyme coded by the plasmid pET9 and c) acc(3')-IV coded by the plasmid pSET152, was determined for different aminoglycoside derivatives at various concentrations ranging from 1mM to 0.25µM. Neomycin, Amikacin and Kanamycin have been used as references. The numbers in the cells represent the OD600 detected (average of three repetitions) after overnight culture. The colors indicate the level of growth of the bacteria grouped by OD600: green) OD600 between 0 and 0.4 (bacteria do not grow), yellow) OD600 range = 0.4-0.6 (partial growth inhibition) , orange) OD600 range 0.6-0.8 (weack growth inhibition), red) OD600 >0.8 (no inhibition)*

The fact that all other new derivatives of Neomycin B, except 148, are ineffective in killing bacteria, suggest that 148 follows a different mechanism of exerting its antimicrobial actibity. Due to its highly amphiphilic character, it might interact with the membrane. A similar effect is seen for antimicrobial peptides, which, like 148, contain positive charges and hydrophobic groups. From the derivatisations of the amino group in 3 position of the 2-streptamine ring, one can conclude that the amine is very important for binding to the ribosome and it might be involved in hydrogen bonding acting as hydrogen donor.

5.3 - Conclusions

Regioselective modification of amynoglicosides allows for fast production of several derivatives with promising potential for the development of new antibiotics. The use of aptamers as supramolecular protective groups and other strategies developed in the last few years in the Herrmann group shortcuts existing fabrication routes to produce new aminoglycoside antibiotics. The activity of such derivatives is hard to predict, minor changes in the structure may lead to very large differences in terms of antibacterial activity. Up to now, we have not found any novel antibiotic with an increased antibacterial activity compared to the original natural compound, neverthless, some of the molecules obtained showed high activity comparable with Neomycin, Amikacin and Kanamycin and one, remarkably, showed low susceptibility to resistance enzymes. In particular, from the data accumulated so far, we can conclude that modifications on ring IV do not lead to a significant drop in activity, whereas almost all the derivatives obtained by modifications on ring II showed very little, if any, antimicrobial activity. An exceptional case, notably, is compound 148, that showed a reasonably high antibacterial activity despite the addition of a long alkyl chain in ring II.

For this compound, other characteristics, like nefrotoxicycty, need to be tested in future experiments.

5.5 - Experimental section

Preparation of electrocompetent cells

This protocol is derived from the work of Ausbel and Miller and it was used for the preparation of any electrocompetent cell described in this thesis[18,19] 500 mL of L-broth was inoculated with 5 mL of an overnight E. coli culture. The cells were grown at 37 °C shaking at 300 rpm until OD600 reached approximately 0.5–0.7. Cells were chilled on ice for ~20 min and then harvested by centrifuging at 4000x g for 15 minutes at 4 °C. The bacterial pellet was gently resuspended with 500 mL of ice-cold 10% glycerol and centrifuged again at 4000x g for 15 minutes at 4 °C. The obtained pellet was resuspended in half of the original volume (250 mL) of ice-cold 10% glycerol. The centrifugation/resuspension procedure was repeated two more times reducing the final resuspension volume every time. The final bacterial pellet was resuspended in 1–2 mL of ice-cold 10% glycerol reaching a final cell concentration of $1–3x10^{10}$ cells/mL. Aliquots of 0.08 mL were prepared and fast freezed in liquid nitrogen and then stored at -80 °C.

Bacterial strains

Escherichia coli ATCC 25922. This strain was purchased from ATCC (http://www.lgcstandards-atcc.org/). The organism is a serotype O6, biotype 1, commonly used as control strain for antimicrobial susceptibility testing of neomycin, colistin, kanamycin, cephalexin, gentamicin, cefamandole, cephalothin, tetracycline, cephaloglycin, cephaloridine, nalidixic acid, and chloramphenicol. A colony picked from a freshly made plate of the bacteria strain E.coli ATCC 25922 was used to inoculate 20 mL of Mueller-Hinton broth and the obtained culture was grown overnight at 37 °C and 250 RPM.

Escherichia coli ATCC 25922 harbouring acc(3′)-IV or aph(3′)-I. Electrocompetent aliquots of ATCC 25922 cells were prepared as reported above. One aliquot was transformed with 4 μl of plasmid pSET152 or pET9 (15 ng/μl) and plated on MH-agar supplemented with Neomycin B. Single colonies were used to inoculate 20 mL of MH

broth supplemented with Neomycin B. Cultures were grown overnight at 37°C shacking at 250 RPM.

Antibiotic disks preparation

Paper disks (6 mm diameter, BBL Microbiology Systems) were wetted through with 20, 25, 30 and 35μl of solution containing the antibiotic sample at a concentration of 0.5 nMol/μl. The wet disks were dried in a desiccator overnight, and used the next day.

Kirby-Bauer test

A refreshed culture was obtained by adding 1 mL of overnight culture to 99 mL of fresh Mueller-Hinton broth. The culture was grown at 37 °C and 250 RPM shaking until it reached an OD_{600} of 0.132 (0.5 McFarland) and a series of Mueller-Hinton-Agar plates preheated at 37 °C were inoculated spreading 200 μL of that culture with sterile cotton. The plates were then dried for 30 minutes. Then on each plate 3 or 4 antibiotic paper disks were placed. The plates were incubated overnight at 37 °C and subsequently the diameter of the inhibition growth zone was measured.

MIC test

A 96-well, round-bottom plate was used to setup a culture made of 200 μL of E.coli ATCC 25922 culture in Mueller-Hinton with an OD_{600} of 0.132 (0.5 McFarland) and an established amount of antibiotic per well. The 96-well plate was incubated overnight at 37 °C and 350 RPM shaking. The OD_{600} of all wells was measured using an E.coli ATCC 25922 culture with an OD600 of 0.132 as reference and the MIC value was determined by taking the lowest concentration where no bacterial growth was observed.

5.5 - References

1. Bastian, A. A., Marcozzi, A. & Herrmann, A. Selective transformations of complex molecules are enabled by aptameric protective groups. *Nature Chemistry* 4, 789–793 (2012).
2. Bastian, A. A., Warszawik, E. M., Panduru, P., Arenz, C. & Herrmann, A. Regioselective diazo-transfer reaction at the C3-position of the 2-desoxystreptamine ring of neamine antibiotics. *Chemistry* 19, 9151–9154 (2013).
3. Waksman, S. A. *Isolation of Antibiotic Substances from Soil Micro-organisms: With Special Reference to Streptothricin and Streptomycin*. (1944). doi:10.1002/jps.3030341102/abstract
4. Waksman, S. A., REILLY, H. C. & JOHNSTONE, D. B. Isolation of streptomycin-producing strains of Streptomyces griseus. *Journal of Bacteriology* 52, 393–397 (1946).
5. SMITH, D. G. & Waksman, S. A. Tuberculostatic and tuberculocidal action of streptomycin. *Journal of Bacteriology* 54, 67 (1947).
6. WAKSMAN, S. P. Streptomycin and neomycin: approach towards a chemotherapy of tuberculosis by antibiotics. *Semaine Des Hopitaux* 26, 3091 (1950).
7. Waksman, S. A. & Lechevalier, H. A. Neomycin, a New Antibiotic Active against Streptomycin-Resistant Bacteria, including Tuberculosis Organisms. *Science* 109, 305–307 (1949).
8. Falagas, M. E., Grammatikos, A. P. & Michalopoulos, A. Potential of old-generation antibiotics to address current need for new antibiotics. *Expert Review of Anti-Infective Therapy* 6, 593–600 (2008).
9. Durante-Mangoni, E., Grammatikos, A., Utili, R. & Falagas, M. E. Do we still need the aminoglycosides? *International Journal of Antimicrobial Agents* 33, 201–205 (2009).
10. Mingeot-Leclercq, M.-P. & Tulkens, P. M. Aminoglycosides: Nephrotoxicity. *Antimicrobial Agents and Chemotherapy* 43, 1003–1012 (1999).
11. Smith, C. R. *et al.* Double-Blind Comparison of the Nephrotoxicity and Auditory Toxicity of Gentamicin and Tobramycin. *New England Journal of Medicine* 302, 1106–1109 (1980).
12. Mingeot-Leclercq, M.-P., Glupczynski, Y. & Tulkens, P. M. Aminoglycosides: Activity and Resistance. *Antimicrobial Agents and Chemotherapy* 43, 727–737 (1999).
13. Wright, G. D. Aminoglycoside-modifying enzymes. *Current Opinion in Microbiology* 2, 499–503 (1999).
14. Shaw, K. J., Rather, P. N., Hare, R. S. & Miller, G. H. Molecular genetics of aminoglycoside resistance genes and familial relationships of the aminoglycoside-modifying enzymes. *Microbiology and Molecular Biology Reviews* 57, 138–163 (1993).
15. Tuerk, C. & Gold, L. Systematic evolution of ligands by exponential enrichment: RNA ligands to bacteriophage T4 DNA polymerase. *Science* 249, 505–510 (1990).
16. Musheev, M. U. & Krylov, S. N. Selection of aptamers by systematic evolution of ligands by exponential enrichment: Addressing the polymerase chain reaction issue. *Analytica Chimica Acta* 564, 91–96 (2006).
17. Bastian, A. A., Rodríguez-Pulido, A., Gruszka, A., Gerasimov, J. Y. & Herrmann, A.

Probing the shielding properties of aptameric protective groups. *Chemistry - An Asian Journal* 9, 2225–2231 (2014).
18. Ausubel, F. M., Brent, R., Kingston, R. E. & Moore, D. D. *Current Protocols in Molecular Biology* (Wiley, 1987).
19. Miller, E. M. & Nickoloff, J. A. in *Electroporation Protocols for Microorganisms* 47, 105–114 (Humana Press, 1995).

Summary

This thesis describes the filamentous bacteriophage M13, its structure, its life cycle and several of its applications in molecular biology and materials science. We have seen how phages are used for the selection of proteins with improved stability, enzyme-inhibitor discovery and selection of binders for inorganic materials and nanostructures through a method called "phage display".

Phage display is based on the expression of an amino acid sequence in fusion with a viral capsid protein that is displayed on the phage particle. Once a large library of sequences is made, an evolution step takes place; each sequence is an individual representative of a wider population and by applying the proper selective pressure, one can drive the evolution of sequences with greater fitness for the desired trait. During this work, phage display was exploited to select peptide aptamers against a variety of targets.

The first target, in Chapter 2, is DXS, an enzyme of the MEP pathway that is indispensible for the survival of bacteria and protozoa among wich there are numerose human pathogens. However, DXS is not produced in higher animals, including mammalians. This fact makes DXS a perfect target for new antibacterial agents. We used a two-step phage display selection protocol for screening of the peptide libraries to select short DXS inhibitors using *D. radiodurans* DXS as a target. While the first step narrowed down the complexity of the library, specific peptides binding to the active site were selected by deep screening using a Darwinian evolution process in the second step. The most representative peptides obtained were tested and we showed that, at least in one case, the *in-vitro* activity of the enzyme is drastically affected upon addition of the aptamer. Through this research, the first peptide inhibitor for the MEP pathway's first rate-limiting enzyme, DXS, was identified. The phage display selection protocol helped in rapid identification of efficient peptide DXS inhibitors with a comparable activity to the best available small organic molecules. Furthermore, using alanine scanning, the significance of the N-terminal serine-rich motif was revealed. Though preliminary, these

findings are an important step towards developing peptide inhibitors with antibacterial potential. Exploitation of these findings and optimization of the binding motifs and delivery process to achieve desired levels of *in vivo* DXS inhibition represent several goals for the future.

In Chapter 3, it was demonstrated how phage display can be instrumental in exploring the host-guest interactions between organic molecules and peptides. The attention was focused on complexes formed by macrocyclic molecules such as the cucurbituril CB8 and aromatic amino acids. Phenylalanine and tryptophan have proven to be very effective to achieve dimerisation of peptides and proteins, and their functionalisation in a reversible and non-covalent fashion in the presence of CB8. Protein dimerisation naturally plays vital roles in regulation of protein activities in many processes including receptor clustering, signal transduction, and apoptosis. Hence, understanding of dimer formation opens the gate to tremendous theoretical and practical implications in biology and medicine.

Using phage display, two different large peptide libraries PhD-7, composed of linear peptides, and PhD-C7C, composed of cyclic peptides, were screened to detect strong CB8 binders. After panning of the libraries on CB8-functionalised surfaces, repeated sequences and small motifs were detected by in depth analysis. All the repeated sequences contained an aromatic residue, and Trp and Tyr residues occurred in repeated sequence, albeit at overall low abundance. The Pro and Ser residues were highly selected and mostly they were followed by positively charged residues like Lys and Arg.

The interaction of the selected peptides and CB8 was investigated using Isothermal Titration Calorimetry (ITC) and optical spectroscopic measurements. Especially the sequences obtained from the acidic selection of the cyclic library were studied. Three sequences showed consistent results with both spectroscopic and ITC measurements, inequivocally proving binding.

Our findings demonstrate for the first time that cyclic peptides form complexes with CB8 and that non-terminal aromatic amino acids are suitable for undergoing the host-guest interactions. These findings underline the importance of having an aromatic residue in the sequence and the need a for positive charge for additional stabilisation of the

complex. In addition to the N-terminal group of a linear peptide that was known to be responsible for the charge stabilisation needed to form the peptide-CB8 complex, we showed that other factors like the protonation state of neighboring residues also play a role in the effective formation of a complex between CB8 and a non-terminal aromatic amino acid. These results open up new possibilities of forming CB8 protein complexes that go beyond the constriction of having only the N-terminus as anchoring point.

In contrast to the previous chapters, Chapter 4 deals with M13 as building block for the fabrication of new materials, in particular water-free liquid crystals. To achieve this objective, the protein p8 that, with 2700 copies forms the capsid of M13, was genetically modified. The N-termini of these proteins are flexible, hydrophilic domains, located on the outer surface of the phage that can be exploited to support a peptide insert of up to 8 amino acids for display on every p8 unit. Further, their self-assembly into one micrometer long filaments has made M13 an ideal building block for many applications. The mutagenesis of M13 was achieved through PCR and confirmed by sequencing and mass spectometry. Several M13 mutants were produced using different mutagenesis protocols. Two of these, M13-K8A and M13-ELA, were explored in this chapter. The M13-K8A variant was derived by replacement of lysine with alanine at position 8, which lead to the exposure of less positive charges of the phage particle. In this modification, only one amino group is exposed at the surface of the phage particle per p8. In contrast, in the wild type phage, two positive charges per p8 are protruding from the phage surface, i.e., Lys 8 and the N-terminus. This results in 5400 and 2700 positive surface charges for wild type phage and the variant M13-K8A, respectively. This single amino acid substitution allowed us to easily tune the charg density of the surface and the degree of functionalisation of the viral particle with a fluorescent dye.

The M13-ELA mutant was more severely modified since the five amino acid long elastin motif (VPGVG) was inserted at its N-terminus. The phages were produced and used to generate liquid-crystals. It was found that complexation of the phage particles with cationic surfactants lead to a smectic mesophase with typical focal-conic birefringence in a temperature range of 14–58 °C. Detailed analysis of these phases showed that the layer spacing corresponds to a bilayer structure made of a sublayer of

phage and an interdigitated sublayer of surfactants. Each repeating layer consisted of tail-to-tail interacting surfactants that protruded from the phage particle. Long-range periodic layer structures in the mesophase were confirmed by FF-TEM studies. The fractured plane revealed individual phages globally, along a preferred direction. Nematic orientational ordering had developed between different phages within the sublayer as a result of the rigidity and large length-to-diameter aspect ratio of the phage.

With our work, we were able to demonstrate how small modifications on the protein p8 can lead to great changes in the chemical and physical properties of the complete capsid.

The results can be summed up as follows:

- Simple amino acid substition can permit control over the chemical functionalisation of the capsid
- The physical characteristics of the partilcles could be fine-tuned with an insertion of a small peptide at the N-terminus of p8
- We showed that phages can be effectively used as building blocks for the fabrication of new hybrid materials that consist of the naturally derived virus and the synthetic surfactant and that form thermotropic liquid crystals.

The last chapter, like Chapter 2, again deals with the development of new antibiotics. In particular, it deals with a new technology developed in the Herrmann group called "aptameric protective groups". This technology was developed for the facile derivatisation of natural products and is based on nucleic acid aptamers that bind to complex molecules bearing several chemical equivalent groups. The groups in contact with the aptamer are transiently protected, while functionalities not in touch with the nucleic acid sequence can be chemically modified. Using this technology, a series of new aminoglycosides was synthesised and their antimicrobial properties were investigated. These aminoglycoside consisted of Neomycin B derivatives that were functionalized at

ring IV. In particular, amino groups in position 2 and 6 were transformed into urea and amide derivatives, respectively.

The aminoglycoside derivatives were evaluated using established standard protocols namely the dilution method and the disc diffusion method. All the tested derivatives showed high antimicrobial activity, demonstrating the significance of the APG technology in deriving active antimicrobial compounds. Moreover, these tests have shown that modification of ring IV of Neomycin B does not impair the antimicrobial proerties of this compound. Following these promising results, other derivatives were synthesized in the laboratory using a different approach that does not require the use of aptameric protective groups. However, this protocol lead to the functionalisation of the C3-position of the 2-desoxystreptamine ring I of neamine antibiotics. Another modification consisted of epimerisation of the hydroxy group of ring II. A comparative MIC test on two strains of *E. coli* expressing different resistance genes showed that one compound, was able to retain a significant antibaterial activity even in the presence of two most common aminoglycoside resistance enzymes. In the future, these promising compounds might be taken further to achieve clinical use. However, this requires testing these compounds against clinical isolates containing multidrug resistant bacteria and determination of their toxicity *in vitro* and *in vivo*.

Samenvatting

In dit proefschrift heb ik de filamenteuze bacteriofaag M13, de structuur, zijn levenscyclus en een aantal van haar toepassingen beschreven in de moleculaire biologie en materiaal wetenschap. We hebben gezien hoe fagen worden gebruikt voor de selectie van eiwitten met verbeterde stabiliteit, enzymremmer ontdekking en selectie van bindmiddelen voor anorganische materialen en nanostructuren door een methode genaamd "phage display".

Faagdisplay is gebaseerd op de expressie van een aminozuursequentie in fusie met een viraal capside-eiwit dat men op het faagdeeltje ziet. Zodra een grote bibliotheek van sequenties wordt gemaakt, vindt een evolutie stap plaats; elke sequentie is een individuele vertegenwoordiger van een bredere populatie en door toepassing van de juiste selectieve druk, kan men de evolutie van opeenvolgingen met een grotere geschiktheid voor de gewenste eigenschap verkrijgen. Tijdens deze werkzaamheden heb ik faag display benut om peptide aptameren tegen een verscheidenheid van doelwitten te selecteren.

Het eerste doel, in hoofdstuk 2, is DXS, een enzym van het MEP traject die onontbeerlijk is voor het overleven van de bacteriën en protozoa onder welke er numerieke menselijke ziektekiemen zijn. Echter, DXS is niet geproduceerd in grotere dieren, inclusief zoogdieren. Dit feit maakt DXS een perfect doelwit voor nieuwe antibiotica. We gebruikten een twee stappen faagdisplay selectie protocol voor het screenen van het peptide bibliotheken om korte DXS-remmers te gebruiken D. radiodurans DXS als doelwit . Terwijl de eerste stap de complexiteit van de bibliotheek versmald zijn specifieke enzymplaats bindende peptiden die werden geselecteerd door screening met een Darwiniaanse evolutie proces in de tweede stap. De meest voorkomende peptiden die verkregen werden getest en toonden we aan dat, ten minste in één geval, de in-vitro activiteit van het enzym drastisch beïnvloed na toevoeging van de aptameer.

Door mijn onderzoek, werd het eerste peptide-remmer voor het MEP traject eerste snelheidsbeperkende enzym, DXS geïdentificeerd. De faagdisplay selectie protocol geholpen bij snelle identificatie van efficiënte peptide DXS inhibitoren met een vergelijkbare activiteit van de best beschikbare kleine organische moleculen. Bovenal, door alanine scanning, de betekenis van de N-terminale serine-rijke motief onthuld. Hoewel voorlopig, deze bevindingen zijn een belangrijke stap naar de ontwikkeling van peptide-remmers met antibacteriële potentieel. Exploitatie van deze bevindingen en optimalisatie van de bindende motieven en leveringsproces te bereiken van het gewenste niveau van in vivo DXS remming vertegenwoordigen verschillende doelen voor de toekomst.

In hoofdstuk 3 werd aangetoond hoe faagdisplay instrumenteel in het verkennen van de host-gast interacties tussen organische moleculen en peptiden kan zijn. De aandacht was gericht op complexen gevormd door macrocyclische moleculen, zoals de cucurbituril CB8 en aromatische aminozuren.

Fenylalanine en tryptofaan zijn zeer effectief gebleken om dimerisatie van peptiden en eiwitten te bereiken, en de functionalisering in een reversibele en niet-covalente wijze in aanwezigheid van CB8. Eiwit dimerisatie speelt natuurlijk een belangrijke rol bij de regulering van proteïne activiteiten in vele processen, waaronder receptor clustering, signaaltransductie en apoptose. Vandaar dat begrip van dimeer vorming opent de poort naar enorme theoretische en praktische implicaties in de biologie en geneeskunde.

Met behulp van faagdisplay, twee verschillende grote peptide libraries PhD-7, bestaande uit lineaire peptiden en PhD-C7C, bestaande uit cyclische peptiden, werden gescreend om sterke CB8 binders te detecteren. Na panning van de bibliotheken op CB8 gefunctionaliseerde ondergronden, herhaalde sequenties en kleine motieven werden gedetecteerd door eendiepgaande analyse. Alle herhaalde sequenties bevatte een aromatische rest, en Trp en Tyr residuen voorgedaan in herhaalde opeenvolging, zij het in het algemeen lage overvloed. De Pro en Ser residuen werden sterk geselecteerd en meestal werden ze gevolgd door positief geladen resten zoals Lys en Arg. De interactie van de geselecteerde peptiden en CB8 werd onderzocht met behulp van Isotherme Titratie Calorimetrie (ITC) en optische spectroscopische metingen. Vooral de uit de zure selectie

van de cyclische bibliotheek werden onderzocht. Drie sequenties toonden consistente resultaten met zowel spectroscopische en ITC metingen ondubbelzinnig bewijzen bindend.

Onze bevindingen tonen voor het eerst aan dat cyclische peptiden complexen vormen met CB8 en dat niet-eindstandige aromatische aminozuren geschikt zijn voor het ondergaan van de hostguest interacties. Deze bevindingen onderstrepen het belang van het hebben van een aromatisch residu in de volgorde en de noodzaak van een positieve kosten voor extra stabilisatie van het complex.

Naast de N-terminale groep een lineair peptide dat bekend is hierin voor de stabilisatie nodig peptide-CB8 te vormen zijn, hebben we aangetoond dat andere factoren zoals het protonering toestand van naburige resten een rol in de effectievevorming van een complex tussen CB8 en een niet-eindstandig aromatisch aminozuur.Deze resultaten openen nieuwe mogelijkheden voor het vormen van CB8 eiwitcomplexen die verder gaan dan de vernauwing van het hebben van alleen de N-terminus als ankerpunt.

In tegenstelling tot de voorgaande hoofdstukken, hoofdstuk 4 behandelt M13 als bouwsteen voor de fabricage van nieuwe materialen, in het bijzonder watervrije vloeibare kristallen. Om deze doelstelling te bereiken, het eiwit p8 met 2700 kopieën vormt de capside M13, werd genetisch gemodificeerd. De N-termini van deze eiwitten zijn flexibel, hydrofiele domeinen, op het buitenoppervlak van de faag die kan worden benut om een peptide tot 8 aminozuren ondersteuning voor weergave op elke p8 unit. Verder is hun zelf-verzameling in één micrometer lange filamenten M13 een ideale bouwsteen voor vele toepassingen.

De mutagenese M13 werd bereikt door PCR en bevestigd door opeenvolging en massaspectrometrie. Verscheidene M13 mutanten werden geproduceerd met verschillende mutagenese protocollen. Twee van deze, M13-K8A en M13-ELA, werden onderzocht in dit hoofdstuk. De M13-K8A variant werd verkregen door vervanging van lysine met alanine op positie 8, die leiden tot de blootstelling van minder positieve ladingen van het faagdeeltje. In deze modificatie is slechts één aminogroep blootgesteld aan het oppervlak van het faagdeeltje per p8. Daarentegen, in het wildtype faag, twee positieve ladingen per p8 steken uit het faag-oppervlakte, d.w.z. Lys 8 en de N-

terminus. Dit resulteert in 5400 en 2700 positieve oppervlakte kosten voor wild-type faag en de variant M13-K8A, respectievelijk. Deze enkele aminozuursubstitutie liet ons gemakkelijk afstemmen van de charg dichtheid van het oppervlakte en de mate van functionalisering van het virale deeltje met een fluorescerende kleurstof.

De M13-ELA mutant werd sterk gewijzigd sinds 5 aminozuren lang elastine motief (VPGVG) werd ingevoegd aan zijn N-terminus. De fagen werden geproduceerd en gebruikt om vloeibare kristallen te genereren. Gevonden werd dat complexering van de faagdeeltjes met kationische oppervlakteactieve tot een smectische mesofase met typische focal-conische birefractie in een temperatuurbereik van 14-58 ° C.

Gedetailleerde analyse van deze fasen bleek dat de laagafstand overeenkomt met een tweelaags structuur gemaakt van een onderlaag van faag en een interdigitated deellaag van oppervlakteactieve stoffen. Elke herhalende laag bestond uit een interactie van oppervlakteactieve stoffen die uitsteekt van het faagdeeltje. Lange-afstands periodieke layer structuren in de mesofase werden bevestigd door FF-TEM studies. Het gebroken vlak onthuld individuele fagen wereldwijd, langs een voorkeursrichting. Nematische oriëntatie geproduceerd ontstaan tussen verschillende fagen in de sublaag ten gevolge van de stijfheid en grote lengte-diameter verhouding van de faag.

Met ons werk, konden we zien hoe kleine modificaties op het eiwit p8 kan leiden tot grote veranderingen in de chemische en fysische eigenschappen van de volledige capside.

De resultaten kunnen als volgt worden samengevat:

- Eenvoudige aminozuur substitutie kan controle mogelijk te maken aan de chemische functionalisering van de capside
- De fysische eigenschappen van de partikels kan ingesteld met een invoeging van een klein peptide aan de N-terminus van p8
- We toonden aan dat fagen effectief kan worden gebruikt als et bouwstenen voor de vervaardiging van nieuwe hybride materialen die bestaan uit de natuurlijk verkregen virus en synthetische surfactant en die vormen thermotroop vloeibaar kristallen.

Het vorige hoofdstuk, zoals Hoofdstuk 2, heeft wederom betrekking op de ontwikkeling van nieuwe antibiotica. In het bijzonder gaat het over een nieuwe technologie ontwikkeld in de Herrmann groep genaamd "aptameric beschermende groepen". Deze technologie werd ontwikkeld voor gemakkelijke derivatisering van natuurlijke producten en is gebaseerd op nucleïnezuur aptameren die binden aan complexe moleculen van verschillende chemisch equivalent groepen. De groepen in contact met de aptameer worden kortstondig beschermd, terwijl functionaliteiten niet in contact met de nucleïnezuursequentie chemisch kan worden gemodificeerd. Met deze technologie werd een reeks nieuwe aminoglycosiden gesynthetiseerd en ik heb hun antimicrobiële eigenschappen onderzocht. Deze aminoglycoside bestond uit Neomycine B derivaten die op ring IV werden gefunctionaliseerd. Met name aminogroepen op positie 2 en 6 werden omgezet in ureum en amidederivaten, respectievelijk.

De aminoglycoside derivaten werden geëvalueerd met behulp van gevestigde standaardprotocollen namelijk de verdunning methode en de disc diffusie methode. Alle geteste derivaten vertoonden hoge antimicrobiële activiteit, tonen het belang van de APG technologie afleiden actieve antimicrobiële verbindingen aan. Bovendien hebben deze tests aangetoond dat de wijziging van de ring IV van Neomycine B doet geen afbreuk aan de antimicrobiële eigenschappen van deze verbinding. Na deze veelbelovende resultaten werden andere derivaten gesynthetiseerd in het laboratorium met een andere benadering die niet het gebruik van aptameric beschermende groepen vereisen. Echter, dit protocol leidde tot de functionalisering van de C3-positie van de 2-desoxystreptamine ring I neamine antibiotica. Een andere modificatie bestond uit epimerisatie van de hydroxylgroep van de ring II. Een vergelijkende proef MIC op twee stammen van *E. coli* die verschillende resistentiegenen gebleken dat één verbinding, kon een significante antibaterial activiteit, zelfs in de aanwezigheid van twee meest voorkomende aminoglycoside resistentie enzymen behouden. In de toekomst zou deze veelbelovende verbindingen verder worden voor klinisch gebruik bereiken. Dit vereist echter het testen van deze verbindingen tegen klinische isolaten die multiresistente bacteriën en bepaling van de toxiciteit *in vitro* en *in vivo*.

Aknowledgements

With these few lines, I would like to express my gratitude to all those who, in one way or another, have been part of this intense chapter of my life and made it of inestimable value. The names below represent only a small part of the people to whom I owe my gratitude, many others should be properly thanked, but I preferred to keep it short. In the chronological order in which my path has become intertwined with them during this adventure, I would like to express my gratitude:

To Prof. Andreas Herrmann, for your confidence in me, for welcoming me into your group and for the countless opportunities for growth received over the years. I started my Ph.D. with the spirit of those who ventured a long training period in preparation for a crucial race. I wanted to train to become a great scientist, and you've given me the opportunity. They were years of intense and exhausting, much like a good workout should be and if today I prepared me to undertake with even more determination the path of science, I owe it to you.

To Diego (being an official document we will use the unofficial name), for sharing together five years of our lives! I still remember like it was yesterday the day when I moved to Groningen, was you to meet me at the station, to host me in your house, to make me feel part of the family. We tied immidiately, we have grown together over the years constantly comparing ourselves, learning from each other by mixing our experience and our world views. You are a guide, a friend, a colleague, a brother. Thanks for everything!

Aan Dennis, voor uw voortdurende nieuwsgierigheid, het verlangen om te leren en de positieve energie die je voortdurend uitstraalt. We brachten samen veel goede tijd door en er zal nog veel meer volgen.

To the whole PCBE group, I infinitely enjoyed the time spent together was a pleasure working with all of you. Thank you so much.

To Karin, always professional and friendly, you helped me on innumerable occasions. Thank you!

To Prof. Anna Hirsch, Prof. Harm-Anton Klok, and Prof. Oren Scherman, for agreeing to be part of the Assessment Committee, for their valuable suggestions and for your time. Thank you.

Un immenso grazie va ai miei genitori, per il loro costante supporto, per i loro insegnamenti, per aver contribuito giorno dopo giorno alla mia formazione con amore, attenzione e dedizione. Siete i migliori! :* :*

Ai miei fratelli, per avermi sempre fatto sentire con forza l'affetto che ci lega, indissolubile alle distanze ed al tempo.

В заключении, я хотел бы особенно поблагодарить Алину. Никто еще не переносил меня так долго ;) Ты замечательный человек и и прекрастный компаньен. Я люблю тебя бесконечно.

THE END